TECHNICAL REPORT HL-90-6

SAN FRANCISCO CENTRAL BAY SUSPENDED SEDIMENT MOVEMENT

Report 1

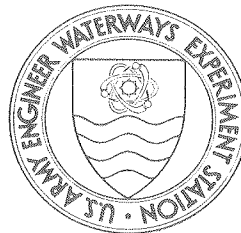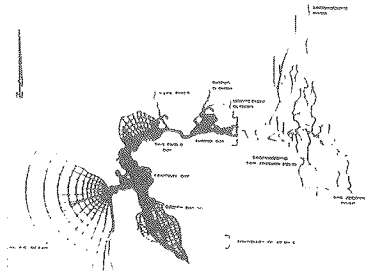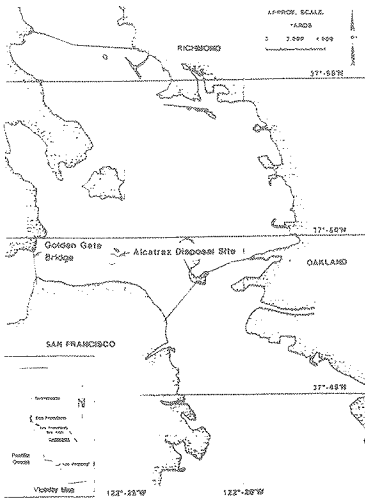## SUMMER CONDITION DATA COLLECTION PROGRAM AND NUMERICAL MODEL VERIFICATION

by

Larry M. Hauck, Allen M. Teeter, Walter Pankow, Robert A. Evans, Jr.
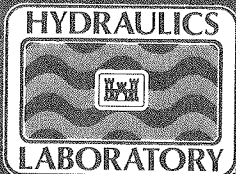
Hydraulics Laboratory

DEPARTMENT OF THE ARMY
Waterways Experiment Station, Corps of Engineers
3909 Halls Ferry Road, Vicksburg, Mississippi   39180-6199

September 1990

Report 1 of a Series

REPORT DOCUMENTATION PAGE

Form Approved
OMB No. 0704-0188

1a. REPORT SECURITY CLASSIFICATION	1b. RESTRICTIVE MARKINGS
Unclassified	

2a. SECURITY CLASSIFICATION AUTHORITY	3. DISTRIBUTION/AVAILABILITY OF REPORT
	Approved for public release;
2b. DECLASSIFICATION/DOWNGRADING SCHEDULE	distribution unlimited.

4. PERFORMING ORGANIZATION REPORT NUMBER(S)	5. MONITORING ORGANIZATION REPORT NUMBER(S)
Technical Report HL-90-6	

6a. NAME OF PERFORMING ORGANIZATION	6b. OFFICE SYMBOL (If applicable)	7a. NAME OF MONITORING ORGANIZATION
USAEWES Hydraulics Laboratory	CEWES-HE	

6c. ADDRESS (City, State, and ZIP Code)	7b. ADDRESS (City, State, and ZIP Code)
3909 Halls Ferry Road Vicksburg, MS 39180-6199	

8a. NAME OF FUNDING/SPONSORING ORGANIZATION	8b. OFFICE SYMBOL (If applicable)	9. PROCUREMENT INSTRUMENT IDENTIFICATION NUMBER
USAED, San Francisco		

8c. ADDRESS (City, State, and ZIP Code)	10. SOURCE OF FUNDING NUMBERS			
	PROGRAM ELEMENT NO.	PROJECT NO.	TASK NO.	WORK UNIT ACCESSION NO.
211 Main Street San Francisco, CA 94105-1905				

11. TITLE (Include Security Classification)
San Francisco Central Bay Suspended Sediment Movement; Summer Condition Data Collection Program and Numerical Model Verification

12. PERSONAL AUTHOR(S)
Hauck, Larry M.; Teeter, Allen M.; Pankow, Walter; and Evans, Robert A., Jr.

13a. TYPE OF REPORT	13b. TIME COVERED	14. DATE OF REPORT (Year, Month, Day)	15. PAGE COUNT
Report 1 of a series	FROM _____ TO _____	September 1990	122

16. SUPPLEMENTARY NOTATION
Available from National Technical Information Service, 5285 Port Royal Road, Springfield, VA 22161.

17. COSATI CODES			18. SUBJECT TERMS (Continue on reverse if necessary and identify by block number)
FIELD	GROUP	SUB-GROUP	Field investigation San Francisco Bay
			Mass flux Sedimentation and deposition
			Numerical modeling Total suspended matter

19. ABSTRACT (Continue on reverse if necessary and identify by block number)

Field data were collected on currents, salinities, and suspended sediments intensively over a lunar day and sporadically over a fortnight in September 1988 for the purpose of identifying transport processes and conditions in central San Francisco Bay and for numerical model verification. Conditions were typical of a low freshwater inflow summer season in this area. A two-dimensional horizontal finite element model was applied and verified to field and physical hydraulic model data. The model is intended for future long-term studies of the fate of dredged material dispersed from the Alcatraz disposal site.

20. DISTRIBUTION/AVAILABILITY OF ABSTRACT	21. ABSTRACT SECURITY CLASSIFICATION
☒ UNCLASSIFIED/UNLIMITED ☐ SAME AS RPT. ☐ DTIC USERS	Unclassified
22a. NAME OF RESPONSIBLE INDIVIDUAL	22b. TELEPHONE (Include Area Code) 22c. OFFICE SYMBOL

DD Form 1473, JUN 86   *Previous editions are obsolete.*

CONTENTS

CONVERSION FACTORS, NON-SI TO SI (METRIC)
UNITS OF MEASUREMENT

Non-SI units of measurement used in this report can be converted to SI (metric) units as follows:

Multiply	By	To Obtain
acres	4,046.873	square metres
cubic feet	0.0283	cubic metres
cubic yards	0.76	cubic metres
degrees (angle)	0.01745329	radians
feet	0.305	metres
inches	2.54	centimetres
metric tons	1,000.0	kilograms
miles (US statute)	1.609	kilometres
ounces (fluid)	0.0296	litres
pounds (force)	4.448222	newtons
pounds (force)-second/square foot	47.88026	pascals-second
square feet	0.0929	square metres
yards	0.9144	metres

SAN FRANCISCO CENTRAL BAY SUSPENDED SEDIMENT MOVEMENT

SUMMER CONDITION DATA COLLECTION PROGRAM
AND NUMERICAL MODEL VERIFICATION

PART I: INTRODUCTION

Background

1.   The dredged material disposal site near Alcatraz Island is a natu-
rally deep open-water site in San Francisco Bay (Figure 1). This particular
site was first designated in 1894 and is the only such remaining site in the
central portion of San Francisco Bay. This site has been the preferred site
for disposal of the sediment materials from the central bay region for both
new work and maintenance dredging. The Alcatraz disposal site was originally
designated because of the depth and the high local velocities, which were
assumed to disperse and carry the sediments out into the Pacific Ocean.

2.   Several dredging projects potentially could use the Alcatraz dis-
posal site in San Francisco Bay. The Oakland Harbor deepening project will
require the removal of approximately 7 million cubic yards* of sediment
material. Other projects include the Richmond project (1.5 million cubic
yards), the J. F. Baldwin III project (9 million cubic yards), and the Navy
improvement dredging project (1.5 million cubic yards). In addition, annual
maintenance dredging is expected to be approximately 4 million cubic yards.
The local public and resource agencies are concerned that disposal of this
material, especially the fine-grained (silt and clay) fraction, might cause
turbidity problems that could adversely affect both fishing and water quality
conditions. According to researchers, phytoplankton primary production is
light limited in the bay, and excessive turbidity could interfere within this
ecologically important process. Deposition of fine-grained sediments over
sandy substrates might affect benthic organisms. In addition, low levels of
contaminants associated with some dredged material have the potential to be
released into the bay environment and the corresponding potential for bio-
accumulation and cycling of any contaminants.

---

* A table of factors for converting non-SI units of measurement to SI
  (metric) units is found on page 4.
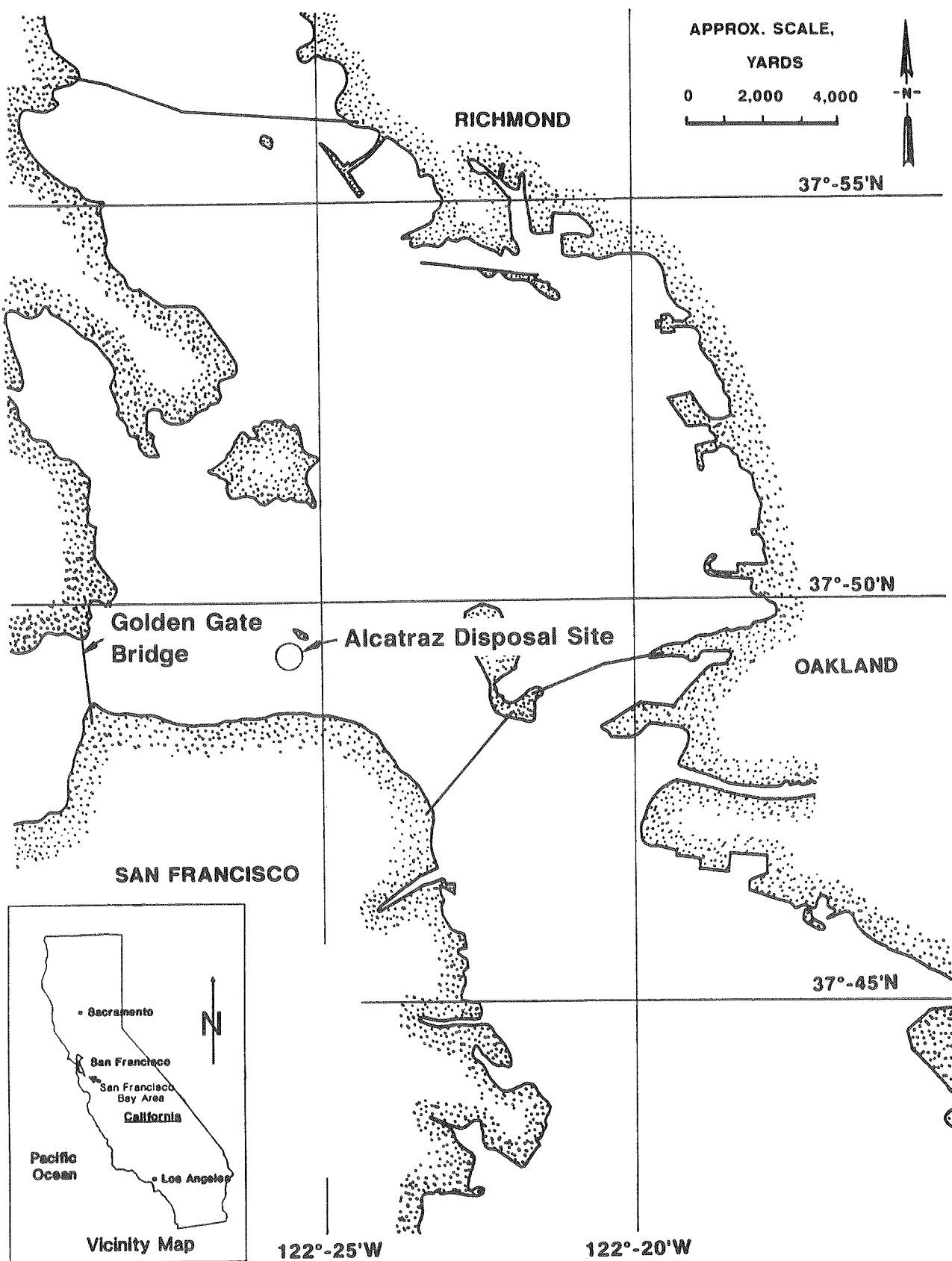
Figure 1. Location map of Central San Francisco Bay

6

3. In 1982, the US Army Engineer District, San Francisco, determined that the dredged materials being disposed at the site were not being dispersed at the rate that they were being introduced and furthermore that a permanent mound was forming. In response to this and the choice of locating alternate but more expensive disposal sites, the San Francisco District formed the Dredged Material Disposal Management Program (DMP). The DMP was tasked with both the determination of the fate of the dredged materials disposed at the Alcatraz site and the development of numerical models to assess various other possible disposal sites within San Francisco Bay. A request was made that the US Army Engineer Waterways Experiment Station (WES) provide assistance with these tasks. This report is the result of the fifth in a series of interrelated studies addressing the problem of open bay dredged material disposal.

4. There have been four WES study reports previously prepared for the DMP:

Title	Report Number	Author	Date
"Alcatraz Disposal Site Investigation"	Miscellaneous Paper HL–86–1	Trawle and Johnson	1986
"Alcatraz Disposal Site Investigation: Report 2, North Zone of Oakland Outer Harbor and Richmond Inner Harbor Sediments"	Miscellaneous Paper HL–86–1	Trawle and Johnson	1986
"Alcatraz Disposal Site Investigation: Report 3, San Francisco Bay–Alcatraz Disposal Site Erodibility"	Miscellaneous Paper HL–86–1	Teeter	1987
"San Francisco Bay: Modeling System for Dredged Material Disposal and Hydraulic Transport"	Technical Report HL–88–27	V. Pankow	1988

The first two reports dealt with the prediction of near field behavior from the instant of disposal through a few hundred seconds until most of the material had descended to the bed. A numerical disposal model was used for this purpose. The third study (Teeter 1987) performed laboratory erosion tests on deposited and remolded Alcatraz sediment beds to determine erodibility. Results of this study were used with field velocity data to predict the capacity of the site to disperse disposed materials.

5. The fourth report (Pankow 1988) developed a hybrid model consisting of a numerical component using verification data and boundary conditions from

the physical model of the San Francisco Bay-Delta Hydraulic Model (SFBM). A two-dimensional vertically averaged hydrodynamic model (RMA-2V) used a computational mesh of San Francisco Bay in conjunction with the SFBM data to define the tidal hydraulics and overall circulation patterns. The Disposal From Instantaneous Dump (DIFID) model was then used to simulate the short-term fate (1 hr or less) of materials disposed from barge or hopper dredge in a high-resolution grid of the Alcatraz dump site. Although the DIFID model can be applied to the short-term fate of materials disposed at the Alcatraz site, it cannot evaluate the baywide movement of materials away from the site. Finally, a sediment transport model (STUDH) was used to simulate the fate of the disposed materials for 3 to 4 hr following discharge using the suspended sediment concentrations predicted by the DIFID model and the hydrodynamics from RMA-2V.

Objectives

6. The major objectives of study tasks reported here were to (a) gage the seasonal concentration and circulation of fine-grained material in Central San Francisco Bay (Central Bay) during a typical low freshwater inflow period of June through October; (b) review and analyze selected previous studies on currents, suspended sediments, and material movement in San Francisco Bay; and (c) verify a numerical sediment transport model to the circulation and concentration of natural suspended sediments in the Central Bay area during the same low freshwater inflow condition.

7. Subsequent study tasks will use the verified numerical sediment model to predict the fate of the dredged material, to provide information for the management of the Alcatraz site, to evaluate environmental impacts from dredge disposal operations, and to relate and compare the predicted suspended sediment levels resulting from dredged material disposal operations to natural levels. Because fine-grained material historically constitutes the majority of the dredged material disposed at the Alcatraz site and since the environmental concerns to be addressed concern turbidity and contaminated dredged material, both phenomena being associated with fine-grained material, this study emphasized fine-grained material and not sand and sand movement as bed load.

Approach

8. The overall study approach was to use a combination of field data collection and analysis, physical model results, and numerical model results to address meteorologic, hydrologic, and hydrodynamic conditions during the typically dry, low freshwater inflow periods of June through October, and to determine the influence of these conditions on the fate of fine-grained dredged materials dispersed from the Alcatraz site. The individual tasks involved in the approach were as follows:

   a. Plan and implement an intensive field survey to obtain velocity, suspended sediment, and related hydrographic information. The survey consisted of a 2-week (spring to neap tide) period of limited data gathering with tide gage and automatic discrete water sampler operation, and a 25-hr (lunar day) intensive survey during a near-mean range tide.

   b. Analyze field survey and other data in the context of suspended sediment behavior, concentrations, currents, and materials.

   c. Review the published literature on San Francisco Bay currents and sediments.

   d. Reanalyze previous physical hydraulic model test data in regard to Central Bay flushing.

   e. Expand the numerical model mesh of San Francisco Bay, a development based upon previous WES numerical efforts.

   f. Verify the expanded hydrodynamic numerical model to SFBM water elevations and velocities and a prototype harmonic tide.

   g. Verify the numerical sediment model using the same expanded mesh to the intensive field survey data and limited historic data.

PART II: DATA COLLECTION PROGRAM

Data Acquisition

9. One of the key factors in successful numerical modeling is the qual-
ity and quantity of the field data used. Prototype data were used to identify
sedimentation and transport processes and geometry of the area, to provide
input for the models, and to provide a standard by which model results could
be compared (verification). Nearly synoptic data were needed (all data col-
lected at the same time) to develop a single, consistent set of boundary con-
ditions to ascribe to all locations and to establish relationships between
processes at the various stations. Long-term monitoring data were also needed
to assess processes at that time scale.

10. The field data for this study were collected by WES personnel in
September 1988. The prototype data acquisition program was performed over a
2-week period and included an intensive 25-hr survey of tidal conditions dur-
ing approximately mean tide. During the week preceding and the one following
the intensive survey, additional data, including water levels, salinities, and
suspended sediment samples, were collected. During the intensive survey,
three to four stations along four transects (ranges) within central San
Francisco Bay were monitored over a 25-hr period to encompass one full tidal
cycle. The intensive survey prototype data acquisition program included tidal
elevation, current speed and direction, salinity, and total suspended material
(TSM) measurements.

Station Locations

11. The program was designed to obtain an overview of the suspended
sediment and salinity conditions in Central Bay during various wind and tidal
conditions. A total of 5 tide gage and 15 point sample station locations
(Figure 2) were established for sampling prior to, during, and after the
intensive survey, with adjustments made in the field to suit actual condi-
tions. For the intensive survey, four transects with three or four stations
each were established (Figure 3). The final station and equipment locations,
along with the descriptions of the equipment used and sample data sheets, will
be presented in subsequent sections.
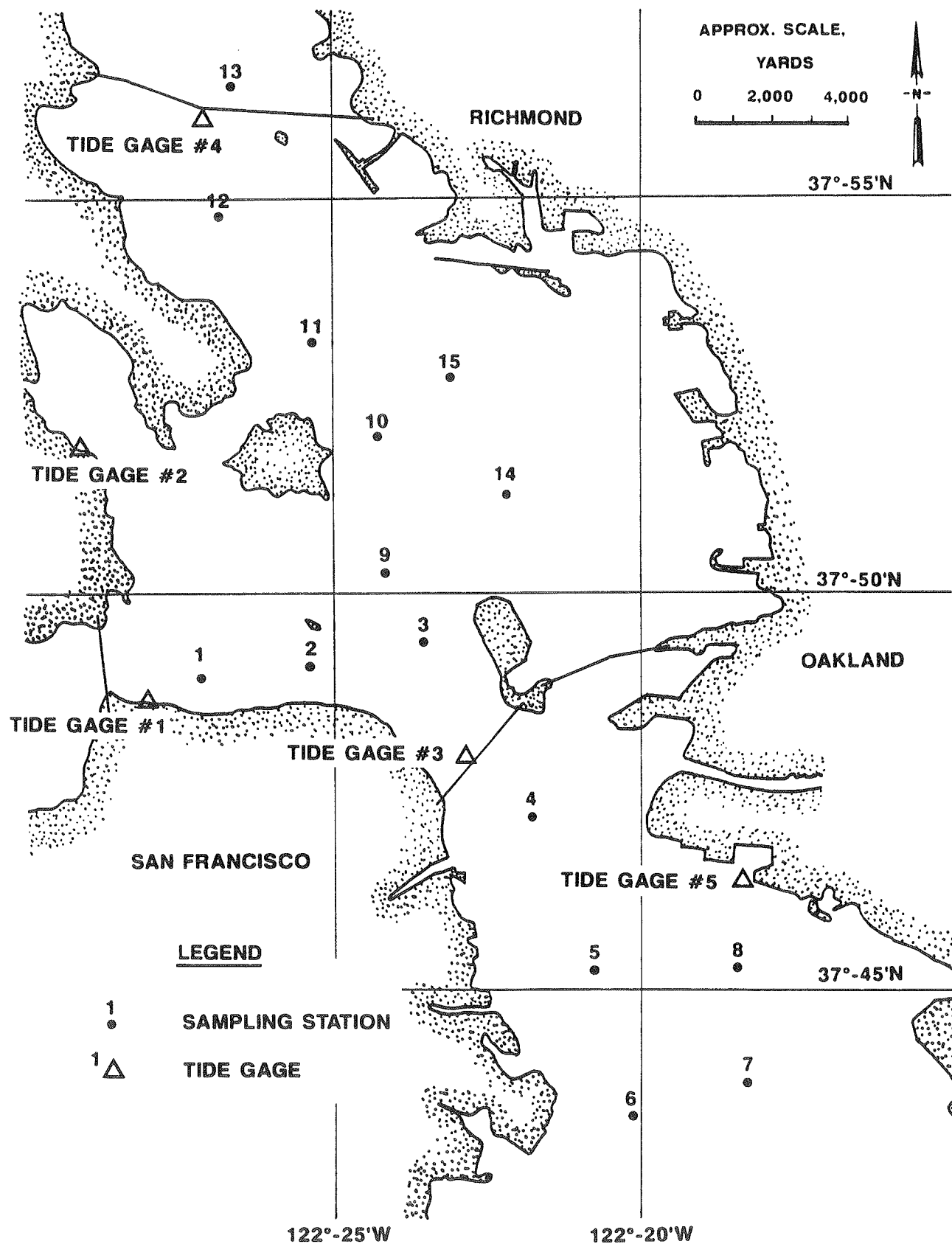
Figure 2. Location of tide gages and point sample locations
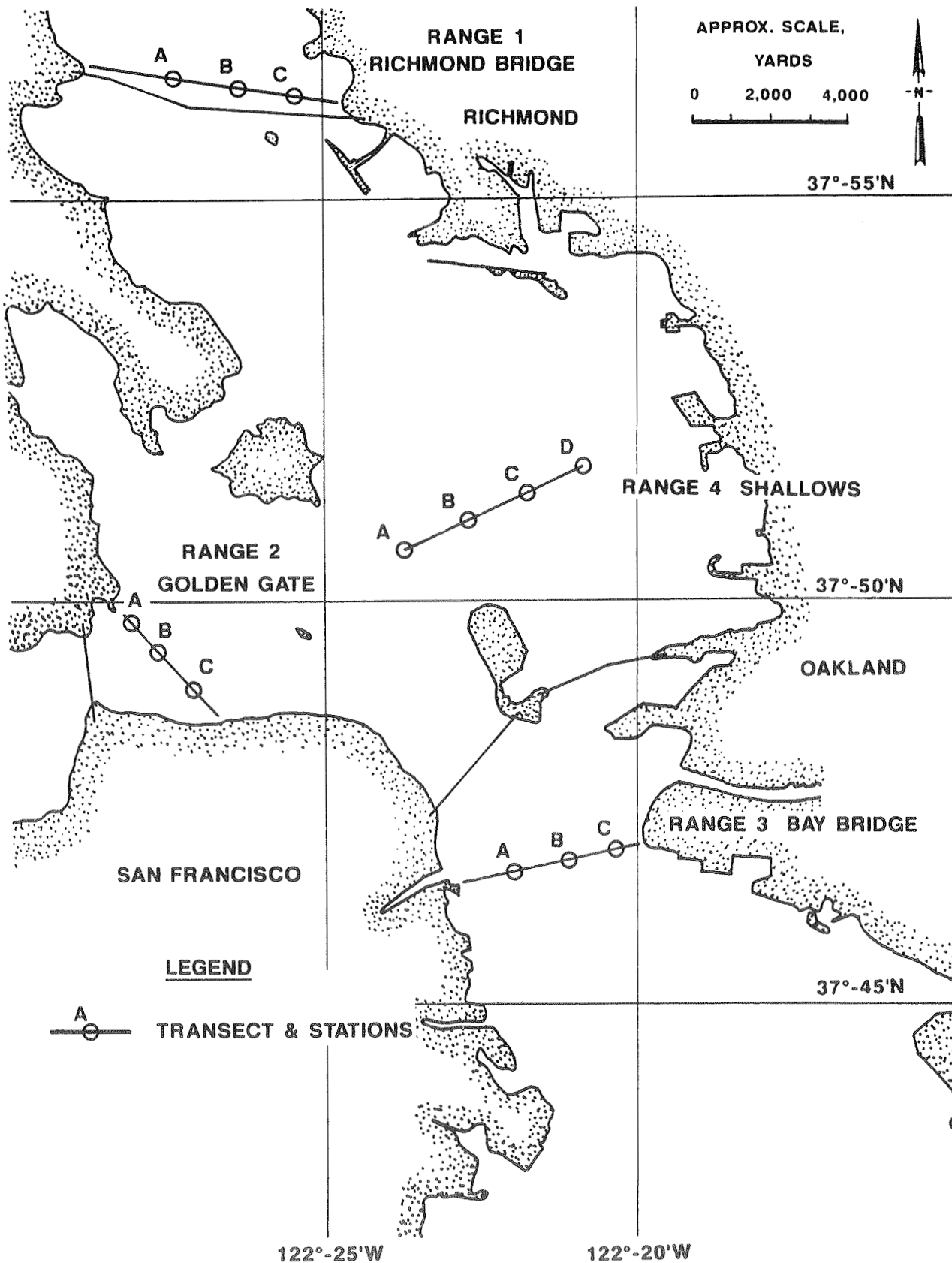
Figure 3. Location of intensive survey transects and stations

Equipment and Collection Methods

12.   This section of the report briefly describes the equipment used in gathering the data. A more specific description of deployment and location, along with other pertinent data, will be given later in this report.

Tidal elevations

13.   Tidal elevations were measured with Fischer and Porter 1550 punched–tape water level recorders (Figure 4). The system consisted of a stilling–well–contained float connected to a recording device by a wire rope. Elevations were recorded to the nearest 0.005 ft. The float elevation was punched on 16–channel, foil–backed paper tape every 15 min by a timer– activated recording mechanism. The 4–in.–diam stilling well was designed to attenuate short–period fluctuations in surface elevation of less than 1 min. Bench tests of the timers have shown them generally accurate to ±2 min per month except for infrequent malfunctions that can cause larger time errors. Relative water level accuracy is affected by the temperature of the water, float, and supporting wire and salinity changes of the water inside the well. Relative accuracy is considered to be within 0.1 ft (Coleman et al. 1988).

Over–the–side equipment

14.   Three of the four survey boats were outfitted with over–the–side equipment consisting of a current meter, direction indicator, wire rope and suspended weight, remote readout device, and a support frame (Figure 5). Cur– rent velocities were measured using a Gurley Model 665 velocity meter with a vertical axis cup–type impeller in conjunction with a Magnesyn directional indicator. This assembly was equipped with a streamlined weight that held the sensors in a vertical attitude facing into the flow. A winch and 1/8–in. wire rope supported by a portable frame was used to raise and lower the assembly (Figure 5). An indicator on the winch showed the sensor depth below the water surface. The Gurley meters have threshold speeds of less than 0.2 fps and an accuracy of ±0.1 fps for speeds less than 1 fps (±5 percent for speeds greater than 1 fps).

15.   Water samples for salinities and total suspended solids were taken with a 12–v d–c pump using 50 ft of 1/4–in. ID plastic tubing attached to the current meter support. Pumps and tubing were flushed with three system vol– umes before individual samples were drawn. The samples and current measure– ments were taken at 3 ft below the surface depth, middepth, and 2 ft above the

13
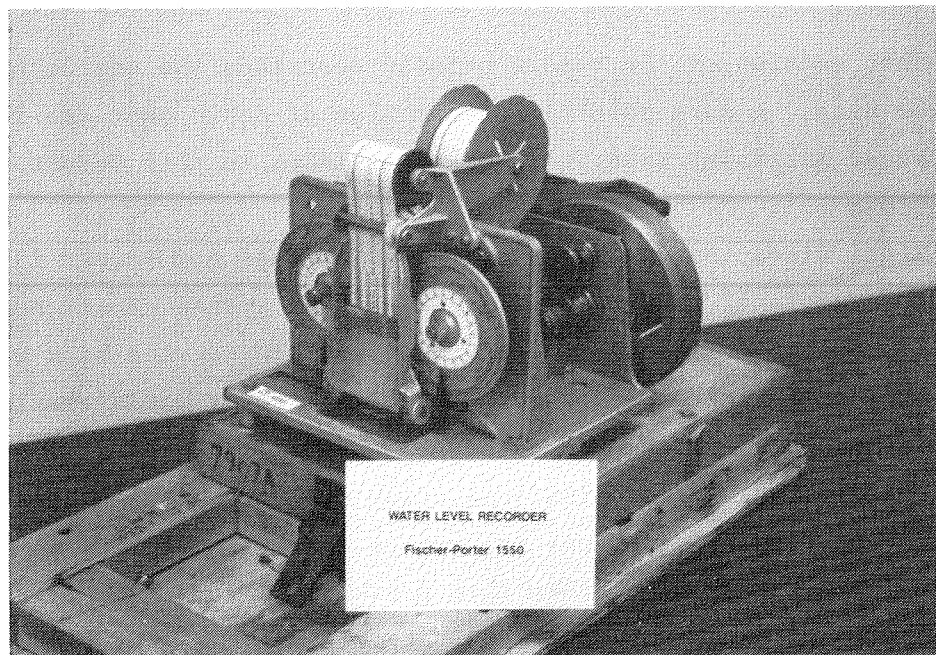
Figure 4.   Fischer and Porter 1550 punched—tape water level recorders
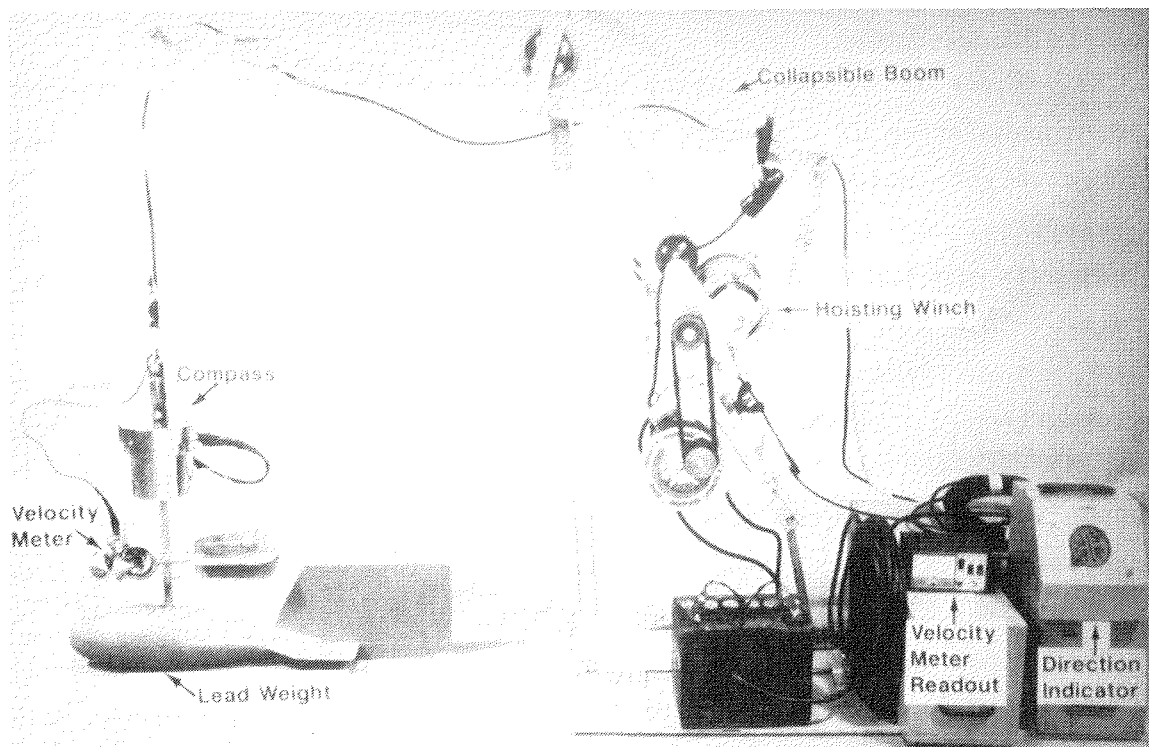
Figure 5.   Over—the—side equipment

bottom at depths less than 35 ft, and at five increments at greater depths. Pumped samples were stored in 8-oz plastic bottles and kept cool (4° C) for shipment back to WES.

Additional equipment used

16.   The fourth survey boat was equipped with an InterOceans Model S-4 velocity meter and 2-ℓ water bottle samplers. This boat was used on the Golden Gate range (Range 2 in Figure 3) to obtain data at depths of up to 200 ft. As the velocity meter was lowered in the water, water bottle samplers were attached to the hydrographic wire. When the velocity meter was at the greatest depth, a messenger weight was sent down the wire to collect a series of water samples.

17.   The InterOceans Model S-4 velocity meter (Figure 6) is another type
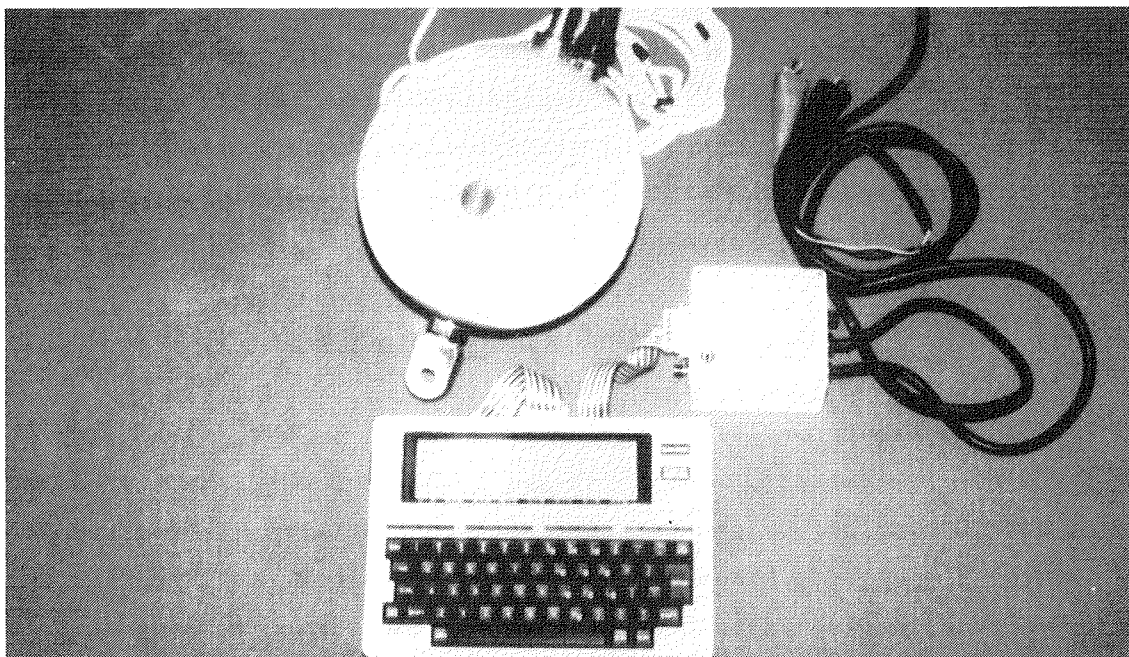
Figure 6.   InterOceans S-4 velocity meter

of over-the-side instrument that measures both current velocity and direction. The 10-in.-diam sphere was used in a tethered configuration so that the variable depth data could be gathered. The device measured the current using an electromagnetic field to sense current induced by the movement of water through the field. A microprocessor coupled with a compass computed referenced current vectors, which were then recorded into the solid-state memory. The data in the memory were periodically loaded onto 3-1/2-in. diskettes using a lap-top computer (Figure 6), and returned to WES for final data reduction.

Synopsis of the Collection Program

18.   Installation of sampling equipment was initiated on 30 August 1988. As described in paragraph 10, during the week preceeding and the week following the intensive survey, point samples were collected at the 15 stations shown in Figure 2 at about 2-day intervals. A total of six sample sets were collected, at arbitrary times usually near slack water. Tide gages were serviced over the same 2-week period.

19.   The intensive survey used four boats to collect data from stations along four separate ranges. Arrangements were made with the San Francisco District Operations Branch to use the 45-ft-long vessel, *GRIZZLY*, in the larger open water areas of the bay. Each range included three stations with the exception of Range 4, which had four stations (Figure 3). Sampling lasted about 25 hr to include one full tidal cycle. Each station was sampled approximately once every hour. This survey design provided synoptic data, which, when compiled, provided the means for verification of a numerical model. The intensive survey began at 0800 PST on 7 September and the final sampling was completed at 1000 PST on 8 September.

Actual Conditions During the Survey

20.   The weather conditions during the overall survey period were cool, breezy, and partly overcast. The worst sea conditions were experienced at the stations adjacent to the Golden Gate Bridge. In that area, late afternoon winds, waves, and current speed and commercial shipping traffic made maneuvering between stations and station keeping difficult. Sampling boat drift was rapid and erratic. For this reason, reliable current measurements could not be made at Range 2. At Range 1 near Richmond Bridge, an anchor line fouled the sampling boat's propeller. Despite the efforts of divers, the boat's maneuverability could not be restored, and only one station (1C) was sampled over the entire survey.

Laboratory Analysis and Data Reduction

21.   Laboratory testing included salinity, TSM, and fall velocity measurement of suspended sediment.

<u>a</u>. Salinities were measured in the laboratory with an AGE Instrument's model 2100 salinometer. Accuracy of the instrument is ±0.003 ppt. Standard seawater, known to better than ±0.001 ppt, was used to calibrate the instrument.

<u>b</u>. TSM was determined by filtration and gravimetric analysis of the samples. Nuclepore polycarbonate filters with 0.40-μ pore size were used. A vacuum system (8-lb vacuum maximum) was used to draw the samples through preweighed filters. After the filters and holders were washed with distilled water, the filters were dried at 105° C for 1 hr and reweighed. Finally, the TSM were calculated based on the weight of the filter and the volume of the filtered sample.

<u>c</u>. Fall velocities were analyzed on a series of composites made on samples from middepth automatic samplers from near the Richmond Bridge. Tests were performed in a 10-cm-diam by 2-m-high clear tube using the pipette method.

22. Data reduction tasks included both transcribing and reformatting raw data, and entering data obtained from both laboratory testing and over-the-side equipment.

Explanation and Selected Samples of the Data

23. The following sections present and describe selected data taken during the survey. In general, most of the data gathered were acceptable; however, as in any large data collection effort, equipment malfunction occurred. Additional stations were included initially to compensate for a possible malfunction of instrumentation. Due to the volume, it was impractical to include all of the data collected in this report; therefore, only a representative sample is presented. The data are on computer file at WES for future reference.

<u>Tide data</u>

24. Figure 7 shows example tide data tabulation and Figure 8 shows a plot of the same data. In the tabulation, a banner is followed by a data listing. Each line lists month, day, year, and sample time for the first data point. The fifth field starts the actual elevation data, in hundredths of feet. Vertical datums were not established for the tide gages.

<u>Over-the-side data</u>

25. Figures 9 through 11 show plots of current speed, salinity, and TSM, respectively. Each shows surface, middepth, and bottom time-series data. Figure 12 shows the depth- and tidal-averaged TSM values for the intensive

17

```
BEGINBANNER
PROJECT          : SAN FRANCISCO BAY
LOCATION         : COAST GUARD DOCK
STATION ID       : TG#1
TYPE DATA        : Tide
UNITS            :  hundrthft
INSTRUMENT TYPE  : papertape
SERIAL NUMBER    : A0610M2
TIME ZONE        : PST
DAYLIGHT SAVINGS : no
SAMPLE INTERVAL  (MINUTES) :  15
DEPLOYED         :  9/ 2/88  945
RECOVERED        :  9/15/88 1145
MEDIA CONVERSION :  9/23/88 1400
REMARK : 9/2=GR 10.01';9/15=GR 12.74'
CNV-REMRK : smpls=    1267., ntgrty=       0., tmo=       1., ovr=       0.
ENDBANNER
 9 288 945 1002 1009 1012 1021 1032 1052 1058 1072 1082 1100
 9 2881215 1122 1145 1160 1180 1199 1217 1230-9999-9999-9999
 9 2881345 1230 1250 1270 1286 1301 1311 1315 1319 1323 1323
 9 2881615 1322 1315 1302 1283 1272 1249 1226 1201 1174 1143
 9 2881845 1109 1071 1044 1012 0978 0946 0918 0893 0868 0844
 9 2882115 0821 0799 0782 0776 0757 0742 0738 0739 0733 0727
 9 2882345 0728 0738 0747 0756 0773 0790 0805 0820 0839 0860
 9 388 215 0883 0903 0923 0938 0958 0984 1006 1023 1038 1057
 9 388 445 1073 1083 1098 1109 1117 1124 1129 1130 1130 1127
 9 388 715 1127 1127 1116 1112 1105 1095 1084 1076 1072 1062
 9 388 945 1055 1049 1044 1038 1038 1039 1044 1045 1056 1060
 9 3881215 1071 1079 1090 1103 1118 1134 1149 1166 1186 1200
 9 3881445 1209 1226 1245 1258 1267 1279 1289 1295 1299 1299
 9 3881715 1300 1290 1285 1273 1259 1244 1223 1201 1175 1140
 9 3881945 1104 1074 1045 1019 0986 0954 0923 0893 0870 0849
 9 3882215 0823 0799 0787 0767 0752 0739 0730 0727 0724 0719
 9 488  45 0718 0722 0731 0741 0753 0770 0785 0800 0817 0840
 9 488 315 0864 0886 0906 0930 0950 0969 0994 1012 1038 1055
 9 488 545 1072 1090 1101 1115 1128 1137 1146 1152 1153 1158
 9 488 815 1158 1152 1149 1143 1136 1131 1123 1114 1108 1098
 9 4881045 1092 1080 1068 1065 1062 1058 1058 1058 1060 1063
 9 4881315 1067 1080 1088 1096 1113 1130 1140 1155 1171 1188
 9 4881545 1201 1216 1231 1246 1264 1268 1278 1288 1296 1299
 9 4881815 1299 1300 1292 1282 1271 1257 1238 1218 1190 1163
 9 4882045 1131 1101 1074 1036 1005 0972 0940 0912 0885 0859
 9 4882315 0833 0814 0793 0778 0755 0738 0734 0724 0723 0722
 9 588 145 0722 0723 0725 0736 0750 0770 0791 0808 0825 0850
 9 588 415 0868 0890 0916 0939 0967 0988 1009 1032 1053 1075
 9 588 645 1095 1110 1133 1145 1158 1166 1176 1182 1189 1194
 9 588 915 1189 1189 1178 1172 1168 1159 1145 1135 1127 1112
 9 5881145 1101 1085 1075 1068 1060 1049 1045 1045 1050 1051
 9 5881415 1055 1062 1074 1084 1092 1108 1128 1140 1156 1175
```

Figure 7. Example tide data tabulation

18

SAN FRANCISCO BAY — COAST GUARD DOCK — TG#1

Tide height — (Ft)

Elapsed time, hrs
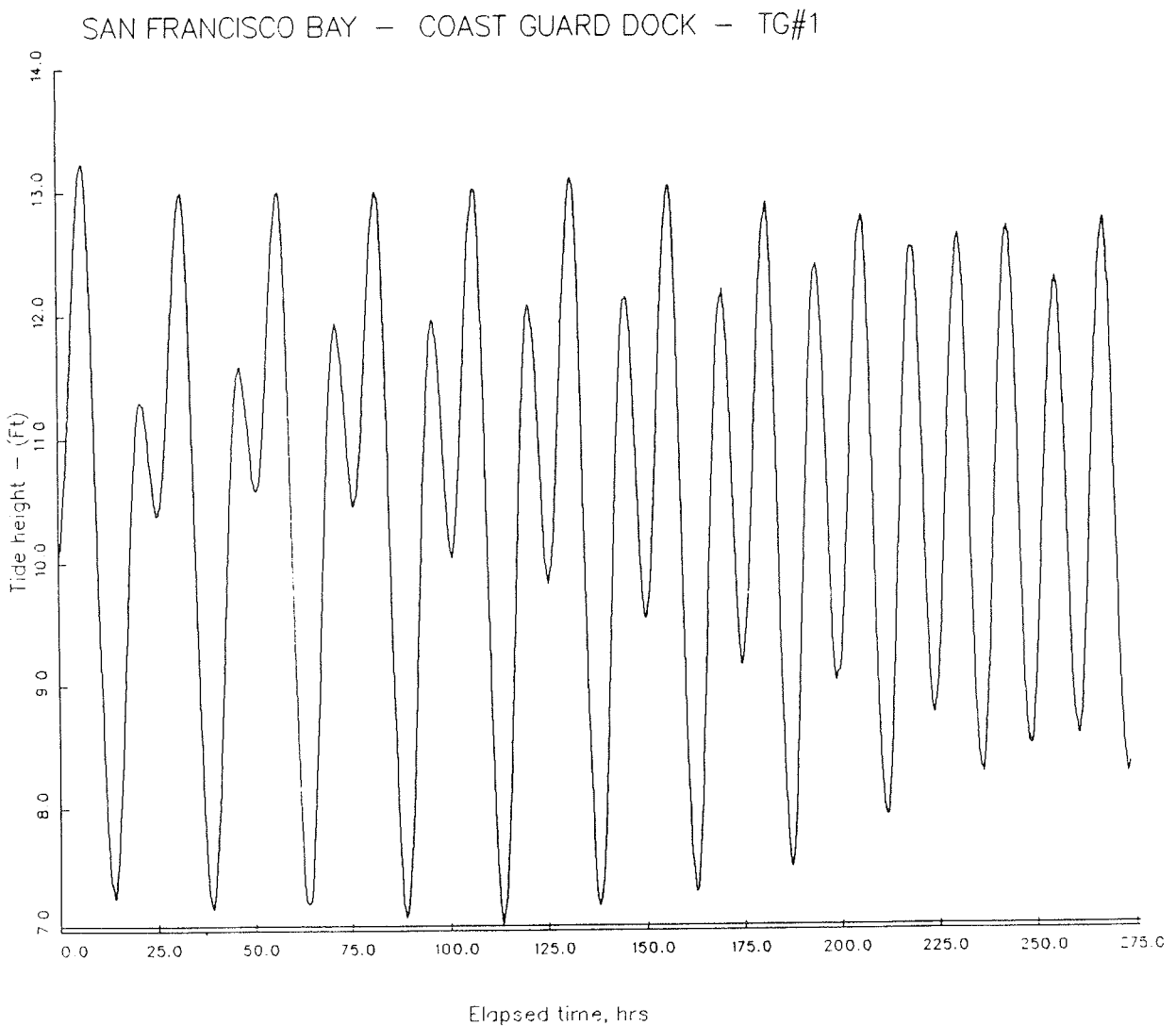
Figure 8. Example tide data plot

survey. Figure 13 shows the depth- and tidal-averaged salinity values for the intensive survey.

Point TSM data

26. Figure 14 shows averages and standard deviations for six sampling periods made between 28 August and 23 September 1988.
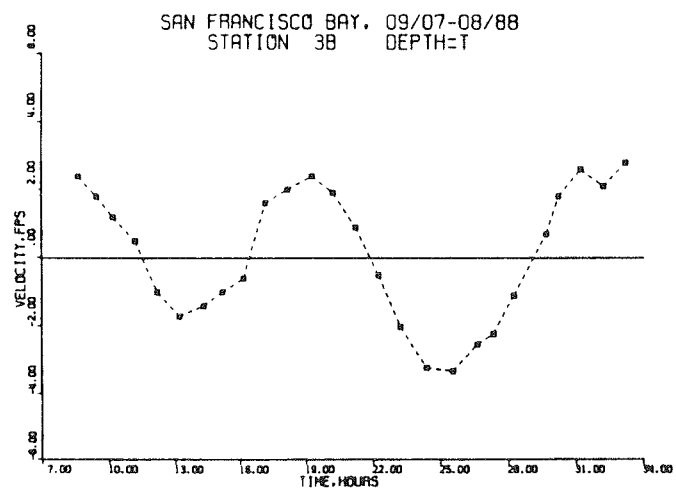
Figure 9. Surface, middepth, and bottom
current speed at sta 3B

20

SAN FRANCISCO BAY, 09/07-08/88
STATION 1C   DEPTH=S

SAN FRANCISCO BAY, 09/07-08/88
STATION 1C   DEPTH=M

SAN FRANCISCO BAY, 09/07-08/88
STATION 1C   DEPTH=B
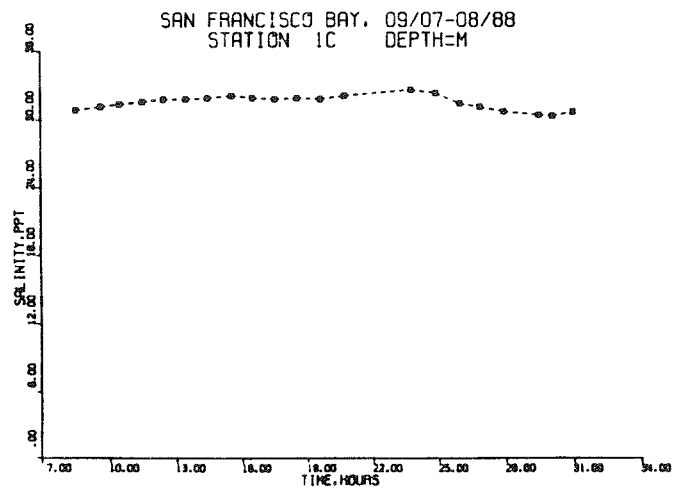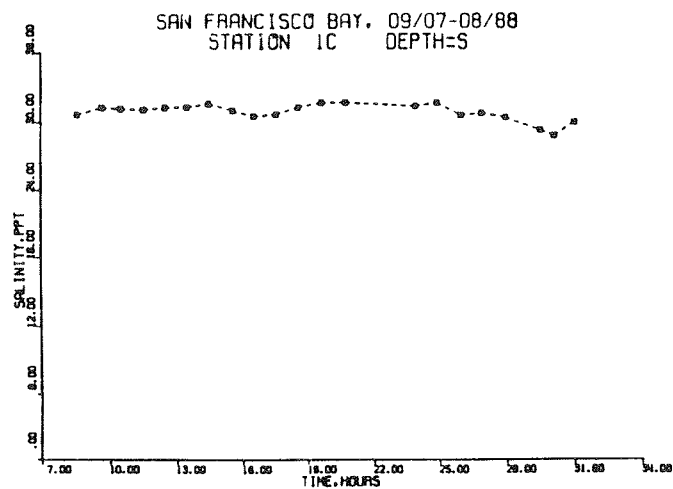
Figure 10. Surface, middepth, and bottom
            salinities at sta 1C

21

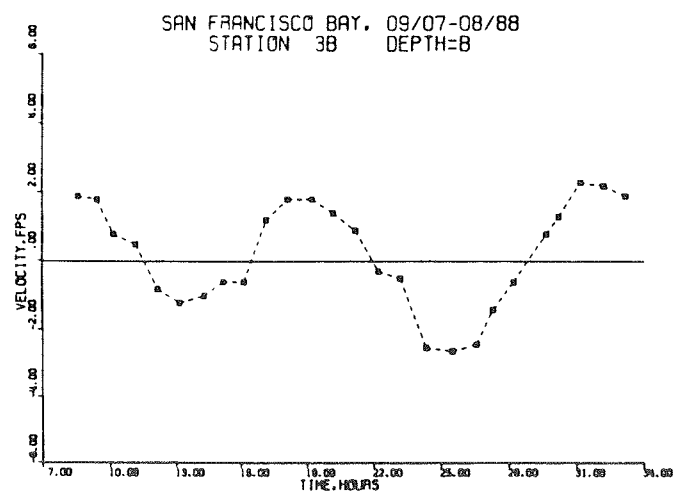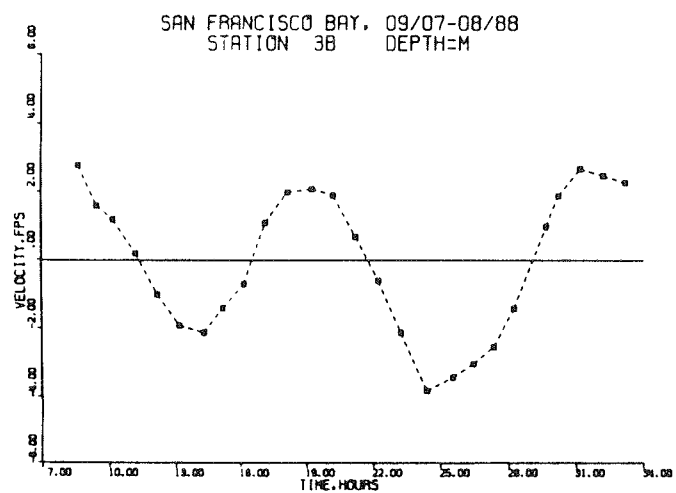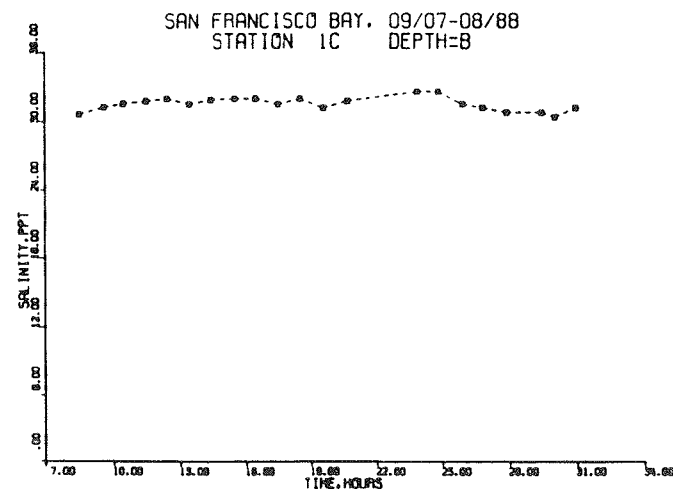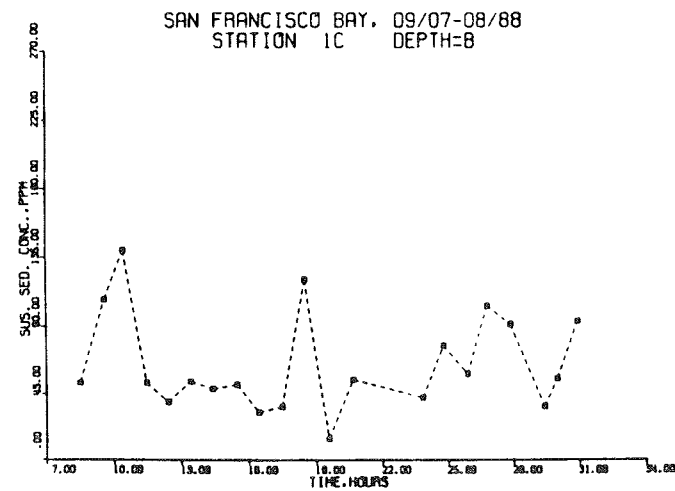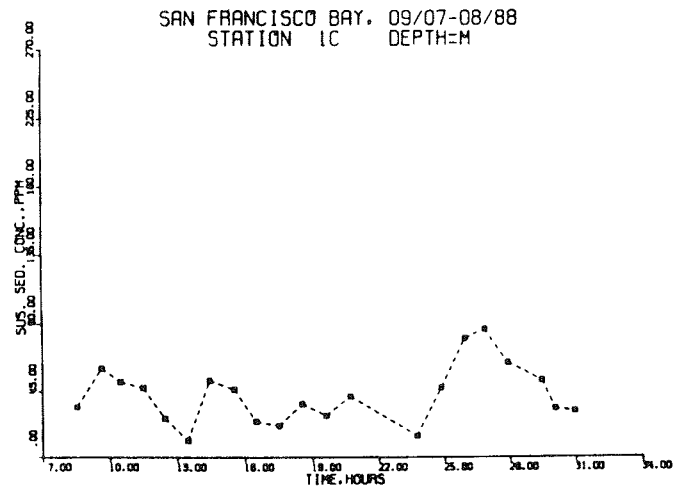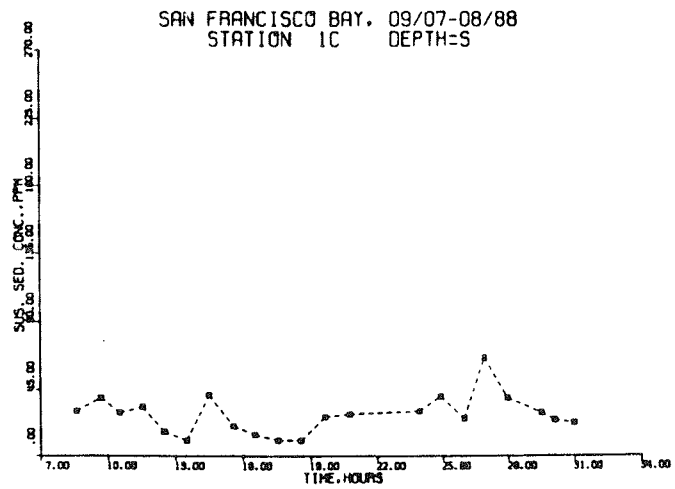Figure 11.   Surface, middepth, and bottom
TSM at sta 1C

22
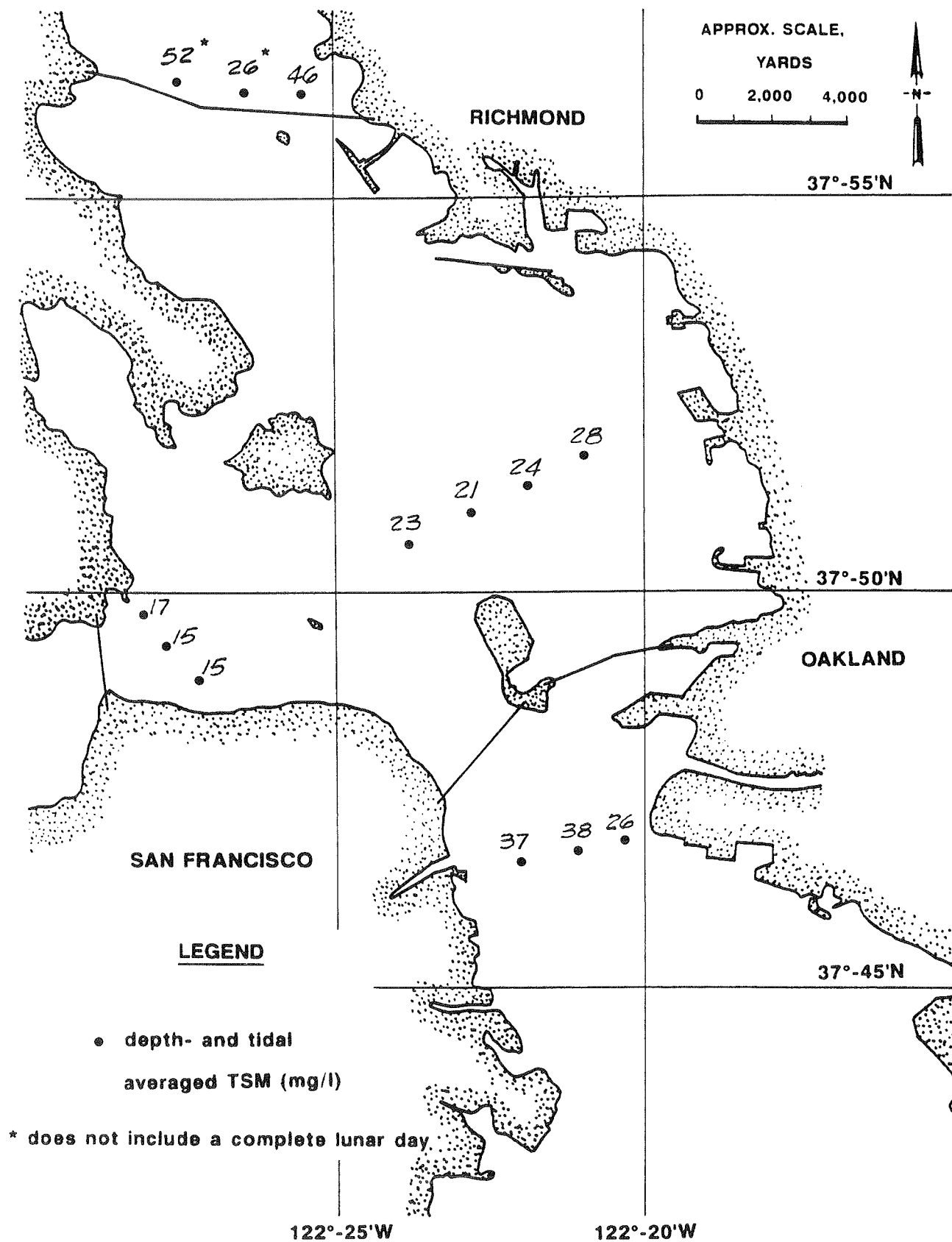
Figure 12. Depth- and tidal-averaged TSM values for the intensive survey
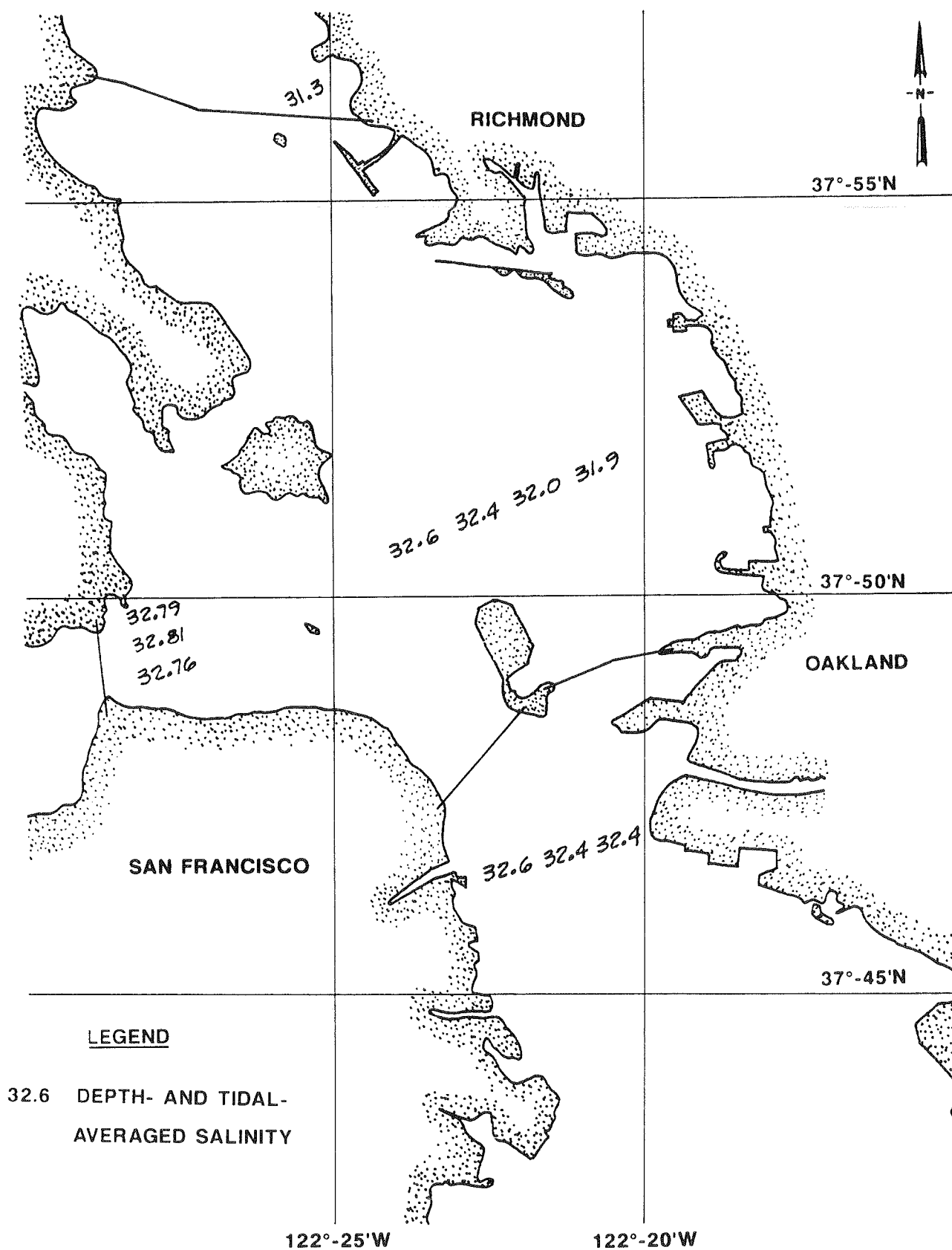
Figure 13. Depth- and tidal-averaged salinities for the intensive survey

24
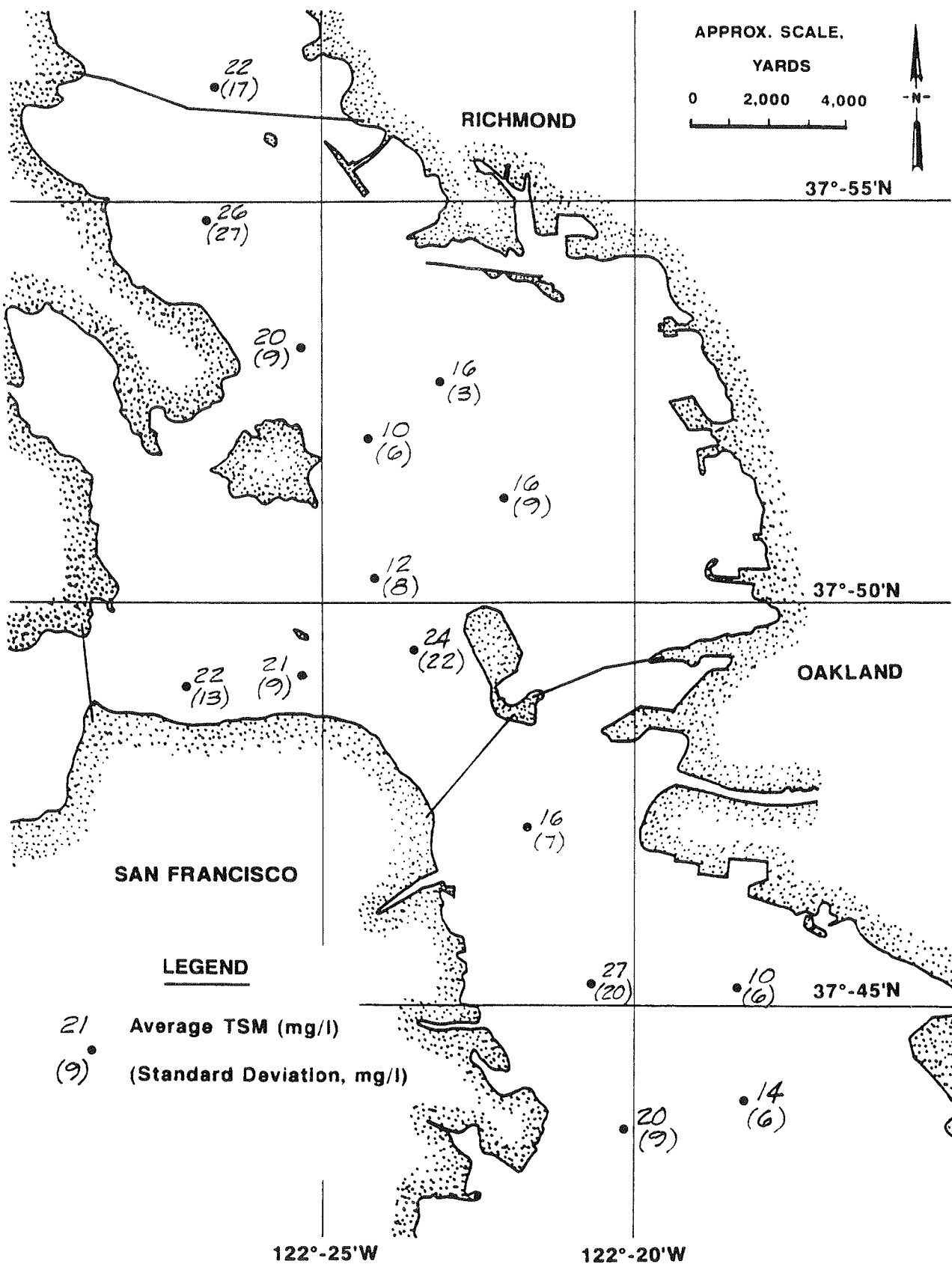
Figure 14. Point sample average TSM and standard deviations

25

PART III: INITIAL PROCESS ASSESSMENT

27.   The long-term fate of fine-grained materials dispersed from the Alcatraz disposal site depends on sediment interactions with flows and individual particle sojourns through the Central Bay area.   This part summarizes initial interpretations of field data related to dry weather seasonal long-term sediment transport in Central Bay.   The field data described in the previous part will be further analyzed here.   Some previous studies that have quantified some relevant aspects of transport processes will also be summarized.

28.   Studies on the movements of natural sediments can be useful to assess the effects of dredged material dispersion from the Alcatraz disposal site.   Measures or parameters are sought that will help answer the following questions:

a.   What is the local flushing rate for the sediments dispersed from the Alcatraz site in Central Bay?   (How fast do sediments move away from the site, and therefore, what is the local buildup of suspended sediments?)

b.   Where are dispersed sediments transported?   (What is the distribution probability of the dispersed materials?)

c.   What is the fate of the dispersed sediments?   (How much deposits in or is transported through various segments of the Central Bay area?)

29.   The present study estimated field sediment fluxes entering and leaving Central Bay by direct observation of suspended transport over a tidal cycle.   The sampled net transport was generally in the landward direction, but net transport was a small fraction of the tidal transport.   It will be shown in this part that the dominant transport mechanism was tidal pumping, and that near-bed currents are very important in this process.   Previous studies have examined tidal-averaged current and bed form patterns.   Those studies have shown variability in Central Bay, with some areas being flood dominated with respect to maximum near-bed currents, and other areas being ebb dominated.

30.   Sediment budget approaches based on changes in bay volumes or input and output accounting have also been used to assess long-term sedimentation in San Francisco Bay.   These studies have been concerned with annual or longer time scales.   Since the purpose here is to examine only dry weather seasonal long-term transport, annual sediment budgets will not be discussed.

31.   The reader is referred to the bibliography in Appendix A for

specific articles on San Francisco Bay sediments. This bibliography includes references on baywide sedimentation, including such topics as the influence of hydraulic mining in the 1800's on riverborne sediment to the bay, the use of various sediment tracers, and global sediment budgets for the bay. However, this bibliography is not intended to be exhaustive.

Baywide Suspended Sediment Behavior

32. In the San Francisco Bay system, sedimentation and suspended sediments have received only limited attention compared to other parameters and hydrographic variables such as water levels, currents, and salinity. Most field surveys have either not included sediment and suspended sediment measurements or have not emphasized such measurements. The complexity of suspended sediment movement in an estuarine environment makes quantitative study of sediment movement a difficult and costly undertaking. However, ample evidence does exist to provide qualitative understanding of sediment and suspended sediment behavior.

33. General agreement exists among most researchers regarding the qualitative behavior and characteristics of riverine sediment loading to the estuary including aggregation, deposition, suspension, erosion, and circulation of sediments in the San Francisco Bay system. To provide background to baywide suspended sediment behavior, a synopsis of some of the available literature on general baywide sediment is provided.

34. In a study of sedimentation in Mare Island Strait, an artificially deepened portion of the lower Napa River at Carquinez Strait, Einstein and Krone (1961) reported on the seasonal sediment pattern in the San Pablo Bay-Carquinez Strait study area. Einstein and Krone, through field observations, determined that despite higher suspended sediment concentrations in bay waters in the winter, much of the deposition in Mare Island Strait occurred during the summer. They concluded that deposition during the winter occurs in the shallow bays and mud flats. The almost daily summer patterns of high mid-morning to late afternoon winds produce wave action that resuspends these winter-deposited sediments. Once the sediments are resuspended, ambient currents move them to relatively quiescent areas such as Mare Island Strait, resulting in deposition in these areas.

35. These early observations by Krone and Einstein have been

substantiated by subsequent research and field data evaluation, and a baywide sediment transport pattern similar to the Mare Island Strait results emerges from the literature. See, for example, Conomos and Peterson (1976), Krone (1976, 1979), and US Army Engineer District (USAED), San Francisco (1977).

36. Approximately 80 to 85 percent of the riverborne sediment to San Francisco Bay originates from the Sacramento-San Joaquin River basin and over 80 percent of this riverborne sediment is contributed during the period of high freshwater inflow in winter and early spring. Furthermore, the measured suspended sediment concentrations reported in Conomos and Peterson (1976) indicate a strong pattern of maximum suspended sediment levels in San Pablo and Suisun Bay areas (the null zone is normally located in either of these bays), the lowest levels near the Golden Gate in Central Bay, and somewhat elevated levels in South San Franciso Bay (South Bay). The seasonal patterns reported by all researchers was riverborne sediment supply and deposition during the winter and sediment resuspension, transport, and redeposition during the summer.

Tidal and Net Fluxes of TSM

37. To evaluate the transport at the boundaries of Central Bay, tidal and net TSM fluxes were computed using the intensive survey data from Ranges 1-3. Not all data sets contained sufficient information with which to make the calculation using the most accurate method. For this reason, computations were made using several methods for comparison. Tidal suspended sediment fluxes were calculated by three methods (direct, decomposition, and tidal prism). Results are presented in Table 1. The most accurate method is the direct method. The direct method calculated average instantaneous fluxes as the product of currents, TSM concentrations, and cross-sectional areas corrected for instantaneous tide height. These results were then integrated over the lunar sampling day. This method calculated vertical averages by weighting the middepth values twice that of the surface and bottom values. The values used for the surface and bottom were actually measured 2 ft down from the surface and 2 ft up from the bottom, respectively. Only Range 3 had a complete data set. Current and TSM data from sta 1C were applied to the entire cross section for Range 1, because only partial data were collected at sta 1A and 1B. Average TSM data for the beginning of the intensive survey were

Table 1

TSM Conditions and Fluxes (Positive = Landward)

Range	Tidal Phase	TSM mg/ℓ	TSM Flux, 1,000 metric tons/lunar day for Method*		
			Direct	Decomposition	Tidal Prism
1	Ebb	44.9	−48	−	−58
(Richmond	Flood	37.5	39	−	49
Bridge)	Net		−9	−37	−9
2	Ebb	14.9	−**	−**	−41
(Golden	Flood	16.3	−	−	45
Gate)	Net		−	−	4
3	Ebb	33.7	−18	−	−29
(Oakland	Flood	36.1	19	−	32
Bay	Net		1	−4	3
Bridge)					

  * See paragraphs 37–40 for explanation.
 ** Unreliability of current measurements at sta 2 prevents evaluation.

comparable at sta 1A, 1B, and 1C. However, the validity of the flux calculation at Range 1 is questionable.

38. The decomposition flux calculation method averaged instantaneous flux per unit areas over the lunar day. Various flux components were calculated as described later in paragraphs 41–43 and summed to a total. The total average flux per unit area multiplied by the average cross section and integrated over the lunar day provided the decomposition method estimate of net TSM flux (Table 1). Ebb and flood fluxes are not available from this method.

39. A tidal prism method was also used to calculate TSM fluxes from ebb and flood tidal prisms and average TSM concentrations. This was the only possible method for Range 2, where current data were lacking. Surface areas for the Central and South Bays were estimated by planimetering National Ocean Service (NOS) nautical charts. Total surface area and tidal prism estimated by a cubature method for the San Francisco Bay system were calculated for an average tide (NOS 1985). The total tidal prism for the bay system for the survey was estimated by tide-range ratio. Then, tidal prisms passing through the various survey ranges were estimated for the observed tide by subtracting various tidal prism segments from the total. Areas, widths, and tidal volumes

passing survey ranges during the intensive survey are given in the following tabulation:

Range	Cross-Sectional Area, m²	Width, m	Tidal Volumes, 10⁹ cu m		
			Flood	Ebb	Average
1	53,800	5,940	1.30	1.28	1.29
2	117,000	3,750	2.75	2.71	2.73
3	66,100	4,500	0.88	0.87	0.87

40.   There was a substantial variation between direct and tidal prism estimates of tidal fluxes, possibly caused by an overestimation of tidal prisms. Tidal prism flux results averaged 44 percent greater than those of the direct method. Range 3 had the best data coverage for any range. The direct method estimate of 1,000 metric tons landward net flux is only a small percentage of the 18,000-19,000 metric ton tidal flux. The tidal prism method gave similar, though larger, values for flux at Ranges 1 and 3. Thus, tidal flux at Range 2 adjusted for the tidal prism method's overestimation was probably about 30,000 metric tons. The decomposition method result at Range 3 was not consistent with other methods, but differences with the direct method were still small in the absolute sense.

Flux Components for TSM

41.   A flux decomposition method was used to examine transport components at individual stations, as well as to estimate total tidal flux as described earlier. Tidal fluxes of TSM were decomposed based on the following equation:

$$\text{Flux of } C = A(\overline{U_o}\,\overline{C_o} + \overline{U_i C_i} + \overline{U_{ov} C_{ov}} + \overline{U_{iv} C_{iv}}) \tag{1}$$

where

C = concentration

A = cross-sectional area

overbar = depth average

U = velocity

o = steady (tidal-averaged)

i = fluctuating component

v = vertical deviations from the depth mean

30

Tidal average values for each of the four terms inside the parentheses were calculated from intensive survey data. The first term is mean-flow transport. The second and fourth terms are tidal pumping components. The third term is transport by vertical circulation.

42. TSM flux decomposition results are shown in Table 2. Also included in Table 2 are the principal salinity flux component, $\overline{U_o}\overline{S_o}$, and salinity and TSM flux totals. Note that all other salinity flux terms were of minor importance, and that, except for mean-flow transport, salinity conditions were nearly balanced. Analysis of several weeks of salinity samples also indicated that salinity conditions were steady. The mean flow component, $\overline{U_o}$, does not always represent a true tidal residual flow and can be influenced by sampling bias.

43. The most important or dominant flux component was $\overline{U_{iv}C_{iv}}$, the tidal pumping component involving vertical deviations in instantaneous or fluctuating fluxes. Near-bed TSM fluctuations were the greatest, as shown in the example (Figure 11). The pattern of net TSM flux suggested by the decomposition totals is indicated in Figure 15.

Table 2

Station Average Flux Components (Positive = Upstream)

Range	Station	Salinity Flux fps × ppt*		TSM Flux, fps × mg/ℓ				
		$\overline{U_o}\overline{S_o}$	Total	$\overline{U_o}\overline{C_o}$	$\overline{U_iC_i}$	$\overline{U_{ov}C_{ov}}$	$\overline{U_{iv}C_{iv}}$	Total
1	C	0.00	1.07	0.0	−9.13	−0.06	−28.28	−37.47
3	A	4.23	4.68	4.79	0.77	0.21	−8.07	−2.30
	B	6.37	6.36	7.68	2.41	1.73	−28.30	−16.48
	C	10.90	10.80	8.68	1.59	−0.13	0.60	10.74
4**	A	−0.35	−0.59	−0.25	7.71	−0.13	−33.16	−25.84
	B	3.62	3.47	2.36	1.68	0.15	−15.92	−11.72
	C	3.34	3.55	2.39	1.80	0.05	−3.36	0.88
	D	4.54	4.67	3.88	2.34	0.09	1.26	7.57

* 1 fps = 0.305 m/sec.
** Positive = south.
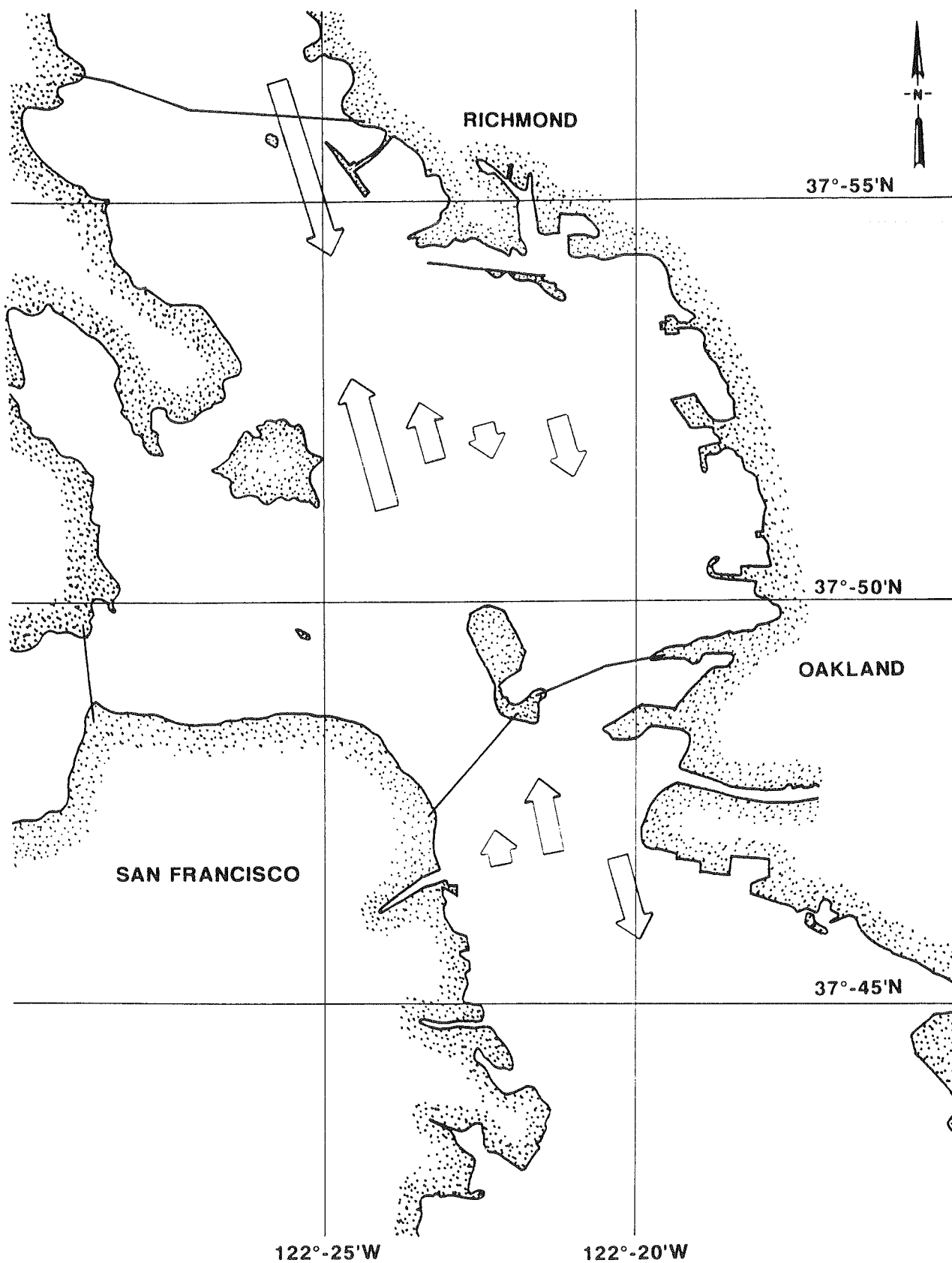
Figure 15.   Relative TSM net fluxes according to station flux
decomposition data

32

44. Certain trace metals were analyzed on the suspended material collected on filters during TSM sample analysis. All filters from each range were divided into ebb and flood composites for analysis. Thus each composite was made up of roughly 100 filter subsamples. Raw trace metals on TSM and normalized trace metals on TSM are given in Tables 3 and 4, respectively. The trace metals manganese (Mn), zinc (Zn), copper (Cu), and nickel (Ni) were normalized with reference to iron (Fe).

45. Trace metals on suspended matter can indicate their source, circulation, and sediment dynamic history. The trace metal iron is enriched in riverborne particles relative to marine particles, and occurs at 5-7 percent by dry weight (Eaton, Grant, and Gross 1980). Dissolved iron becomes bound to particulates at low salinities, and total iron remains conservative through estuarine systems. Ratios of manganese, zinc, and other trace metals have

Table 3

Trace Metals on TSM

Range	Tidal Phase	Concentration, mg/g dry weight				
		Fe	Mn	Zn	Cu	Ni
1	Flood (F)	61.4	1.06	0.142	0.092	0.138
	Ebb (E)	60.0	1.02	0.185	0.087	0.133
	(F − E)	1.4	0.04	−0.043	0.005	0.005
2	Flood	41.0	0.816	−	0.083	0.101
	Ebb	44.8	0.872	0.178	0.076	0.106
	(F − E)	−3.8	−0.056	−	0.007	0.005
3	Flood	44.4	0.843	0.152	0.069	0.107
	Ebb	42.5	0.854	0.149	0.067	0.121
	(F − E)	1.9	−0.011	0.003	0.002	−0.014
4	Flood	39.8	0.686	0.139	0.057	0.092
	Ebb	46.4	0.828	0.175	0.069	0.107
	(F − E)	−6.6	−0.142	−0.036	−0.008	−0.015

Table 4

Normalized Trace Metals on TSM

Range	Tidal Phase	Fe mg/g dry weight	Trace Metal Ratios			
			Mn/Fe	Zn/Fe	Cu/Fe	Ni/Fe
1	Flood	61.4	0.0173	0.0023	0.0015	0.0022
	Ebb	60.0	0.0170	0.0031	0.0015	0.0022
2	Flood	41.0	0.0199	–	0.0020	0.0025
	Ebb	44.8	0.0195	0.0040	0.0017	0.0024
3	Flood	44.4	0.0190	0.0034	0.0016	0.0024
	Ebb	42.5	0.0201	0.0035	0.0016	0.0028
4	Flood	39.8	0.0172	0.0035	0.0014	0.0023
	Ebb	46.4	0.0178	0.0038	0.0015	0.0023

been used to examine the origins of estuarine particulates. Helz et al. (1985) gave the following ratios for zinc and manganese:

Source	Mn/Fe	Zn/Fe
Continental crust	0.017	0.0012
Sedimentary rock	0.020	0.0028
Soils	0.022	0.0013

46. Dissolved manganese is high (3–12 mg/ℓ) in bed pore water, and increases in the flow where resuspension occurs (Morris, Bale, and Howland 1982). Thus manganese is nonconservative due to remobilization of dissolved manganese from bed sediments. Manganese returns to bed sediments by the deposition of suspended sediments. The fraction of manganese in fine silts and clay (<16 μ) has been found to be a constant for a particular sediment source and may vary between sources (deGroot 1964).

47. Only a few inferences can be drawn from the trace metals data presented in Tables 3 and 4. The strongest riverine influence was detected at Range 1, as indicated by the highest iron concentrations (6 percent by dry weight). Particulate iron was not conservative with respect to the fraction of fresh water as suggested for other estuarine systems. The influence of an

alternate sediment source (nonriverine) is indicated for Ranges 2-4 where particulate iron was appreciably reduced. The origin of the alternate sediment source and the extent of its influence could not be determined from the data. Estuarine and oceanic sediments are both possible sources.

Near-Bed Transport Inferred from Bed Forms

48. The net direction of bottom sediment transport was determined in a previous study (Rubin and McCulloch 1979) using observations of the movements and shapes of sand bed forms. A 100-kHz side-scan sonar was towed along known tracks to detect bed forms. Some track lines were repeated over several tidal cycles, and some fixed points were monitored over longer periods. However, the exact dates of various surveys were not reported, and it is not known whether these conditions vary between summer and winter conditions, or with tidal conditions.

49. Transport directions were inferred from the orientations of crests and asymmetry of sand waves. Sand ripples were too small to detect. Sand waves covered about half of the area in depths greater than about 10 m in Central Bay. Flat bed was the second most abundant form. Flat beds were bare rock areas near the Golden Gate and low-velocity areas along the eastern edge of Central Bay. Transport directions based on sand wave migration direction were determined for the areas of sand waves. Figure 16 shows a plot of the results. Arrows indicate direction of dominant transport (not magnitude), and lines indicate boundaries between ebb- and flood-dominated areas. The patterns indicated in Figure 16 are consistent with a flood-dominated channel area east of the Golden Gate flanked by ebb-dominated areas to the north and south. The Golden Gate appears to contain a convergence zone in the south and a divergence zone in the north.

50. The Alcatraz disposal area is indicated as ebb dominated. Previous corings at the Alcatraz disposal site indicated a westward encroachment of sand in the sedimentation record.* As presented later, various current velocity studies confirm the Alcatraz disposal area to have ebb-dominant maximum currents.

---

* R. Farmer. 1985. "Geotechnical Investigation, Alcatraz Disposal Site, San Francisco Bay, California," Draft Report, US Army Engineer District, San Francisco, San Francisco, CA.
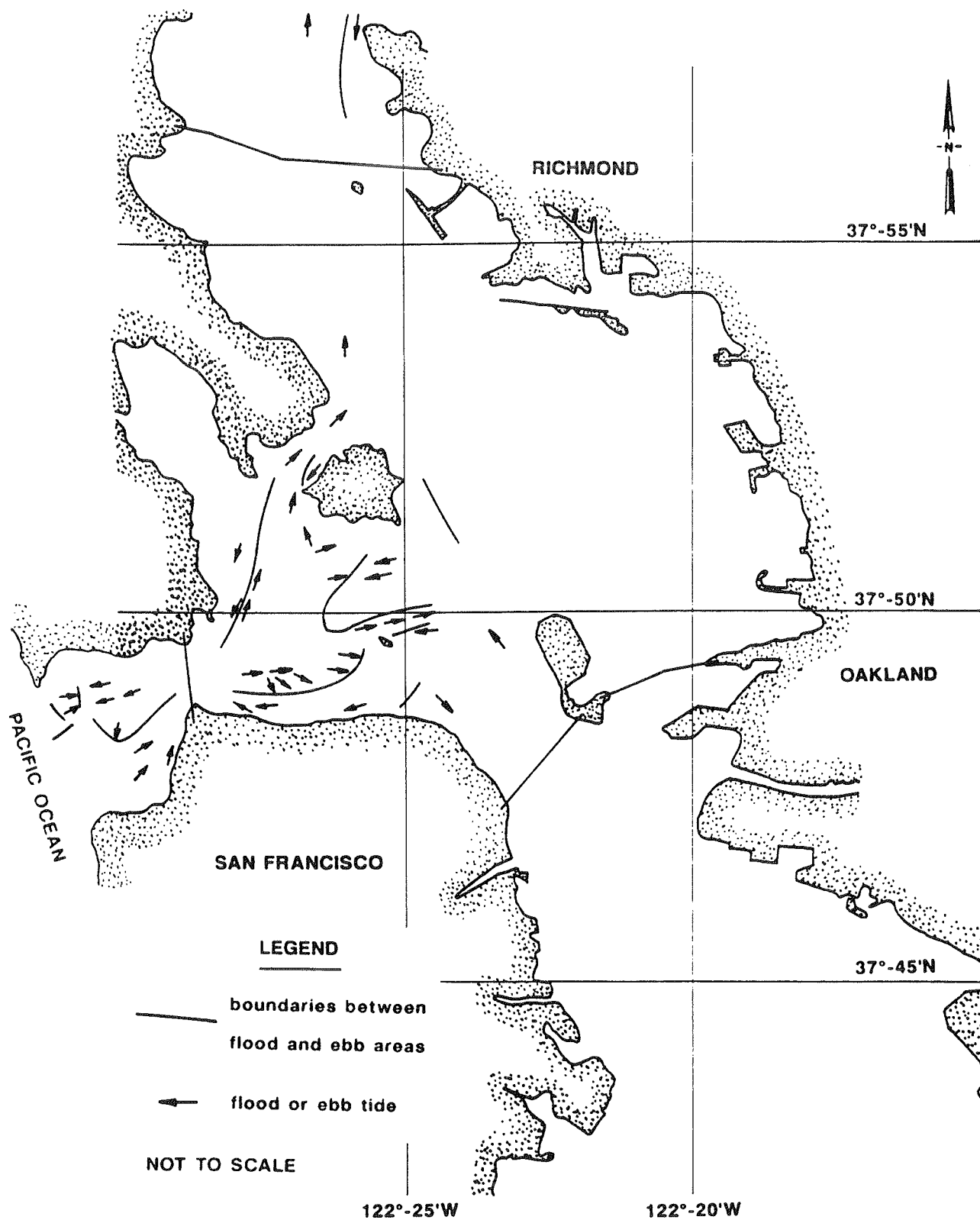
Figure 16. Direction of near–bottom current maximums

36

<u>Near-Bed Current Dominance</u>

51. Winzler and Kelly (WK) (1985), Science Applications International Corporation (SA) (1987a and 1987b), and the US Geological Survey (USGS) (Cheng and Gartner 1984) have previously reported on near-bed currents based on field programs. WK and SA studies were commissioned by the San Francisco District, and their measurements were carried out near the Alcatraz disposal site. USGS made measurements throughout the San Francisco Bay system, including Central Bay.

<u>Alcatraz disposal site area</u>

52. WK performed current measurements between 5 and 11 July 1985. Four current meter arrays, designated WK-A, WK-C, WK-D, and WK-E were deployed within a 1,500-ft radius of the Alcatraz disposal site. Sta WK-A was located at the center of the site, and sta WK-C through WK-E were located at the east, south, and west compass points of the site perimeter, respectively. A fifth array (WK-F) was located 900 ft westward from the west edge of the disposal site. At each array Aanderaa RC-4 current meters were positioned at a 4-m depth, middepth, and 1.5 m off the bottom. At sta WK-A an additional instrument system consisting of a wave recorder, electromagnetic current meter, and transmissometer was deployed 0.75 m above the bottom.

53. Table 5 presents means and 5 percent exceedences for flood and ebb current speeds measured by the WK current meters. In all cases the ebb current speeds are greater than flood speeds.

54. SA performed current measurements near the Alcatraz disposal site between 4 July and 10 December 1986. General Oceanics 6011 MKI current meters (Niskin standard wing-type recording tilt) were deployed 1.5 m above the bed at three stations: SA-E (east); SA-W (west); and SA-S (south). The same type meters were deployed at 2-m depth, 12-m depth, and 1.5-m above the bed at sta SA-3M. A Sea Data electromagnetic current meter and Sea Tech transmissometer were deployed at sta SA-tripod 1.5 m above the bed. See Figure 17 for current meter locations.

55. Table 6 presents 5 percent exceedence maximum currents. Ebb current speeds are generally greater than corresponding flood current speeds, although at SA-S and SA-3M (bottom), maximum ebb and flood current speeds are similar. Sta SA-W was located west of the disposal site and recorded

Table 5

Currents Near Alcatraz Disposal Site

14-21 July 1985 (Winzler and Kelly 1985)

| Station (Station Depth) m	Position Meter	Depth m	Current Speed, cm/sec			
			Flood		Ebb	
			5% Exceeded	Mean	5% Exceeded	Mean
WK-A	Top	4	80	51	114	62
(13.7)	Middle	6	77	50	104	59
	Bottom	12	67	43	86	48
	Tripod	13	62	40	83	44
WK-C	Top	4	81	51	123	64
(12.5)	Middle	6	95	56	130	71
	Bottom	11	70	43	90	50
WK-D	Top	4	90	57	125	65
(21.0)	Middle	10	93	63	129	74
	Bottom	20	54	37	71	40
WK-E	Top	4	64	33	73	36
(16.5)	Middle	8	87	57	116	67
	Bottom	15	60	38	68	40
WK-F	Bottom	23	36	20	40	21
(24.7)						
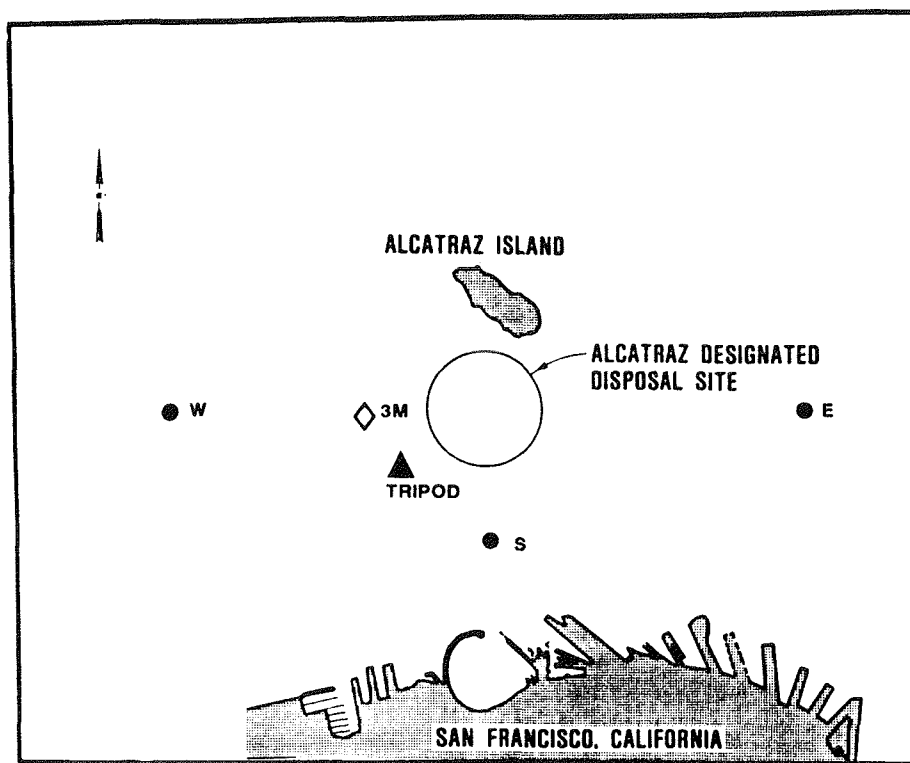
Figure 17. SA current meter locations

Table 6

Current Near Alcatraz Disposal Site

4 July–10 December 1986 (SA 1987a)

Sta	Position	Current Speed, cm/sec, at 5% Exceedence							
		Flood				Ebb			
		7–4 7–28	7–31 9–4	9–9 10–30	11–7 12–10	7–4 7–28	7–31 9–4	9–9 10–30	11–7 12–10
SA–E	Bottom	59	*	60	59	70	*	64	69
SA–W	Bottom	97	105	88	95	80	90	74	75
SA–S	Bottom	84	77	84	86	93	86	86	85
SA–3M	Surface	107	*	91	*	129	*	115	*
SA–3M	Middepth	89	*	73	*	102	*	84	*
SA–3M	Bottom	63	*	59	*	64	*	56	*
SA–tripod	Bottom	62	66	44	49	75	69	48	54

Note: Top figure in each column is the deployment date; bottom figure is the retrieval date.
   * No data available.

39

greater flood currents than ebb, consistent with the pattern suggested in Figure 16.

Central Bay tidal dominance

56. Tides in Central Bay are a nearly equal mixture of diurnal and semidiurnal harmonic tidal constituents. Tides have two high waters and two low waters like semidiurnal tides, but with unequal amplitudes. Higher high water (hhw) normally precedes lower low water (llw). Tidal currents following this pattern would be expected to be strongest during this hhw-llw ebb tidal phase.

57. Tidal current observations from a large data set collected in 1979-1980 (Cheng and Gartner 1984) were examined to determine tidal dominance. Evaluating maximum current speeds by harmonic analysis technique requires a minimum record length of 14 days and preferably 28 days or longer. Daily tidal dominance can change during a lunar month.

58. Tidal dominance was estimated by computing the relative phase between the M_2 (the principal harmonic constituent) and the M_4 shallow-water harmonic constituent (similar to Friedrichs and Aubrey 1988). Using twice the M_2 phase less the M_4 phase, symmetric tidal currents were defined as having relative phases of about 90 or 270 deg while ebb dominated were between 90 and 270 deg and flood dominated between 270 deg clockwise through 90 deg. Current data plots were spot checked to confirm these relationships.

59. Bottom current results are shown in Figure 18 for long time series (greater than 28 days). Results were not always consistent with other analyses. For example, the area south of Alcatraz Island was indicated as flood dominant, while other analyses in this general area indicated ebb dominance.

Hydraulic Residence Time

60. This section evaluates hydraulic residence time characteristics of the Central Bay area. Hydraulic residence time is the average time for a parcel of water initially residing in a certain area or volume of concern to leave permanently. Previous physical model test results were reanalyzed and used for this purpose. The purpose of reviewing hydraulics residence time characteristics is primarily to examine flow and mixing regimes in a descriptive way, and to gain insight into sediment dispersal in the Central Bay area.

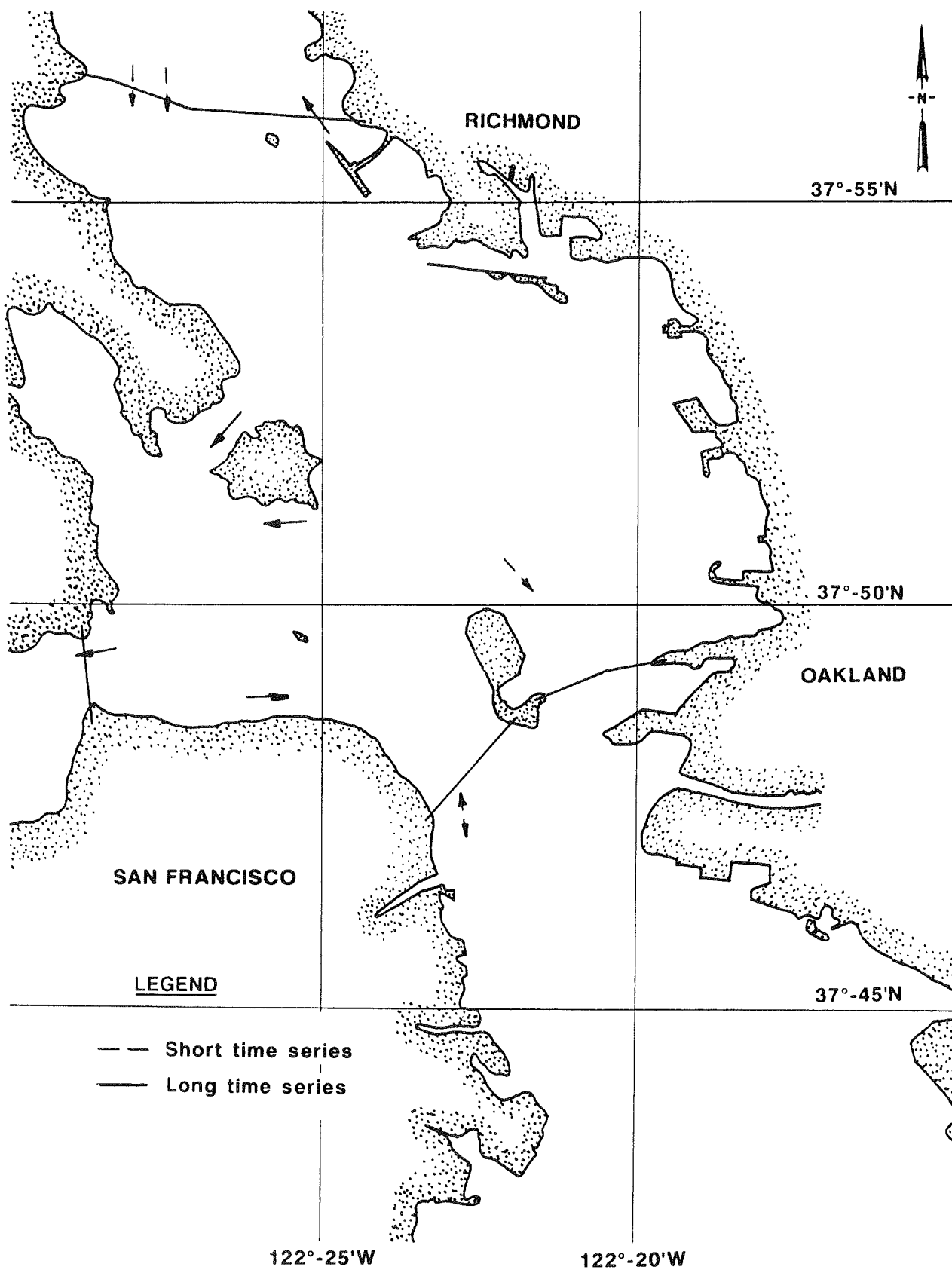61. When injected into model or prototype estuaries, dyes and other

40

Figure 18.   Tidal dominance of bottom currents

41

conservative tracers follow the flow and do not behave exactly like sediments. Sediments do not mix irreversibly with water as dyes do. They readily settle and/or stratify vertically during flow slacks, and can concentrate in areas and in ways different from dye. Still, dye tracers are representative of nonsettling sediment wash loads. Dye tracer tests can be descriptive of the same flow and mixing regimes that strongly influence sediment transport.

62. Dye dispersion tests were previously performed in the physical hydraulic model of the SFBM operated by the San Francisco District. (The SFBM is described in Part IV.) The tests were performed for the purpose of tracing the movements of pollutants and gaging the effects of proposed tidal barriers (USAED, San Francisco, 1963). A net delta outflow of 16,000 cfs and 19-year mean tide were used for these tests.

63. Dye loss and/or decay was accounted for in the model tests. Pontacyl Brilliant Pink-B dye, an acid form of Rhodamine-B dye, was found to be most conservative and was used in the tests. Special tests were conducted in several areas of the model to determine dye loss. Dye concentration data for a given tidal cycle, without respect to location in the hydraulic model or initial concentration of the dye release, were averaged to construct correction curves. Individual dye loss curves varied by less than 5 percent during 30 tidal cycles. After 40 cycles, about 83 percent of the initial dye was retained in the model according to the average correction curve.

64. For each test, a solution of dye was mixed with seawater to the tidal average density of flow at the injection point. Dye pulses were injected over a lunar day at uniform rates beginning about 12 hr before local hhw. Injections were made at the surface but were seen to mix vertically throughout the depth. Samples were taken at times of local hhw slack current. Between 1,500 and 3,000 samples were generally collected during each test. Three data sets were used in analyses presented here with injections as follows:

Injection	Shoreside Location
I	Passenger Pier, San Francisco
R	Point Richmond, Richmond
H	Islais Creek, South Bay

65. Dye test results were used to calculate residence times π and transition probabilities P_{ij} . A compartmental analysis was used.

Central Bay and adjoining areas were segmented into five areas as shown in Figure 19, and defined as follows:

Segment	Description	Area, sq ft
1	Lower San Pablo Bay	0.91E9
2	Upper Central Bay	1.76E9
3	Offshore bar area	1.89E9
4	Lower Central Bay	1.66E9
5	Upper South Bay	1.57E9

66. Three phases of dispersion can be identified in the physical model dye tests. During the short initial phase of one to two tidal cycles, the dye was advected in parcels at high concentration by tidal currents, usually into all five segments. During the second phase, local longitudinal concentration gradients were large, and dye concentrations fell rapidly especially near the injection segment. In the third phase, after 5 to 10 tidal cycles, concentrations were more uniform and dye concentrations fell slowly.

67. In a one-dimensional flow-through system, the local flushing rate U_j can be defined by tracer experiment as:

$$U_j = \frac{M}{\int_o^\infty C_j(t)\ dt} \tag{2}$$

where M is the mass of tracer injected upstream, t is time, and C_j is the average concentration (mass per unit volume) in segment j. Then:

$$\pi = \frac{V_j}{U_j} \tag{3}$$

where V_j is the volume of the segment. In this method, the integral dye concentration history at a point is used to define a flushing rate for a segment, implying a compartment analysis. An alternate approach might be to calculate dispersion coefficients from the second moments of the dye concentration histories. However, second moments are sensitive to the distribution
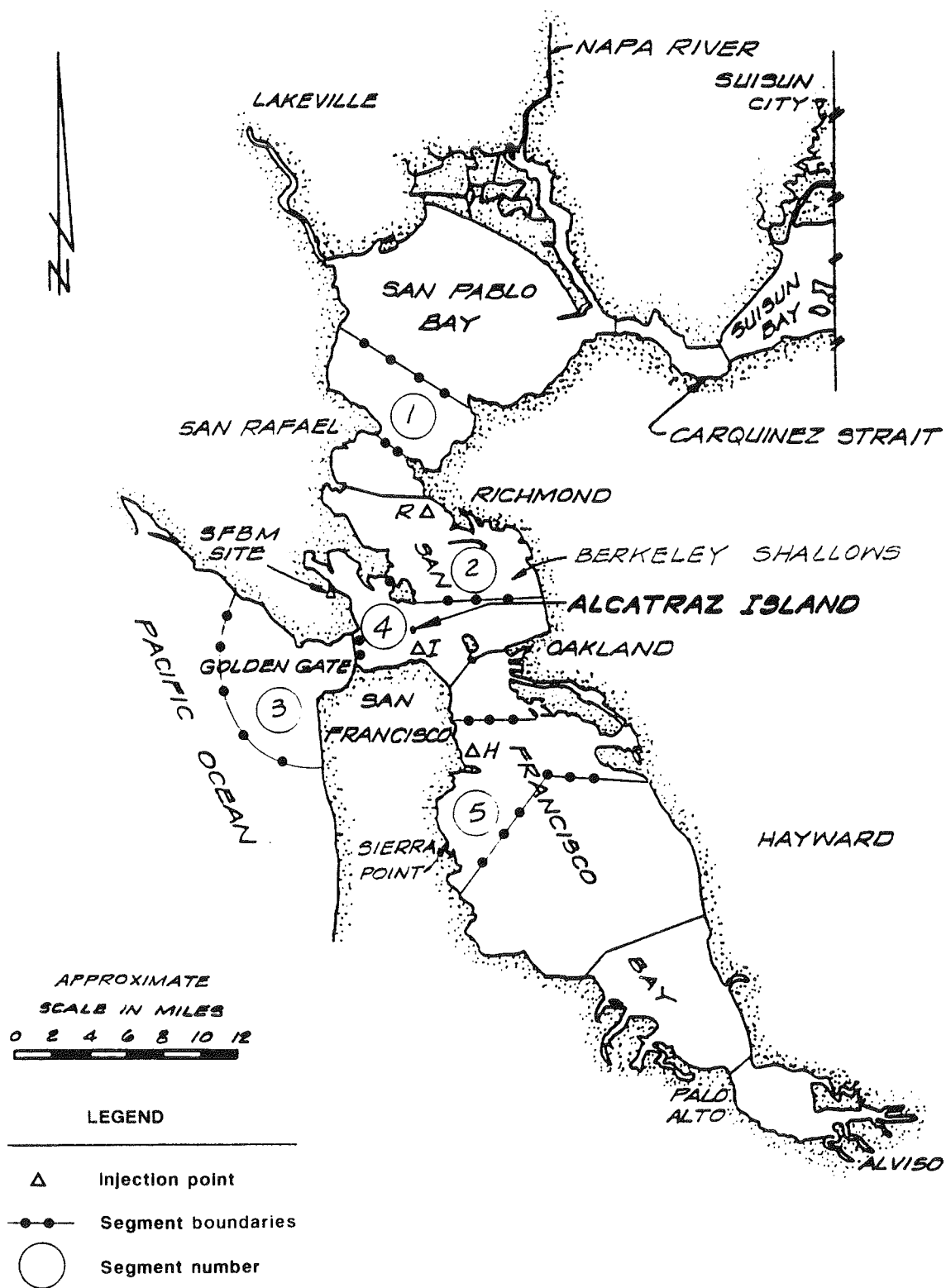
Figure 19. The five areas used in conjuction with the dye tests

tails, and the test data are of insufficient length and temporal resolution to perform such computations accurately.

68. Some additional considerations are required for the analysis of San Francisco Bay with its unsteady flow and its multiple connections or branches. The local flushing rate under these conditions (Zvirin and Shinnar 1976) can be expressed as:

$$U_j = \frac{M_i}{\int_o^\infty C_j(t) \, dt} P_{ij} \qquad (4)$$

where P_{ij} is the probability that a particle launched in segment i would pass through segment j at least once, and M_i is the mass launched at i. P_{ij} can be evaluated from the tracer tests. In each segment j, transition probabilities were calculated as:

$$p_{ij}(t) = \frac{C_j(t) \, V_j(t)}{M_i} \qquad (5)$$

where $p_{ij}(t)$ is the fraction of particles residing in segment j and released from segment i at time t. Then:

$$P_{ij} = \frac{\int_o^\infty p_{ij}(t) \, dt}{\int_o^\infty p_{jj}(t) \, dt} \qquad (6)$$

Theoretically, P_{ij} for any segment between the injection segment and a single outlet would be unity, and $P_{jj} = 1$; however, the interpretation of π for a branched, unsteady system is more complicated than that for a linear flow-through system, as will be discussed later.

69. Concentration and mass of dye for the five segments were estimated for each of the model data collection periods 1, 3, 5, 10, 20, 30, and 40 tidal cycles after injections I and R, and 1, 3, 5, 10, and 20 cycles after injection H (a shorter test). Mass values for tidal cycles 1 and 3 were used

45

to extrapolate back to time zero and estimate the initial mass injected.

70. Dye test results from the SFBM generally indicated that the main portion of Central Bay was a well-flushed section of San Francisco Bay, and that dye releases resulted in low concentrations with respect to the amount of dye released. Results of the π and P_{ij} analyses were as follows:

Segment	π, Tidal Cycles for Injection Test			P_{ij} for Injection Test		
	I	H	R	I	H	R
1	0.0	0.1	1.4	0.1	0.3	0.6
2	0.7	0.7	4.1*	0.6	0.7	1.0*
3	2.5	1.4	1.7	1.2	1.0	0.6
4	1.8*	1.9	6.5	1.0*	1.2	1.3
5	0.6	1.4*	0.6	0.5	1.0*	0.4

* Indicates injection segment.

71. In a simple system (not San Francisco Bay) the value of π should be independent of injection location, and hence should be consistent between tests. Some of the variation in π results can be explained by local effects near injection points R and H. Following injection R, high concentrations persisted in the shallow areas near Richmond, and were subsequently transported into the shallow area off Berkeley. Dye was slow to disperse into the main portion of the flow from these shallow locations. The initial dye mass, estimated as described earlier, was only about half that of other tests, indicating that some of the dye may have stayed near the injection point and was not immediately sampled. Residence times for segments 2 and 4 were much larger for this test, and reflected the slower flushing rates of the shallow area of these segments. The injection at H similarly produced highest concentrations in shallow-water areas, in this case near Sierra Point in South Bay, and the greatest π for the injection segment (5).

72. These shallow-water effects have implications with respect to the dispersion of wave-resuspended sediments from those areas. Flushing of dye from the shallow area off Berkeley in the SFBM was particularly slow. Therefore, resuspended sediments would have the opportunity to redeposit before being mixed with the main portions of the flow and transported away from this area. This applies to shallows on the west side of upper South Bay to a lesser extent. The slow flushing of the shallow-water areas, if

46

representative of the prototype, would reduce the influence of these areas and the processes affecting them (i.e., wind waves) on overall transport of suspended sediments.

73. The extremely short values of π for lower San Pablo Bay (segment 1) are unrealistic, a limitation of the analysis pointed out by Zvirin and Shinner (1976). Segment 1 was poorly connected to the other regions according to values of P_{ij}. Only a small amount of mass reached segment 1, which had strong local mixing.

74. As discussed earlier, P_{ij} is dependent on injection location, has a theoretical maximum of 1.0, and should be 1.0 in the injection segment and in all segments downstream from the injection segment. The calculated P_{ij} indicates a strong connection between segments 3-5 for injection H. P_{ij} has a theoretical maximum of 1.0, and the occurrence of values greater than 1.0 indicate that model test results were probably accurate only to within ±20 percent or so.

75. The injection at I produced the most immediate dispersion. Maximum concentrations were in the main portions of the flow. Results of π for injection H were similar to I except for segment 5, which, as explained earlier, was affected by low shallow-water flushing.

76. Local residence times are descriptive of flushing conditions, and can also be used to calculate equilibrium concentrations resulting from a continuous discharge. The results for the injection at I were used to estimate the buildup of turbidity $\hat{C}$ caused by a constant release of material. The previously mentioned qualifications apply. A constant release rate R_o would roughly correspond to the continuous release of a conservative, passive tracer at the Alcatraz disposal site. Then the release rate into any segment is

$$R_j = \alpha_j R_o \qquad (7)$$

where α_j is a distribution parameter, and

$$\alpha_j = \frac{P_{ij}}{\sum\limits_{j} P_{ij}}$$

47

then at steady state,

$$\hat{C}_j = \pi_j \, \alpha_j \, \frac{R_o}{V_j} \tag{8}$$

Results for a 10,000-metric-ton release per tidal cycle were as follows:

Segment j	$\hat{C}_j$, mg/ℓ
1	0.0
2	0.7
3	2.3
4	2.0
5	0.9

Caution should be exercised when interpreting these results. As described previously, dye is a poor analog for sediment. The physical model from which these data were developed was never verified to residence times, and scale distortion effects may have affected dye test results. The only cross-check on the estimated residence times on hand is the prototype hydraulic residence time estimated by dividing segment volumes by tidal prism. Tidal prisms are available only at the three boundaries of Central Bay, and segments 2 and 4 had to be combined for this analysis. Using a mean tide, the hydraulic residence time of Central Bay (segments 2 and 4) was 1.6 tidal cycles.

PART IV: DESCRIPTION OF THE MODELS

Model Overview and Procedures

77.   The prediction of TSM concentration in San Francisco Bay was accomplished with mathematical models. A hydrodynamic model generated the time-varying currents and water elevations at computational nodes in a numerical mesh representing San Francisco Bay. These hydrodynamics were used in a sediment transport model to solve the convection–diffusion equation with appropriate sink/source terms for TSM. The two numerical models, RMA–2V (A Two-Dimensional Model for Free Surface Flows) and STUDH (Sediment Transport in Unsteady 2–Dimensional Flows, Horizontal Plane), are included in the TABS modeling system, which is supported by the US Army Corps of Engineers (Thomas and McAnally 1985). Data from the SFBM were the principal source of verification currents and water levels for the hydrodynamic model.

The San Francisco Bay–Delta Physical–Hydraulic Model

78.   The SFBM is a fixed–boundary, distorted–scale, tidal hydraulic model. This physical model provides a means of reproducing, on a manageable scale, the three–dimensional hydrodynamic phenomena that occur throughout the large and complex estuarine system. Similarity between model and prototype is established using laws of similitude expressed by a set of dimensionless numbers. These may include the Froude, Reynolds, Weber, and Cauchy numbers, which are the ratios of inertial forces to the forces of gravity, viscosity, surface tension, and elasticity, respectively. Perfect similitude would require that each of these numbers be the same for model and prototype. Physical hydraulic models cannot be designed to provide similitude with respect to all forces, but are designed to simulate the dominant forces affecting the conditions being modeled. This requires different horizontal and vertical scales, and therefore a distorted–scale model. The scales were selected so that the remaining forces are negligible or do not cause fundamental dissimilarities in the processes of interest.

79.   In the San Francisco Bay complex, the depth, surface slope, and other features of tidal flow are controlled by the joint effects of inertial and gravitational forces. The major hydraulic quantities vary according to

49

the Froude number. For the SFBM, different model scales were chosen for horizontal and vertical dimensions to reduce construction and operation time and cost as well as reproduce flows faithfully and permit measurements of the desired parameters with satisfactory accuracy. The effect of distortion on boundary roughness was reproduced during verification tests by the use of metal strips embedded in the model. These strips were adjusted to obtain reproduction of the bay's tides, currents, and salinities. The selected scaling ratios of model to prototype are as follows:

Characteristic	Scale Relations Model:Prototype
Horizontal length	1:1,000
Vertical length	1:100
Time	1:100
Velocity (horizontal)	1:10
Discharge	1:1,000,000
Salinity	1:1

80.   The SFBM occupies an area of about 1 acre and is completely enclosed in a 128,500-sq-ft shelter to protect it from the weather and thus permit uninterrupted operation. The limits of the model, shown in Figure 20, encompass a portion of the Pacific Ocean extending 17 miles west of the Golden Gate, San Francisco Bay, San Pablo Bay, Suisun Bay, and all of the Sacramento-San Joaquin Delta east of Suisun Bay to the cities of Sacramento on the north, Stockton on the east, and Tracy to the south.

81.   The model is equipped with the necessary appurtenances including freshwater and saltwater supply sumps, primary saltwater inflow and mixing pumps, computer-controlled tide generator capable of reproducing repetitive ocean tides by regulating two motorized gate valves, precise flowmeters to regulate major river inflows to the delta plus other inflow and withdrawal facilities, major pumping plant exports, and electrically operated one-way head gates. The model represents the state of the art in model operation, real-time data acquisition using miniature sensors, data analysis, and information storage/retrieval capability.

The TABS Numerical Modeling System

82.   The TABS is a modular system composed of distinct computer programs

Figure 20. Limits of SFBM (from USAED, San Francisco, 1981)
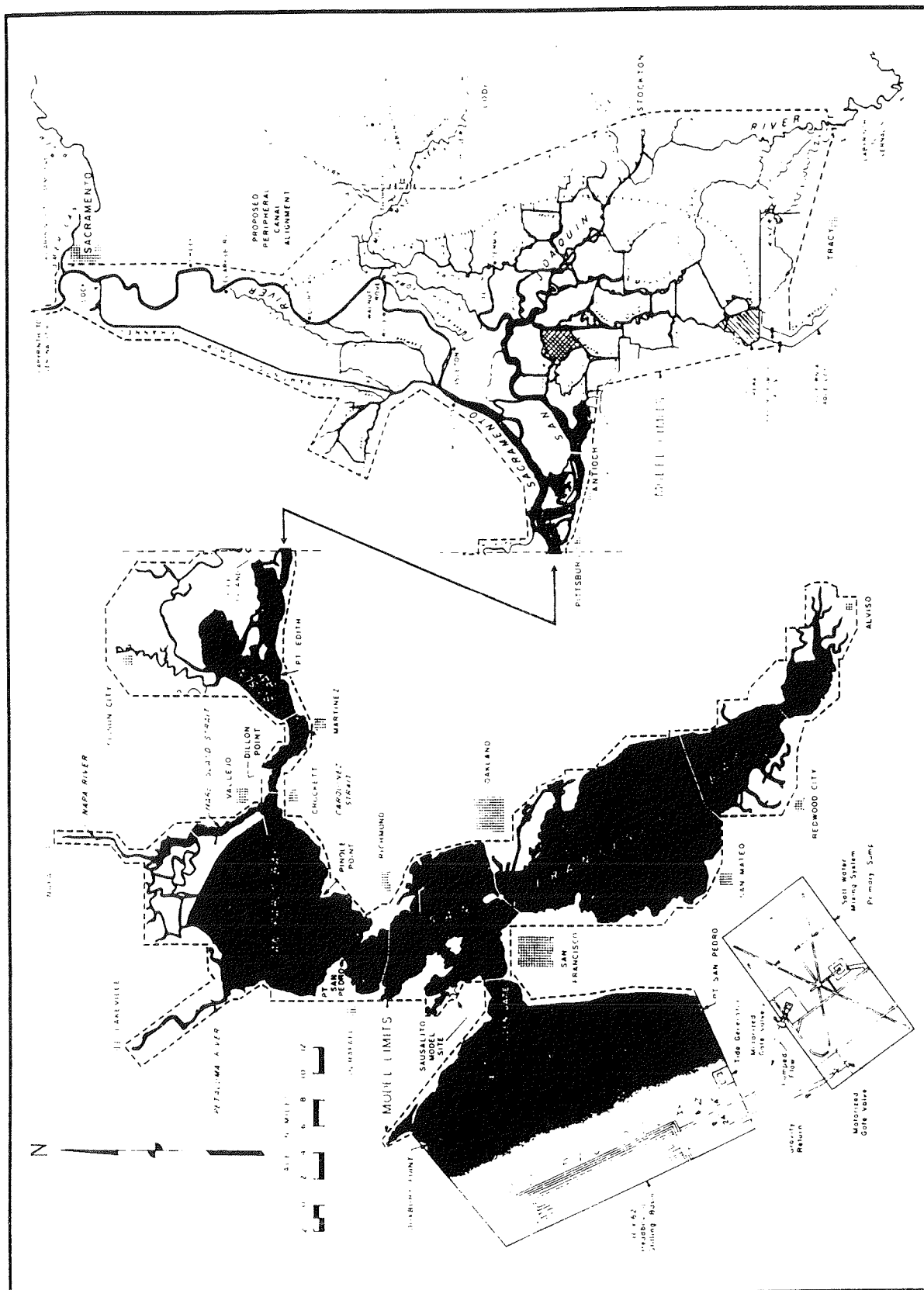
linked together by preprocessors and postprocessors. Each of the major computer programs solves a particular type of problem: hydrodynamics (RMA-2V), sediment transport (STUDH), or constituent transport (RMA-4). These programs employ the finite element method to solve the governing equations. A brief description of RMA-2V and STUDH appears in Appendix B.

Numerical-Hydrodynamic Model

83. RMA-2V is a finite element solution of the Reynolds form of the Navier-Stokes equations for turbulent flows. Friction is calculated with Manning's equation, and eddy viscosity coefficients are used to define turbulent exchange characteristics. A velocity form of the basic equation is used with side boundaries treated as either slip (parallel flow) or static (zero flow). The model recognizes computationally wet or dry elements and corrects the mesh accordingly. Boundary conditions may be water-surface elevations, velocities, or discharges and may occur inside the mesh as well as along the outer boundaries.

Numerical Mesh

Model limits

84. A comprehensive mesh of the San Francisco Bay system was developed using the original global mesh from the previous numerical study of the Alcatraz disposal site reported in Pankow (1988). The new mesh includes expansions to the Pankow (1988) global mesh through the two-dimensional representation of Suisun Bay, a larger ocean boundary in the Gulf of the Faralones (the Pacific Ocean), and the one-dimensional representation of the Napa River, Suisun Slough, Montezuma Slough, and the Sacramento-San Joaquin Delta (Figure 21). The numerical representation of the Pacific Ocean encompasses the region between Drakes Bay to the north, the Farallon Islands to the west, and Half Moon Bay to the south, which are all approximately 22 nautical miles from the Golden Gate Bridge. The mesh consists of 2,330 elements with 7,049 nodes. Quadrilaterals and triangles compose the 2,019 two-dimensional elements representing the open bay and ocean waters, while 311 one-dimensional elements define the riverine portions of the system. This mesh is referred to as Mesh A.
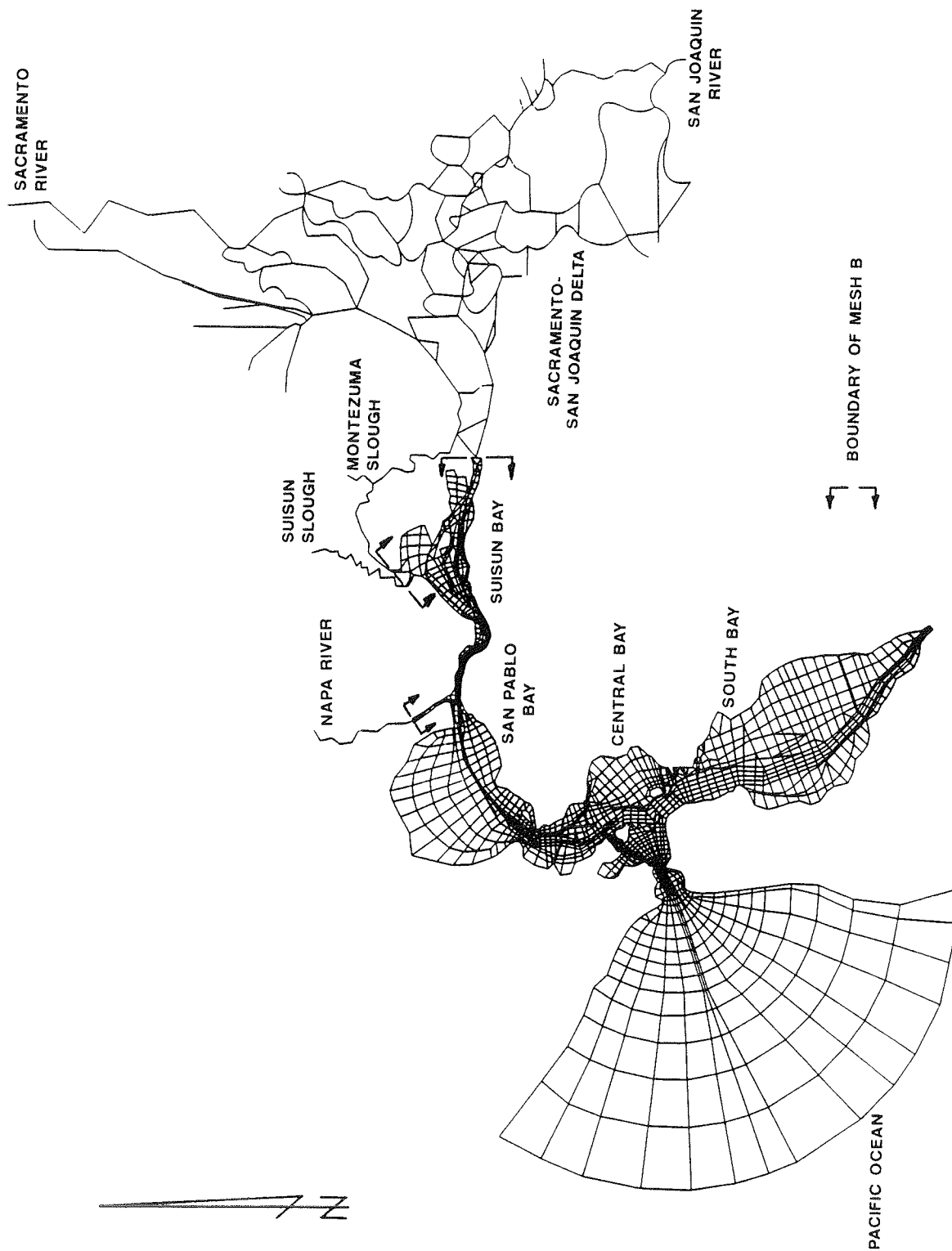
Figure 21. Numerical model representation of San Francisco Bay (Mesh A and Mesh B)

85. Because the sediment transport model is presently limited to using two-dimensional elements, a second mesh (Mesh B) was developed that was identical to the expanded comprehensive mesh except for the exclusion of the 311 one-dimensional elements (Figure 21). The method of using both meshes is described in the boundary conditions section. A second reason for using Mesh B is the lack of resolution in the one-dimensional portion of Mesh A to address adequately sedimentation and TSM values in the Sacramento-San Joaquin Delta.

Bathymetry

86. The bathymetric data required by the numerical models were obtained from the following NOS nautical charts:

Chart No.	Location	Scale	Date
18645	Gulf of the Faralones	1:100,000	1976
18651	San Francisco Bay-southern part	1:40,000	1978
18649	Entrance to San Francisco Bay	1:40,000	1986
18654	San Pablo Bay	1:40,000	1988
18656	Suisun Bay	1:40,000	1983

A state coordinate (x-coordinate and y-coordinate) and a z-value (bed elevation) were assigned to each node in both Meshes A and B through use of a digitizer. The vertical datum was set to mean lower low water (mllw).

Time-step

87. The time-step used in the hydrodynamic numerical simulations is identical to that used in the SFBM for data collection. This allows the direct comparison of physical model and numerical model results. A time-step of 37.26 min (0.621 hr) was used, which provides 40 equal steps in the 24.84-hr lunar day.

Boundary conditions

88. If no boundary condition is specified at a node, RMA-2V computes an x- and y-component of velocity and a water depth. For boundaries along land/water interfaces, slip flow parallel to the boundary is specified. Along the Pacific Ocean outer boundary, a time-dependent head specification (water-surface elevation) was assigned to all boundary nodes to represent tidal elevation fluctuations. In the Sacramento-San Joaquin Delta, velocity specifications were made at the Mesh A headwaters of the San Joaquin and Sacramento Rivers and withdrawals of water were specified at pumping locations of the Contra Costa Canal and the US Bureau of Reclamation Tracy Pumping Plant. All

other riverine freshwater inflows were considered sufficiently small to be assumed to be zero, which is a reasonable assumption for the low inflow conditions of this study. In Mesh A, the Napa River, Suisun Slough, Sacramento River, and San Joaquin River one-dimensional reaches were extended sufficiently to include a majority of the tidal prism associated with each riverine system. While none of these one-dimensional riverine reaches was extended upstream beyond the influence of the tide, the reaches were extended sufficiently so that the tide had appreciably damped and minor spurious tidal reflections induced by the boundaries had been sufficiently reduced or removed from all areas of interest to this study. A final boundary condition in Mesh A was the boundary in extreme South Bay at the Dumbarton Bridge. Data obtained from the SFBM were used to supply the velocity boundary conditions at this location.

89. Mesh B used the same time-dependent water level specification for boundary nodes in the Pacific Ocean and the same time-dependent velocity specification for boundary nodes in extreme South Bay as for Mesh A. However, with the deletion of one-dimensional elements from Mesh B, new boundary specification locations occurred at the termination of the two-dimensional elements in Mesh B at the Napa River, Suisun Slough, Montezuma Slough, and eastern Suisun Bay (Figure 21). The velocity specifications at these locations were determined through the laborious but necessary process of extracting them from the results generated from the execution of RMA-2V for Mesh A.

Numerical-Sediment Transport Model

90. The sediment transport model in the TABS system is STUDH, which solves the convection-diffusion transport equation with bed source terms. These terms are structured for either sand or cohesive sediments. The Ackers-White (1973) procedure is used to calculate a sediment transport potential for the sands from which the actual transport is calculated based on the availability. Clay erosion is treated as described in Ariathurai, MacArthur, and Krone (1977), and the deposition of clay uses Krone's (1962) equations. Deposited material forms layers, and bookkeeping within the STUDH code allows up to 10 layers at each node for maintaining separate material types, deposited thickness, density, and age. The identical Mesh B used by RMA-2V

was used by STUDH. Boundary conditions were specified as a TSM concentration, which may be time-varying.

Time-step

91. STUDH was operated with a time-step equal to one-half the value used in RMA-2V; that is, 80 time-steps of 18.63 min each represented a lunar day. The hydrodynamic conditions used in STUDH were obtained by linearly interpolating RMA-2V results to generate the hydrodynamic conditions for each STUDH time-step.

Boundary conditions

92. At all boundary locations specified in RMA-2V, a STUDH TSM boundary concentration was supplied. While in actuality this boundary is undoubtedly time and spatially varying with tidal fluctuations and other factors, insufficient data existed at boundary locations to allow elaborate representation. Instead, a single representative value appropriate for each boundary location, e.g., Pacific Ocean or Napa River, was determined and used throughout the application of STUDH.

PART V: MODEL VERIFICATION TO SUMMER CONDITION

Physical Model Verification

93. The verification report of the San Francisco physical model (USAED, San Francisco, 1963) indicated that the model could reproduce a prototype mean tide (21-22 September 1956) with good results. Maximum error in elevation in model reproduction at 23 gages throughout the bay was 0.4 ft prototype, with the model amplitudes being slightly less than those of the prototype. At most stations the error was only 0.1 ft prototype. Water levels were found to repeat cycle to cycle and test to test. The standard deviation of water levels was found to be 0.04 to 0.08 ft prototype. Forty percent or more of the standard deviation was attributed to the tide generator (USAED, San Francisco, 1984).

94. The verification procedure indicated that local model velocities may vary up to 20 percent from those in the prototype, the model velocities tending to be generally higher than those in the prototype. Additional prototype to model comparisons made in 1976 (USAED, San Francisco, 1976) were similar.

Hydrodynamic Model Verification

95. Verification of the RMA-2V model employed in the previous dredged material disposal study, which used a global mesh of San Francisco Bay, is reported in Pankow (1988). The expanded mesh (Mesh A) for the present study, including the one-dimensional representation in important riverine areas, was verified to measured water levels and velocities from the SFBM for mean and spring tide conditions. In addition, Mesh A was verified to water levels generated from a least squares harmonic analysis of prototype tide gage locations in the San Francisco Bay system. The tide gages were operated and harmonic analysis performed as the result of a comprehensive tidal survey of the bay system conducted jointly by the USGS and NOS/National Oceanic and Atmospheric Administration (NOAA) during 1979 and 1980 (Cheng and Gartner 1984; Welch, Gartner, and Gill 1985).

Model coefficients

96. The process of numerical model verification resulted in one final

set of model coefficients valid for all verification cases for Meshes A and B. The model coefficients subject to adjustment during model verification are bottom roughness as represented by Manning's n value and eddy viscosity coefficients. Based on water depths and bottom conditions, the Manning's n values in the Gulf of the Faralones (Pacific Ocean) ranged from 0.018 to 0.027 with the smaller values in the deeper waters. In a similar manner, Manning's n values ranged from 0.015 in the deep waters of San Francisco Bay to 0.025 in the shallow waters. In the one-dimensional sections, slightly higher Manning's n values indicative of riverine conditions with a range of 0.024 to 0.035 were employed. Eddy viscosity values were assigned based upon the element size in the mesh. In San Francisco Bay the eddy viscosity coefficients were all set to 200 $lb-sec/ft^2$; in the one-dimensional areas of the Sacramento-San Joaquin Delta, Napa River, Suisun Slough, and Montezuma Slough to 1,500 $lb-sec/ft^2$; and in the Gulf of the Faralones to a range from 400 to 4,000 $lb-sec/ft^2$. Extremely large element areas in the gulf necessitated the large eddy viscosity values in this area. The largest values (greater than 1,000 $lb-sec/ft^2$) were used in the northeast corner of the mesh representation of the Gulf of the Faralones. The interaction of Coriolis force with a specification of a uniform water level along the entire gulf boundary resulted in spurious current patterns localized in the elements in the extreme upper (northeast) gulf boundary. This slight irregularity was controlled through specification of large eddy viscosities that artificially damped it. A natural sloping water surface along the ocean boundary would have accounted for the influence of the Coriolis force, avoiding this spurious current. Since no data of sufficient detail exist to allow specification of this slope and since the irregularities were confined to the extreme northeast portion of the Gulf of the Faralones, far removed from the areas of interest, the damping from eddy viscosity was selected as the most expedient manner to control the phenomenon.

Mean tide verification, Mesh A

97. The numerical model (Mesh A) was operated for nearly 35 hr with the 19-year mean tide to produce a mixed tide with extremes of approximately 0.0, 4.6, 2.3, and 5.8 ft mllw at tide sta T8, Golden Gate location. The ocean boundary conditions were specified to closely reproduce the tide at the Golden Gate measured in the physical model. Net delta outflow in the numerical and physical models was specified at 4,400 cfs. Numerical and physical model

results for water levels and velocities are compared in Plates 1-7. The station locations for comparisons are shown in Figure 22. Comparisons are provided only for selected stations that demonstrate the general trend of model verification with emphasis on Central Bay stations. The complete set of comparisons at numerous water level and velocity stations is provided in Hauck, Heltzel, and Teeter (in preparation), the report to the San Francico District on the salinity intrusion and ship simulation study for the proposed John F. Baldwin III Ship Channel project.

98. Since the first 5 to 10 hr of numerical model results for this mesh are influenced by the model initial condition specification, only the last complete tidal cycle (24.84 hr) of the total 35-hr simulation is used for comparison. Because the RMA-2V code determines vertically averaged values, the physical model data were averaged to estimate a comparable vertically averaged value. Generally, near-bottom and near-surface measurements were taken in the physical model, though only a middepth measurement was made at some shallow stations and for sta 1 at the Golden Gate only a surface velocity was measured. The mean velocity at sta 1 was determined as 85 percent of the surface velocity.

99. The water-surface elevations for the mean tide conditions compare closely. Phasing of the numerical and physical model is in general agreement, though a trend of RMA-2V results preceding physical model measurements by approximately one-half hour is apparent. Amplitude and tidal plan (mean elevation) agreement is also favorable. Only in the Suisun Bay area do appreciable discrepancies occur between the tidal planes in the physical and numerical models. This discrepancy is the result of the constant water density limitation in RMA-2V, while the physical model contains the density effects (as in the prototype system) of water of varying salinity from least density (nearly freshwater conditions) in Suisun Bay to greatest density (seawater) in the vicinity of the Golden Gate. This may be interpreted that, hydrostatically, a higher level of low-density water is required to equal the pressure of higher density water. The constant water density in RMA-2V manifests itself in an underprediction of the tidal plane in the lower density portions of the system, i.e., Suisun Bay and the Sacramento-San Joaquin Delta.

100. Comparison of RMA-2V velocities to physical model averaged results are good considering the errors involved in the process of measuring velocities in the physical model and errors resulting from representation of a
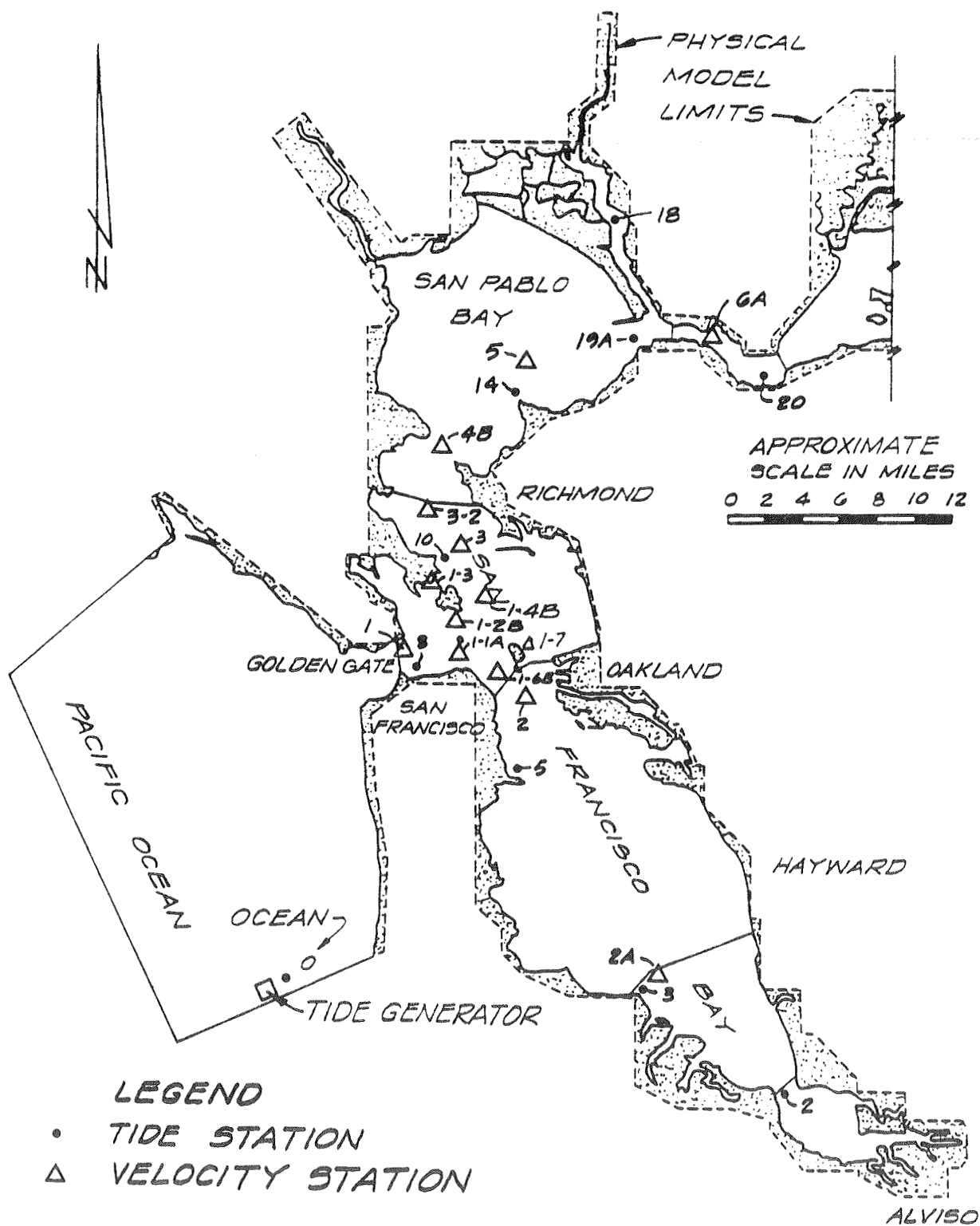
Figure 22. San Francisco Bay area with physical model station locations

60

vertical mean velocity by the simple arithmetic mean of a surface and bottom measurement. The phasing of the numerical model velocities compared to physical model velocities is good. At several stations, RMA-2V results precede the physical model results by 0.5 to 1 hr, e.g., sta 1A, 1B, and 1-1B, while at other stations the phasing is very close, e.g., sta 1-3, 1-4A, and 1-6A. Generally, the RMA-2V velocity magnitudes underpredict the results from the physical model. However, as mentioned under physical model verification, physical model velocities tended to be slightly higher than prototype velocities, so the RMA-2V values are considered to show a good verification to expected prototype velocities.

101. The residual or tidally averaged currents for the mean tide as determined with RMA-2V are depicted in Figure 23 for the central San Francisco Bay area. With the inherent limitation that RMA-2V results are vertically averaged, the residual currents indicate the net direction and magnitude of currents in an estuarine system where currents vary with time. The residual current pattern in Figure 23 is of interest not only for the predicted patterns, but also because of the similarity to Figure 16, which displays near-bottom current direction ebb and flood dominance determined from physical measurements and bed form observations. The patterns in Figures 16 and 23 are very similar, especially in the areas to the south and west of Alcatraz Island, around the Golden Gate Bridge, in Raccoon Strait, and south of Richardson Bay. An exception is the bay area north of Alcatraz Island where the numerically predicted residual current pattern has some notable discrepencies from field measurements. However, RMA-2V predicted residual current patterns are generally remarkably similar to near-bottom patterns determined from the physical measurements, including the locations of boundaries between flood and ebb dominance.

Spring tide verification, Mesh A

102. The numerical model was operated in essentially the identical manner for spring tide verification as for the mean tide verification. Again, net delta outflow was specified as 4,400 cfs for numerical and physical models. The numerical model was operated with time-varying water level boundary specifications in the Pacific Ocean to reproduce the physical model mixed tide with extremes of -1.7, 4.6, 2.3, and 6.8 ft mllw at tide sta T8, Golden Gate.

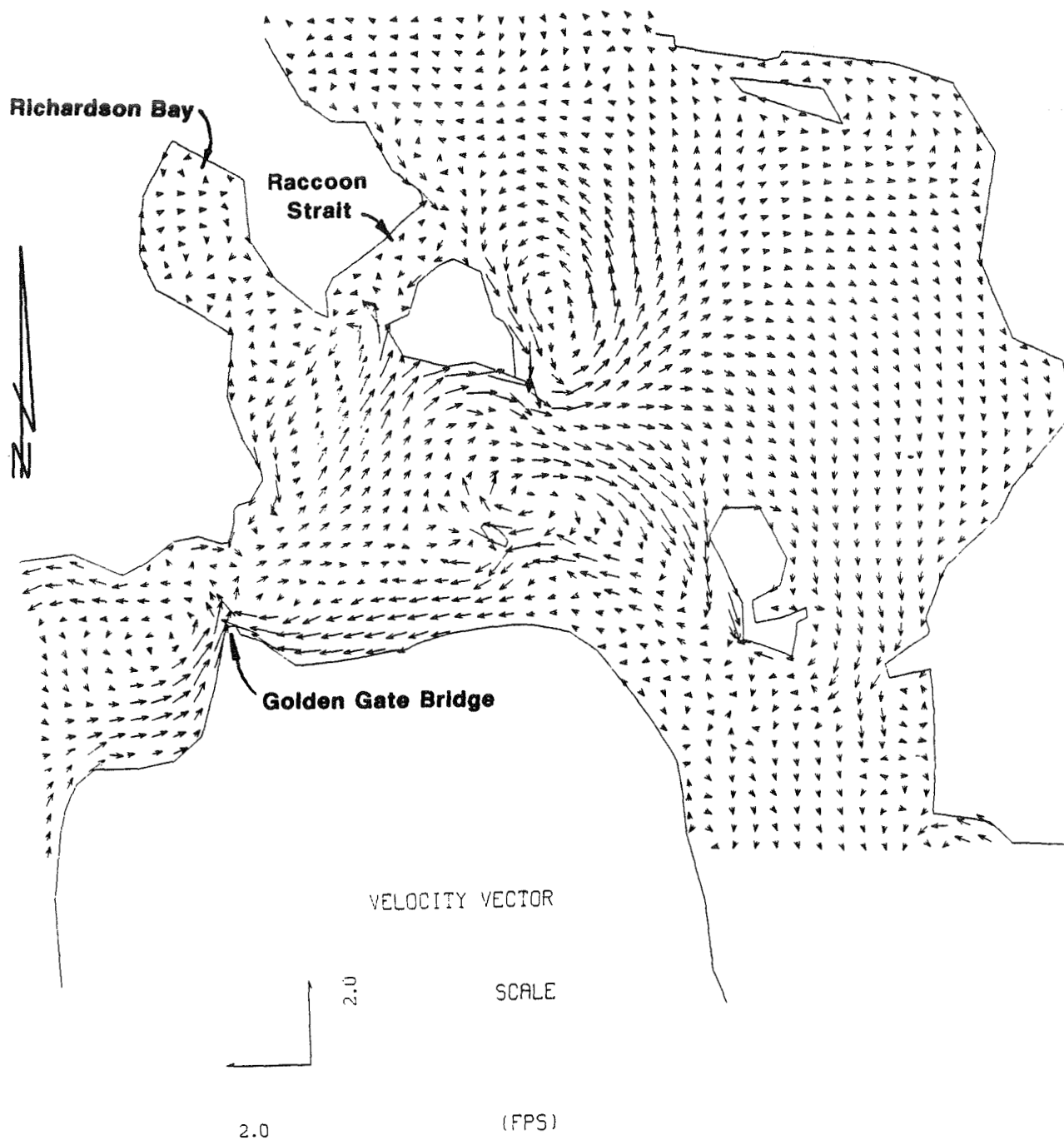103. The same trends and characteristics were observed in the spring

61

Figure 23. Numerical model predicted residual current pattern for central San Francisco Bay

tide verification as in the mean tide verification. Because the verification
is similar and since the mean tide, not the spring tide, was used in the sedi-
mentation modeling, only a limited, representative number of velocity and
water level verification stations are presented (Plates 8-10). The complete
presentation of spring tide verification is presented in Hauck, Heltzel, and
Teeter (in preparation). For the spring tide, tidal phasing, amplitude, and
plane are still in good agreement. The half-hour lag of physical model phas-
ing to numerical model phasing still occurred, as did the tidal plane discrep-
ancy in Suisun Bay due to the constant water density assumption in RMA-2V.
The RMA-2V velocities were in general slightly lower than the vertically aver-
aged physical model results, though numerical results were very close or
greater than physical model velocities at some stations. Generally, the
phasing of the velocities showed reasonable agreement.

Harmonic tide verification, Mesh A

104. The USGS and NOS/NOAA analyzed tide (water level) records obtained
during their joint study by least squares harmonic analysis. The tide records
for the various locations were obtained for different lengths of time and at
different times during the 1979-80 study period. In an attempt to minimize
discrepancies arising in the harmonic analysis, the stations used in verifying
RMA-2V were limited to those with 8 months or more of water level records.
The five major tidal constituents (or harmonic constituents) O1, K1, N2, M2,
and S2 were selected for use in the model verification. Using these five
major harmonic constituents for each station, the astronomical tide was pre-
dicted for the period of 6 and 7 September 1988. The astronomical tide during
this period was midway between the extremes of spring and neap tides, there-
fore representing an average tide.

105. The numerical model was operated with no freshwater inflow and
with a tide that closely reproduced the harmonically constructed tide at
sta T8, Golden Gate (Figure 22). Comparisons of RMA-2V results after model
spin-up to the harmonically constructed tide at sta 3, 8, 19, and 20 are pro-
vided in Plate 11. Results of these comparisons are good. While the RMA-2V
tide phasing still preceded the verification data at sta 3 and 19, the differ-
ences are not as great as observed with physical model results and are gener-
ally much less than 0.5 hr. At sta 19, the RMA-2V results actually lag the
harmonic tide by 0.5 hr. Tidal amplitudes from RMA-2 are somewhat too large,
and this is most prominent at the first high water. No tidal plane

63

comparisons could be made since the reference datums of the tide gages were not published.

Verification, Mesh B

106. Mesh B may be viewed as an inset to Mesh A necessitated by two factors: (a) the importance of riverine/deltaic systems to circulation in portions of the bay system, especially Suisun Bay, and (b) the limitation in STUDH that allows only two-dimensional elements. Verification of Mesh B was limited, since the expectation was that by operation of Mesh B with boundary conditions generated from Mesh A applications of RMA-2V, nearly identical results should be obtained. This indeed was the case. RMA-2V was operated with Mesh A for mean tidal conditions. Time-varying velocity boundary conditions were obtained directly from Mesh A results for the two-dimensional/one-dimensional interfaces of the delta, Napa River, and Montezuma and Suisun Sloughs. Otherwise Mesh B was operated with boundary conditions and model coefficients identical to Mesh A. Results of Mesh A and Mesh B were identical based on comparison of results at selected locations.

Sediment Model Verification

107. Concentration (TSM) verification of the sediment model, STUDH, was performed to conditions and measurements during the 7-8 September 1988 intensive survey in the Central Bay area. The verification data were supplemented with limited surface TSM data obtained by the USGS during low freshwater inflow periods during 1969 through 1976 and 1980 (Smith, Herndon, and Harmon 1979; Schemel*).

Model coefficients and parameters

108. Several model coefficients and parameters required refinement during the verification process. These values were selected to allow the best practical verification of natural sediment movement. Special care is necessary to deal with the steep gradients in time and space of natural sediments due to resuspension and deposition with tidal variations in velocities. At some locations, temporal variations in TSM exceeded one order of magnitude.

109. The diffusion coefficients were specified at 25 m^2/sec for the

---

* Personal communication, October 1988, from L. Schemel, US Geological Survey, Menlo Park, CA.

x- and y-directions. The Crank-Nicholson implicitness coefficient θ was set at 0.66, which is the recommended value for operation of STUDH. (The Crank-Nicholson scheme is used for time-stepping in STUDH.) A value for θ of 0.5 produces the most model sensitivity while a value of θ of 1.0 produces the least sensitivity. Increased values of θ smoothed results, as did increased values of the diffusion coefficients. The selected values of θ and the diffusion coefficients allowed stable model operation without excessive numerical and diffusive smoothing.

110. The time-step used in RMA-2V of 37.26 min (40 per 24.84-hr tidal cycle) was too large to maintain stable conditions in STUDH. By using a time-step of 18.63 min (80 per tidal cycle), STUDH produced reasonable results. The hydrodynamics required by STUDH at each time-step were created through postprocessing of RMA-2V results. In the postprocessing, linear interpolation was used to calculate the intermediate time-step hydrodynamics between RMA-2V time-steps.

111. Other model parameters and characteristics describing TSM and sediment beds are presented in Table 7. Boundary concentrations were estimated from the intensive field survey data and historic surface TSM measurements. TSM characteristics and sediment bed characteristics were based on previous laboratory results on San Francisco Bay sediments (Teeter 1987). The average settling velocities from separate settling tests conducted on the September 1988 survey samples were in the range of 0.086 to 0.187 mm/sec. Teeter (1987) reported average settling velocities ranging from 0.437 to 0.840 mm/sec. The process of model verification gave satisfactory results with a settling velocity of 1.0 mm/sec, which is higher than the values of the September survey and those reported in Teeter (1987). However, the size distribution analysis of dispersed samples from the field survey indicated a median particle size of 14 μ, which is in the silt range and which substantiates a settling velocity on the order of 1.0 mm/sec.

112. In the Gulf of the Faralones, the settling velocity was reduced beginning approximately 7 miles west of the Golden Gate Bridge or at the western limits of the Fourfathom Bank. The settling velocity was reduced from 0.5 mm/sec at the Fourfathom Bank to 0.01 mm/sec at the Farallon Islands. This was found necessary to prevent excessive deposition and loss of TSM concentration in the deeper, slow-moving gulf waters. The reduced settling velocities in this model area are required because the present numerical model

Table 7

Cohesive Sedimentation Coefficients and Model Parameters

Coefficient	Value
Initial suspended sediment concentration, kg/m^3	0.070
Boundary concentrations, kg/m^3	
Ocean	0.015
Delta	0.125
South bay	0.030
Napa River	0.060
Suisun Slough	0.060
Montezuma Slough	0.040
Particle settling velocity, mm/sec*	1.0
Particle specific gravity	2.65
Critical shear stress for deposition N/m^2	0.15
Critical shear stress for erosion N/m^2	0.20
Erosion rate constant, kg/m^2/sec	0.0001
Sediment bed initialization	Noneroding
Dry weight density—newly deposited layer, kg/m^3	450
Point source, Alcatraz Island, kg/sec**	8
Wind speed, mph	10
Wind fetch length, miles	4

 * Except in ocean area (see text).
** Represents dredged material disposal during the period of the September
    1988 study.

does not incorporate offshore currents known to exist in the region, and for which inadequate knowledge exists to quantify current magnitudes accurately. Secondly, at the low concentrations of TSM in the gulf, settling velocities would be expected to be reduced. Generally, settling velocities are directly proportional to TSM concentration, until hindered settling occurs at concentrations much higher than those of this study.

113. The critical shear stress for erosion and deposition used in STUDH is in the range of values from the University of Florida flume studies (Teeter 1987) on San Francisco Bay muds. However, in a much earlier study (Krone 1962), a minimum bed shear to allow deposition of 0.06 to 0.08 N/m^2 was determined. Values from Krone (1962) used in STUDH produced poor results and did not provide adequate deposition periods during the tidal cycle to allow reproduction of observed TSM patterns. In STUDH and Teeter (1987), bed shear was calculated by the Manning shear stress equation, whereas in Krone (1962) the smooth-wall log velocity profile was used. Therefore some of the discrepancy in bed shear values may be due to the manner of calculation. (In STUDH, bed shear can be calculated by the smooth-wall log velocity profile or the Manning shear stress equation. However, when wave-induced bed shear is important, as it is in San Francisco Bay, a Jonsson-type equation for wave and current caused shear is used, which incorporates the Manning shear stress equation.)

114. When a Jonsson-type equation is used to determine bed shear as a function of tidal currents and waves, a wind speed and wind fetch are used to calculate wave height and frequency in order to determine wave orbital velocity. For the typical summer conditions, a daily average wind speed of 10 mph was selected with a fetch length of 4 miles. Monthly average wind speeds at the San Francisco Airport for June through October range from 9.3 mph to 13.9 mph (NOAA 1985), which is somewhat greater than other more inland stations. The 4-mile fetch length is a representative average for the bay system. This wind speed and fetch produced wave heights of 0.5 ft with a period of 2 sec. The Jonsson-type equation has the following general form:

$$U^* = \sqrt{\frac{1}{2}\left[\frac{f_w\, U_{om} + f_c\, \bar{U}}{U_{om} + \bar{U}}\right](\bar{U} + U_{om})^2} \tag{9}$$

where

U^* = shear velocity

f_w = shear stress coefficient for waves

U_{om} = maximum orbital velocity of waves

f_c = shear stress coefficients for currents

U = vertically averaged velocity

115. In the model verification, a point source was included at the Alcatraz site (mesh element 809) to approximate the level of dredged material disposal that occurred during the intensive study timeframe. Based upon San Francisco District records, 49,700 cu yd of material was disposed at the Alcatraz site in August 1988 and 44,500 cu yd were disposed in September 1988, which are moderately low levels of disposal. All this material came from clamshell operation. Using a bulk wet density of 1.52 (approximately 8,000 mg/ℓ) for the in situ sediment, a 15 percent sand content, and 15 percent material retention at the Alcatraz site, the average rate of readily erodible cohesive dredged material disposed at the Alcatraz site during August and September was 8 kg/sec.

Verification procedure

116. The STUDH verification required the following procedural steps:

a. RMA-2V was operated with Mesh A for three tidal cycles, not including 10 hr allowed for model spin-up, with a repetitive mean tide ocean boundary condition and a net delta outflow of 2,500 cfs. The average net delta outflow obtained from the USGS* for the month prior to the 7-8 September 1988 intensive field survey was 2,450 cfs (or 2,500 cfs). By the third tidal cycle, Mesh A hydrodynamics had closely approached dynamic equilibrium conditions. (Dynamic equilibrium is the condition in which identical water levels and currents occur at the same tidal phase for successive tidal cycles.)

b. The third tidal cycle hydrodynamic results from Mesh A provided the necessary time-varying velocity boundary conditions for Mesh B.

c. RMA-2V was operated with Mesh B for two tidal cycles with mean tide conditions. Since Mesh B did not include the extensive Sacramento-San Joaquin Delta and used the dynamic velocity boundaries developed from Mesh A, Mesh B approached dynamic equilibrium more quickly than Mesh A.

---

* Personal communication, November 1988, from M. Taylor, US Geological Survey, Sacramento, CA.

<u>d</u>. The RMA-2V hydrodynamics for the second tidal cycle of opera-
tion of Mesh B were sent through appropriate postprocessing
codes to develop the hydrodynamics necessary to operate STUDH.

<u>e</u>. Beginning with constant TSM value of 0.07 kg/m^3 and the other
coefficients shown in Table 7, STUDH was operated for three
repetitive tidal cycles with the hydrodynamics developed for
Mesh B. The three tidal cycles allowed ample time for the
solution to adjust from initial conditions and to develop
depositional beds, erosion/deposition patterns, and TSM pat-
terns both spatially and temporally.

<u>f</u>. Using the ending hydrodynamics of the third tidal cycle from
step <u>a</u>, RMA-2V was operated using Mesh A for the verification
period tidal cycle of 8 a.m., 7 September, to 9 a.m.,
8 September 1988. (The mean tide of steps <u>a</u> through <u>e</u> was
oriented in time so that it could be directly phased into the
verification period tide in a smooth, consistent manner.)

<u>g</u>. The Mesh A results for the 7-8 September tide were used to
generate time-varying velocity boundary conditions for Mesh B.

<u>h</u>. RMA-2V was operated with Mesh B for the 7-8 September tide.

<u>i</u>. The hydrodynamic results from Mesh B were sent through post-
processing to develop the hydrodynamics to operate STUDH for
7-8 September.

<u>j</u>. Using the ending TSM concentrations and sediment bed structure
from the third mean tide cycle, STUDH was operated for the
verification period of 7-8 September 1988.

<u>Verification results</u>

117. The results from RMA-2V for Mesh B simulation of the verification
period of 8 a.m., 7 September, to 9 a.m., 8 September (model hour 50 to 75),
are displayed with field-measured velocities in Plates 12-14. (Figure 3 dis-
plays the field sample sites used in verification.) The field measurements
were weight-averaged vertically (see next paragraph) to obtain values for
comparison with RMA-2V results. Good comparisons of RMA-2V and field measure-
ment were obtained at all locations with the exceptions of the very shallow
water, sta 4D (depth) and to a lesser extent sta 4C (depth). The exact cause
of the poorer comparisons at these shallow stations is unknown, but some dis-
crepancy is probably the result of high wind and wave action corrupting field
measurements at these shallow, lower velocity stations. The phasing of numer-
ical results is in good agreement with the physical data at all stations, and
velocity magnitude comparisons are good, especially at sta 3A, 3B, and 3C.

118. The results from STUDH for the verification period 8 a.m.,
7 September, through 9 a.m., 8 September, are displayed with the field-
measured verification data in Plates 15-21. (Figure 3 displays the field

sample sites used in verification.) The verification data from the field measurements were vertically averaged for comparison with the vertically averaged STUDH results. The field data averaging process involved weighting to approximate the percent of the vertical water column represented by a value. For stations with three vertical measurements, the vertically averaged value $\overline{X}$ was determined as

$$\overline{X} = 0.25\ X_s + 0.50\ X_m + 0.25\ X_B \tag{10}$$

where

X_s = near-surface value

X_m = middepth value

X_B = near-bottom value

For the situation with five vertical measurements, then

$$\overline{X} = 0.1X_s + 0.25X_1 + 0.3X_m + 0.25X_3 + 0.1X_B \tag{11}$$

where

X_1 = one-fourth depth value

X_3 = three-fourths depth value

A simple arithmetic mean was not used in Equations 10 and 11 because the near-surface and near-bottom measurements are not representative of the same percentage of the water column as an interior measurement point. The numerical results are generally satisfactory considering the following: potential biases and errors induced from sampling and the high variability of natural TSM values in San Francisco Bay in space and time resulting from the interaction of periods of deposition followed by periods of resuspension. In the numerical and prototype TSM values, the fluctuations within tidal cycles were pronounced. Generally during slack water, TSM values decreased only to increase rapidly in response to velocity increase (resulting in a resuspension of material). The numerical model results generally mimicked the measured patterns and responded similar to current speed (and thus bed shear and sedimentation (deposition and resuspension)) variations. A notable exception was the numerical model's inability to reproduce the pronounced magnitude of increase in TSM concentration occurring during the strong ebb current from hhw

to llw at approximately hour 18 on the plots or approximately 2 a.m., 8 September; for example, see sta 1C, 3A, and 3B. This temporary surge in concentration was adequately reproduced at shallow sta 4A and 4D. The complexity of sediment movement in the bay system is indicated by survey measurements showing no significant surge during the strong ebb current at sta 3C, though a sharp concentration rise was measured at approximately 11 p.m., 7 September, near slack water, while adjacent sta 3A and 3B showed the ebb current response. A general weakness of the numerical results is in reproducing the magnitude of the response of the prototype system to variations in bed shear manifested through the temporal changes (acceleration/deceleration) in tidal currents. The numerical simulation also had some difficulty in reproducing the lateral variation in TSM across Range 1, sta 1A, 1B, and 1C. Relatively good simulations were obtained at sta 1B, 2A, 2B, 2C, 4A, and 4B.

119. As a second less exacting verification, historical USGS TSM data were used (Smith, Herndon, and Harmon 1979; Schemel*). These data were taken along the deep ship channels transecting the bay system from the delta to the end of South Bay and were generally taken at a depth of 2 ft (surface readings). Based on the WES intensive survey data, an average factor by which to multiply a surface concentration to estimate the vertical average value is 1.6. This factor was determined by dividing the average of all surface TSM concentrations for the 7-8 September intensive survey into the average vertically averaged value for each deepwater station (excluding shallow sta 4C and 4D). The factor ranged from 1.2 to 2.0. While it is not exacting to compare numerically determined TSM concentrations from one tide condition and one net delta outflow to field measurements taken during various tide conditions from spring to neap and for a wide range of low to extremely low net delta outflows, the exercise did indicate whether the model replicated the generally observed trends in the natural system (Table 8). The stations for comparison had a minimum of 17 surface TSM measurements taken during the summers of 1972, 1973, 1976, and summer and fall of 1980, which were periods with low monthly average delta outflows ranging from 3,000 to 15,000 cfs. The numerical model minimum, maximum, and mean values for nodes close to the USGS stations generally compared very favorably with the field measurements. In Suisun Bay (sta 6), the numerical results appeared to be somewhat low, whereas in South

---

* Op. cit.

Table 8

Comparison of STUDH Simulation of 7-8 September 1988 to Historical Low Inflow Data

Station	STUDH, kg/m³			Historic Data, kg/m³			Location
	Minimum	Maximum	Mean	Minimum	Maximum	Mean	
6	0.011	0.110	0.047	0.025	0.261	0.128	Suisun Bay, Roe Island
9	0.017	0.060	0.041	0.006	0.207	0.056	Carquinez Strait, Benicia
12	0.003	0.070	0.032	0.006	0.184	0.038	San Pablo Bay, Pinole Shoal
13	0.002	0.051	0.027	0.003	0.125	0.030	San Pablo Bay, Pinole Point
14	0.007	0.052	0.026	0.005	0.152	0.031	San Pablo Bay, Southwest Pinole Point
15	0.010	0.036	0.025	0.004	0.077	0.030	San Rafael Bay
17	0.006	0.025	0.014	0.004	0.043	0.019	Central Bay, near Raccoon Strait
19	0.009	0.020	0.015	0.004	0.029	0.012	Golden Gate Bridge
21	0.009	0.029	0.017	0.003	0.042	0.015	Central Bay, Bay Bridge
24	0.002	0.112	0.039	0.003	0.032	0.014	South Bay, Hunters Point
27	0.002	0.053	0.025	0.004	0.070	0.019	South Bay, near Coyote Point
30	0.007	0.058	0.034	0.004	0.108	0.026	South Bay, Redwood Creek

Bay (sta 24), the numerical results were too high. For the remaining stations in Central and San Pablo Bay, the numerical and field results compared favorably.

PART VI: CONCLUSIONS AND RECOMMENDATIONS

120. This study was limited in that only a late summer/early fall low freshwater inflow condition was considered. The subsequent study phase will include the winter/spring high freshwater inflow period so that seasonal variations within the system can be determined. Upon the completion of that phase of this study, the results of the two phases will be integrated and an explanation of the fate of dredged material will be presented.

Field Data Conclusions

121. The field data collected during the low freshwater inflow period of September 1988 indicated that Central Bay had near-oceanic salinities, was vertically well mixed, and had moderately low total suspended material (TSM). Net delta outflow of fresh water into the bay system was only about 2,500 cfs during this period. TSM at the Golden Gate survey range averaged about 16 mg/ℓ, increased upstream to 34 mg/ℓ at the entrance to South Bay, and increased to 45 mg/ℓ at the Richmond Bridge near the entrance to San Pablo Bay. Peak TSM values were greater than average values by a factor of about three.

122. Tidal fluxes of TSM were large, commensurate with the tidal prism of this system. Observed tidal fluxes were roughly 30,000 metric tons per lunar day at the Golden Gate range, 19,000 metric tons per lunar day at the entrance to the South Bay, and 44,000 metric tons per lunar day at Richmond.

123. Despite the general tidal characteristic of Central Bay, which favors ebb-dominated flows, net landward TSM fluxes were observed through the ranges at the Golden Gate, and the entrance to South Bay. These landward fluxes had relatively small magnitudes, 5-10 percent of the tidal fluxes. The station data suggest possible clockwise net TSM flux for that part of Central Bay where estimates could be made. The net fluxes were south along the east side of the bay near the Richmond Bridge, Berkeley shallows, and into South Bay. The net flux was northward on the west side of the entrance to South Bay.

124. The overall flux balance for Central Bay was not determined. The flux at sta 1C at the Richmond Bridge was seaward, but a large portion of the range cross section was not sampled.

125. The phenomenon responsible for the largest fraction of the TSM

74

flux was fluctuation in TSM during high current speeds, called tidal pumping. Such fluctuations were most pronounced near the bottom. TSM fluctuations were apparently more rapid than the 1-hr sampling rate, and were therefore not well resolved.

126. The question remains how well the intensive survey was representative of low freshwater inflow conditions. Tidal and wind conditions were about normal. There were no strong variations in salinity or TSM conditions during the 2-week period surrounding the intensive survey. However, the variability in fluxes over days or weeks is not known, and therefore how well the intensive survey represents seasonal conditions remains an open question.

127. Data from previous published studies were used in an attempt to determine near-bed tidal dominance. Although results were not always consistent, a complex pattern with both ebb- and flood-dominant areas across most cross sections emerged. The area near the Alcatraz disposal site was indicated to be ebb dominated.

Dye Test Conclusions

128. Previous physical model dye test data from the San Francisco Bay-Delta Physical-Hydraulic Model (SFBM) were reanalyzed to determine dispersion of dissolved materials. Although dyes in general are a poor analog for suspended sediments, they are representative of nonsettling wash load and are affected by the same flow and mixing regimes that influence sediment transport. Flushing rates and residence times were estimated for five segments in the Central Bay area. Results indicated that most segments had hydraulic residence times of 1-2 lunar days, except for shallow areas, which had residence times of 4-7 lunar days. A maximum concentration increase of about 2 mg/ℓ for any segment was estimated for a continuous discharge of 10,000 metric tons per tidal cycle near the Alcatraz disposal site.

Numerical Modeling Conclusions

129. The model RMA-2V, which predicts two-dimensional vertically averaged velocities, was successfully verified for the San Francisco Bay system to water levels developed from harmonic analysis of prototype tide data and to physical model velocities and water levels from the SFBM.

130. The sediment transport model, STUDH, which uses the hydrodynamic results from RMA-2V, was verified to field-measured total suspended matter (TSM) concentrations from an intensive survey conducted for 25 hr during 7-8 September 1988 and to historical field data gathered by the US Geological Survey (USGS). STUDH was only moderately successful in replicating the highly variable TSM values obtained during the intensive survey. However, the model results did compare favorably with the less exacting ranges of the historical USGS data. Generally, the model results did not completely reproduce the short pulses of high TSM concentrations of the field survey, which frequently, though not always, coincided with periods of high tidal velocities and bed shear.

Recommendations

131. Several areas of field data paucity were identified during this study. Further coordinated field investigations are recommended to improve the general understanding and predictive/diagnostic modeling of suspended sediment transport in Central Bay.

a. Map surficial bottom sediment size, metals content, and physico-chemical characteristics related to fine-sediment erodibility seasonally over an annual cycle, and, if possible, over storm events.

b. Analyze historical surveys to identify long-term deposition and erosion trends.

c. Deploy near-bed instrument arrays at various positions in Central Bay to obtain high temporal descriptions of suspended sediment pulses, and associated flow conditions. Simultaneously, investigate local suspended sediments at high spatial resolution using towed sensors.

132. To complete the analysis of long-term transport, additional data sets are needed to quantify transport conditions and for use in future sediment model verification. Such data sets should include, at the minimum, a high-flow wet-weather survey, and possibly a winter frontal passage condition. Duplicate data sets would be desirable. Areas of long-term deposition and erosion within Central, San Pablo, and South Bays should be identified and quantified by comparisons of historical bathymetric surveys, radioisotope tracer studies, and/or grain size characterizations.

133. Several areas of potential numerical model modification,

improvement, or redirection are recommended for future sediment modeling of the Alcatraz site and San Francisco Bay:

a. The ocean boundary in the hydrodynamic model, RMA-2V, should be modified to produce an appropriate, seasonal longshore current in the Gulf of the Farallones. This will more accurately define the exchange of waters between the gulf and San Francisco Bay. The nearshore currents off the California coast can be very complex, seasonally varying, and subject to anomalies most often attributed to eddies, meanders, and counterflows. The California current is a slow southward current generally close to shore during late winter through early fall. A northward countercurrent, the Davidson Current, persists nearshore generally in late fall and early winter. There is some limited evidence of a nearshore poleward flow throughout the year along the central California coast that is not resolved by normal hydrographic data, which is taken too far offshore.

b. The present numerical mesh should be extended to include the southern extremity of South Bay, below Dumbarton Bridge, and to refine the resolution in the immediate vicinity of the Alcatraz site. The mesh extension will directly resolve a difficult boundary condition and the mesh refinement will facilitate the accuracy and stability of the material injection at the disposal site.

c. Settling velocity should be included as a function of TSM concentration in STUDH. Such a relationship has been noted in settling tests on sediments from San Francisco Bay, as well as other estuarine systems.

d. Wind-wave induced bed shear should be incorporated more accurately as a function of wind direction and actual fetch in STUDH. Because wind direction and speed varies both temporally and spatially over the San Francisco Bay system, this may be an important consideration and will require the application of a wind model.

e. The wind-surface stress and density gradient options in operation of RMA-2V should be included, especially to determine the influence on STUDH verification results to the intensive survey data.

f. Improved boundary conditions should be obtained, especially TSM values, for the Gulf of the Faralones. This can be obtained by a more thorough literature search and/or field measurements.

g. The benefit of having multiple grain sizes, essentially silt and clay, for representation of fine-grained material in STUDH should be investigated. The observed rapid temporal fluctuations in field TSM may be the result of a silt fraction that settles rapidly. Because of the computational requirements, this option becomes viable only when a large mainframe or supercomputer is available. The WES supercomputer became available during January 1990.

134. The viability of three-dimensional hydrodynamic and sediment transport numerical modeling should be investigated. A coarse mesh for limited three-dimensional hydrodynamic-salinity simulations was used on the John F. Baldwin Phase III Ship Channel Project, and the mesh is available for adaptation as a three-dimensional sediment mesh. However, three-dimensional sediment modeling is not presently an off-the-shelf application, and must be approached with much forethought.

REFERENCES

Ackers, P., and White, W. R. 1973 (Nov). "Sediment Transport: New Approach and Analysis," Journal, Hydraulics Division, American Society of Civil Engineers, Vol 99, No. HY-11, pp 2041-2060.

Ariathurai, R., MacArthur, R. D., and Krone, R. C. 1977 (Oct). "Mathematical Model of Estuarial Sediment Transport," Technical Report D-77-12, US Army Engineer Waterways Experiment Station, Vicksburg, MS.

Cheng, R. T., and Gartner, J. W. 1984 (Feb). "Tides, Tidal and Residual Currents in San Francisco Bay, California-Results of Measurements, 1979-1980," Water Resources Investigations Report 84-4339, US Geological Survey, Menlo Park, CA.

Coleman, C. J., Teeter, A. M., Donnell, B. P., Fisackerly, G. M., Crouse, D. A., and Parman, J. W. 1988 (Jun). "The Atchafalaya River Delta; Report 2, Field Data; Section 1: Atchafalaya Bay Program Description and Data," Technical Report HL-82-15, US Army Engineer Waterways Experiment Station, Vicksburg, MS.

Conomos, T. J., and Peterson, D. H. 1976. "Suspended-Particle Transport and Circulation in San Francisco Bay: An Overview," Estuarine Processes; Volume II, Circulation, Sediment and Transfer of Material in the Estuary, Academic Press, San Francisco, CA, pp 82-97.

deGroot, A. J. 1964. "Origin and Transport of Mud (Fraction <16 Microns) in Coastal Waters From the Western Scheldt to the Danish Frontier," Deltaic and Shallow Marine Deposits, Proceedings, Sixth International Sedimentation Congress, The Netherlands and Belgium, 1963, L. M. J. U. Van Straaten, ed., Elsevier Publishing, New York, pp 93-100.

Eaton, A., Grant, V., and Gross, M. G. 1980. "Chemical Tracers for Particle Transport in the Chesapeake Bay," Estuarine and Coastal Marine Science, Vol 10, pp 75-83.

Einstein, H. A., and Krone, R. B. 1961 (Mar). "Estuarial Sediment Transport Patterns," Journal, Hydraulic Division, American Society of Civil Engineers, Vol 87, No. HY 2, pp 51-59.

Friedrichs, C. T., and Aubrey, D. G. 1988. "Non-linear Tidal Distortion in Shallow Well-Mixed Estuaries: A Synthesis," Estuarine, Coastal, and Shelf Science, Vol 27, pp 521-545.

Hauck, L. M., Heltzel, S. B., and Teeter, A. M. "San Francisco Bay Hydrodynamic and Salinity Modeling: John F. Baldwin Phase III Channel Modifications" (in preparation), US Army Engineer Waterways Experiment Station, Vicksburg, MS.

Helz, G. R., Sinex, S. A., Ferri, K. L., and Nichols, M. 1985. "Processes Controlling Fe, Mn, and Zn in Sediments of Northern Chesapeake Bay," Estuarine, Coastal, and Shelf Science, Vol 21, pp 1-16.

Krone, R. B. 1962. "Flume Studies of Transport of Sediment in Estuarial Shoaling Processes," Final Report, Hydraulics Engineering Research Laboratory, University of California, Berkeley, CA.

Krone, R. B. 1976. "Ultimate Fate of Suspended Material in Estuaries," Pro-ceedings of the Specialty Conference on Dredging and its Environmental Ef-fects, American Society of Civil Engineers, Mobile, AL, pp 180-201.

_____. 1979. "Sedimentation in the San Francisco Bay System," San Francisco Bay: The Urbanized Estuary, American Association for the Advance-ment of Science, Pacific Division, San Francisco, CA, pp 85-96.

Morris, A. W., Bale, A. J., and Howland, R. J. M. 1982. "The Dynamics of Estuarine Manganese Cycling," Estuarine, Coastal, and Shelf Science, Vol 14, pp 175-192.

National Ocean Service. 1985 (Nov). "National Estuarine Inventory - Data Atlas, Volume 1: Physical and Hydrologic Characteristics," US Department of Commerce, National Oceanic and Atmospheric Administration, Rockville, MD.

Pankow, Virginia R. 1988 (Nov). "San Francisco Bay: Modeling System for Dredged Material Disposal and Hydraulic Transport," Technical Report HL-88-27, US Army Engineer Waterways Experiment Station, Vicksburg, MS.

Rubin, D. M., and McCulloch, D. S. 1979. "The Movement and Equilibrium of Bedforms in Central San Francisco Bay," San Francisco Bay: The Urbanized Estuary, American Association for the Advancement of Science, Pacific Divi-sion, San Francisco, CA, pp 97-113.

Science Applications International Corporation. 1987a (Apr). "Alcatraz Dis-posal Site Survey, Phase I, San Rafael Clamshell/Scow Operation Technical Report," SAIC Report #87/7513-142, Newport, RI.

_____. 1987b (May). "Alcatraz Disposal Site Survey, Phase II, Richmond Channel Hopper Dredge Operation Technical Report," SAIC Report #87/7517-144, Submitted to US Army Engineer District, San Francisco, San Francisco, CA.

Smith, R. E., Herndon, R. E., and Harmon, D. D. 1979. "Physical and Chemical Properties of San Francisco Bay Waters, 1969-1976," Open File Report 79-511, US Geological Survey.

Teeter, A. M. 1987 (May). "Alcatraz Disposal Site Investigation, Report 3, San Francisco Bay - Alcatraz Disposal Site Erodibility," Miscellaneous Paper HL-86-1, US Army Engineer Waterways Experiment Station, Vicksburg, MS.

Thomas, W. A., and McAnally, W. H., Jr. 1985 (Aug). "User's Manual for the Generalized Computer Program System; Open-Channel Flow and Sedimentation, TABS-2, Main Text and Appendices A through O," Instruction Report HL-85-1, US Army Engineer Waterways Experiment Station, Vicksburg, MS.

Trawle, M. J., and Johnson, B. H. 1986a. "Alcatraz Disposal Site Investiga-tion," Miscellaneous Paper HL-86-1, US Army Engineer Waterways Experiment Station, Vicksburg, MS.

_____. 1986b. "Alcatraz Disposal Site Investigation; North Zone of Oakland Outer Harbor and Richmond Inner Harbor Sediments," Report 2, Miscel-laneous Paper HL-86-1, US Army Engineer Waterways Experiment Station, Vicksburg, MS.

US Army Engineer District, San Francisco. 1963 (Mar). "Comprehensive Survey of San Francisco Bay and Tributaries, California; Appendix H, Hydraulic Model Studies; Volume I, Text and Figures; and Volume II, Plates: Verification and Tests of Barriers, to the Technical Report on San Francisco Bay Barriers," San Francisco, CA.

US Army Engineer District, San Francisco. 1976 (Jun). "San Francisco Bay and Sacramento, San Joaquin Delta Water Quality and Waste Disposal Investigation, San Francisco Bay; Model Verification and Results of Sensitivity Test," Delta Model Technical Memorandum No. 1, San Francisco, CA.

_____. 1977 (Feb). "Dredge Disposal Study, San Francisco Bay and Estuary," Main Report and Appendices A-M, San Francisco, CA.

_____. 1981 (Dec). "User's Guide for the San Francisco Bay-Delta Tidal Hydraulic Model," San Francisco, CA.

_____. 1984 (Oct). "Repeatability Study: San Francisco Bay-Delta Hydraulic Model," San Francisco, CA.

Welch, J. M., Gartner, J. W., and Gill, S. K. 1985 (Nov). "San Francisco Area Circulation Survey: 1979-1980," NOS Oceanographic Circulation Survey Report No. 7, National Ocean Service, Rockville, MD.

Winzler and Kelly. 1985 (Sep). "Oceanographic Investigation at the Alcatraz Disposal Site, San Francisco Bay, California," prepared by Winzler and Kelly, Consulting Engineers, San Francisco, CA, for the US Army Engineer District, San Francisco, San Francisco, CA.

Zvirin, Y., and Shinnar, R. 1976. "Interpretation of Internal Tracer Experiments and Local Sojourn Time Distributions," International Journal of Multiphase Flow, Vol 2, pp 495-520.
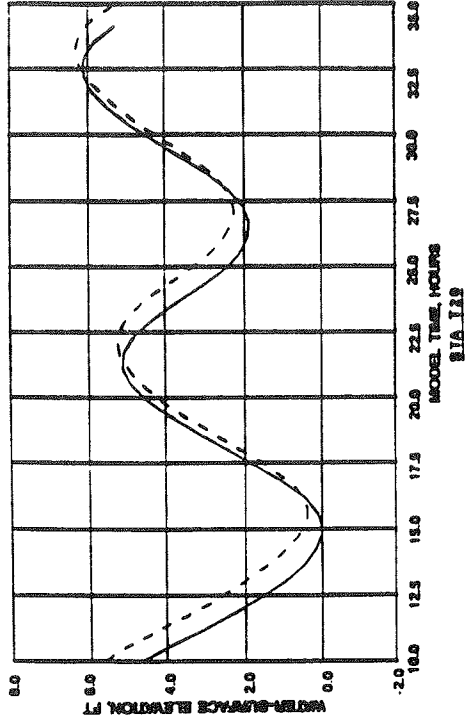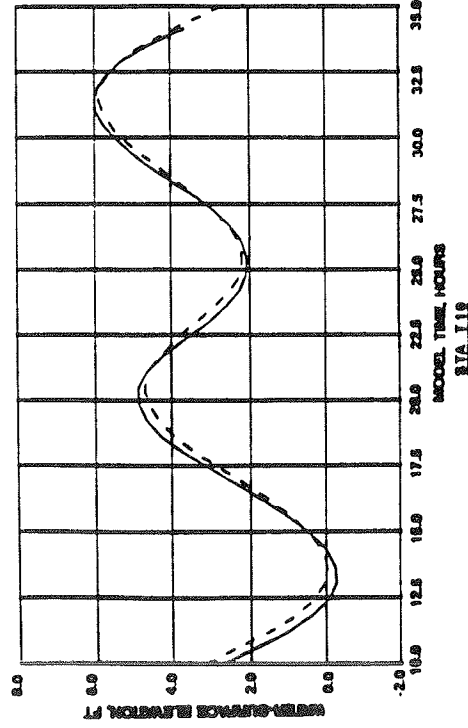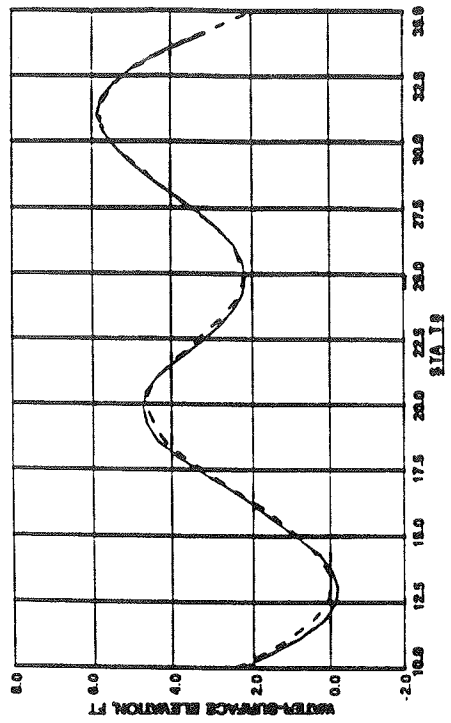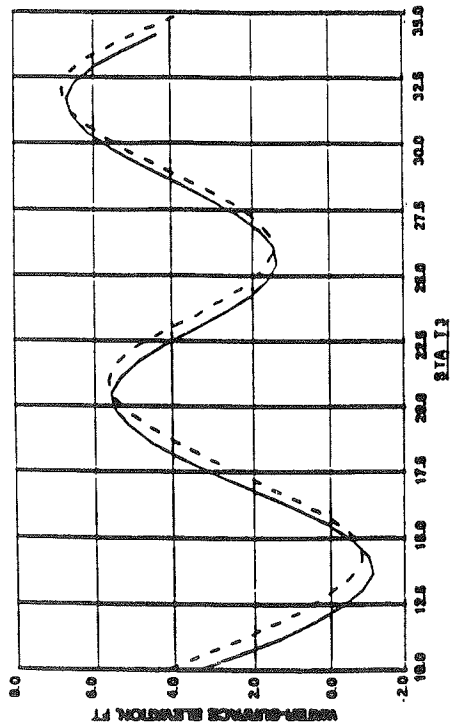
MESH A
MEAN TIDE WATER-SURFACE DATA
RMA-2V VERSUS PHYSICAL MODEL
STA T3, T8, T10, T20
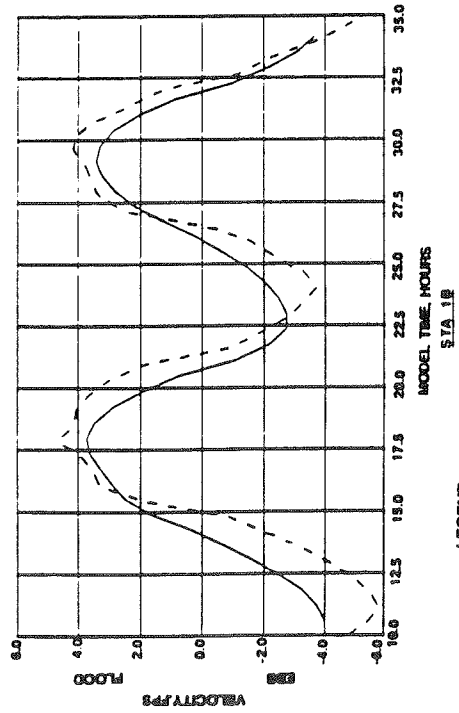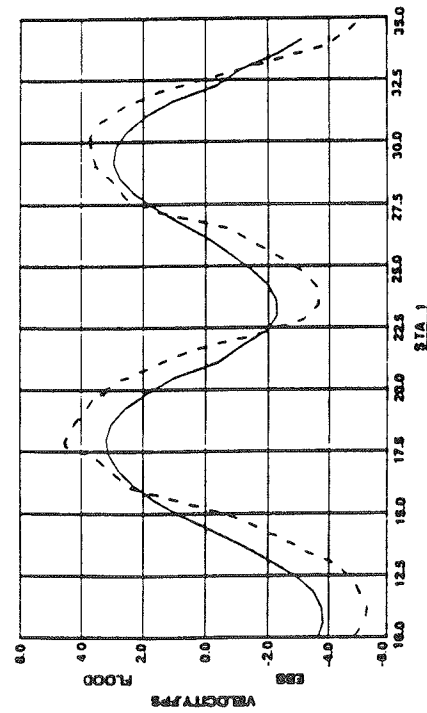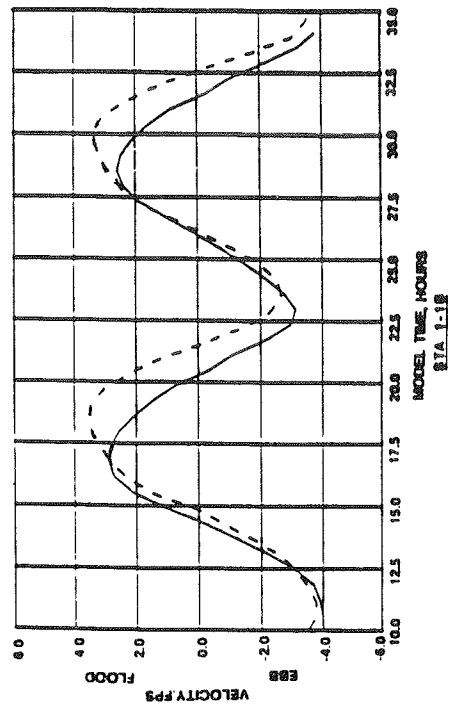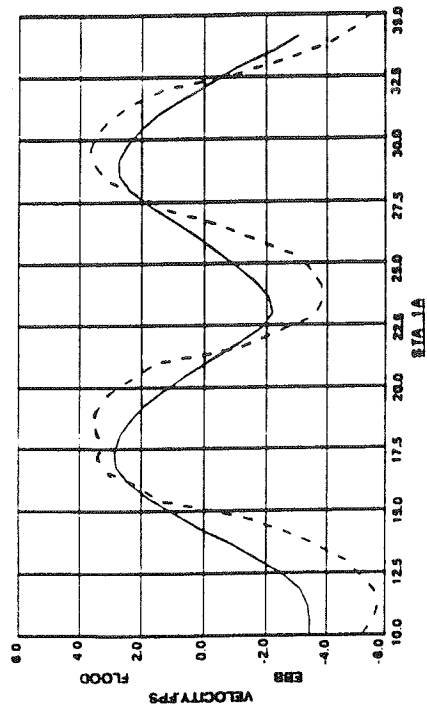
PLATE 1

MESH A
MEAN TIDE VELOCITY DATA
RMA-2V VERSUS PHYSICAL MODEL
STA 1, 1A, 1B, 1-1B
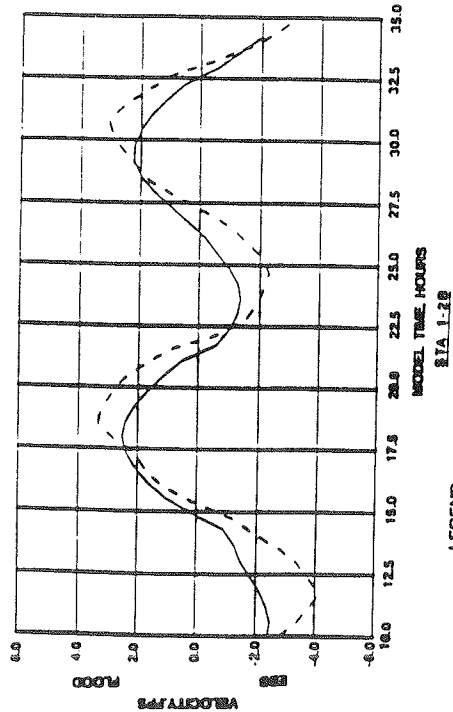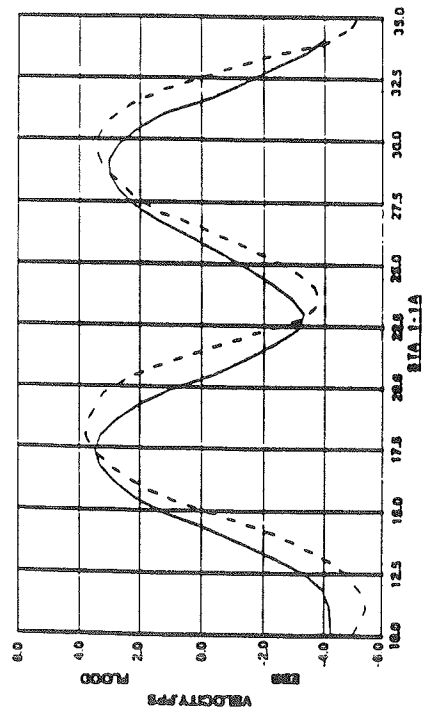
PLATE 2
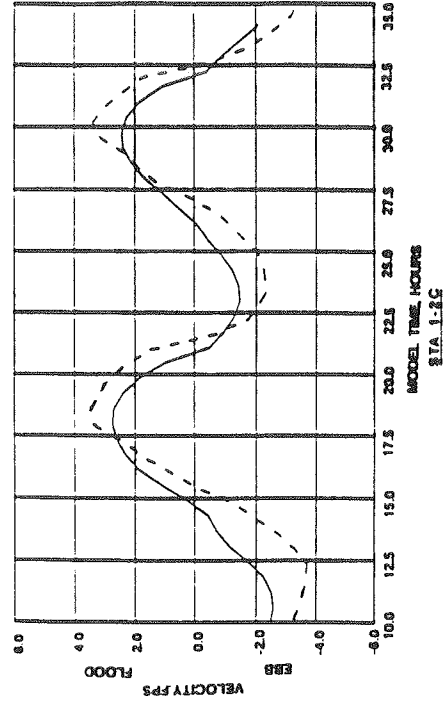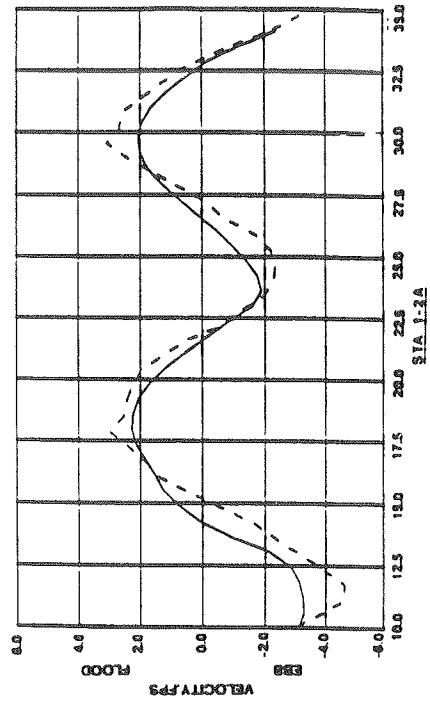
MESH A
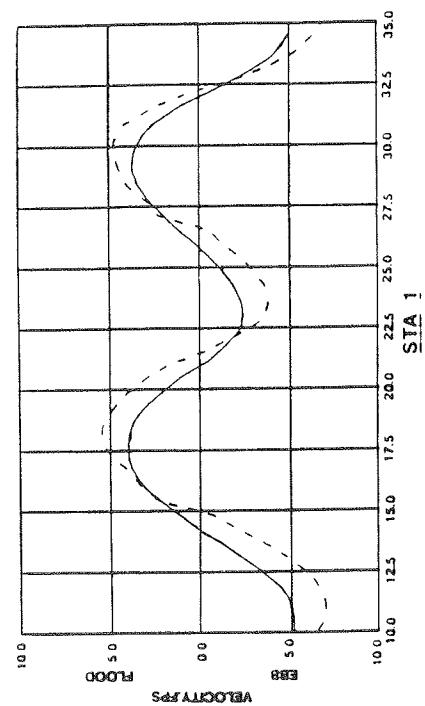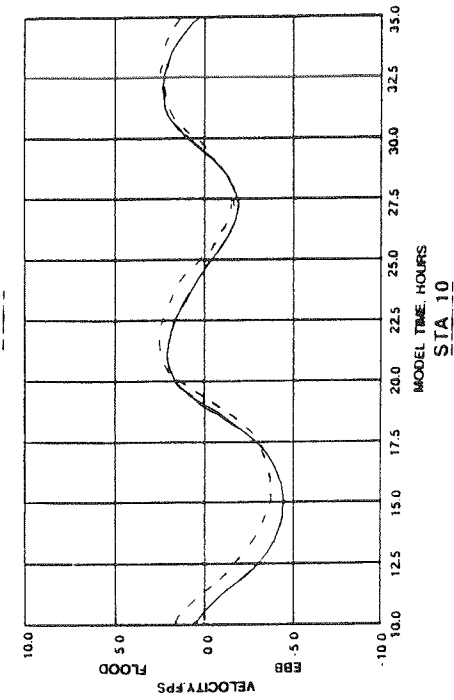MEAN TIDE VELOCITY DATA
RMA-2V VERSUS PHYSICAL MODEL
STA 1-1A, 1-2A, 1-2B, 1-2C
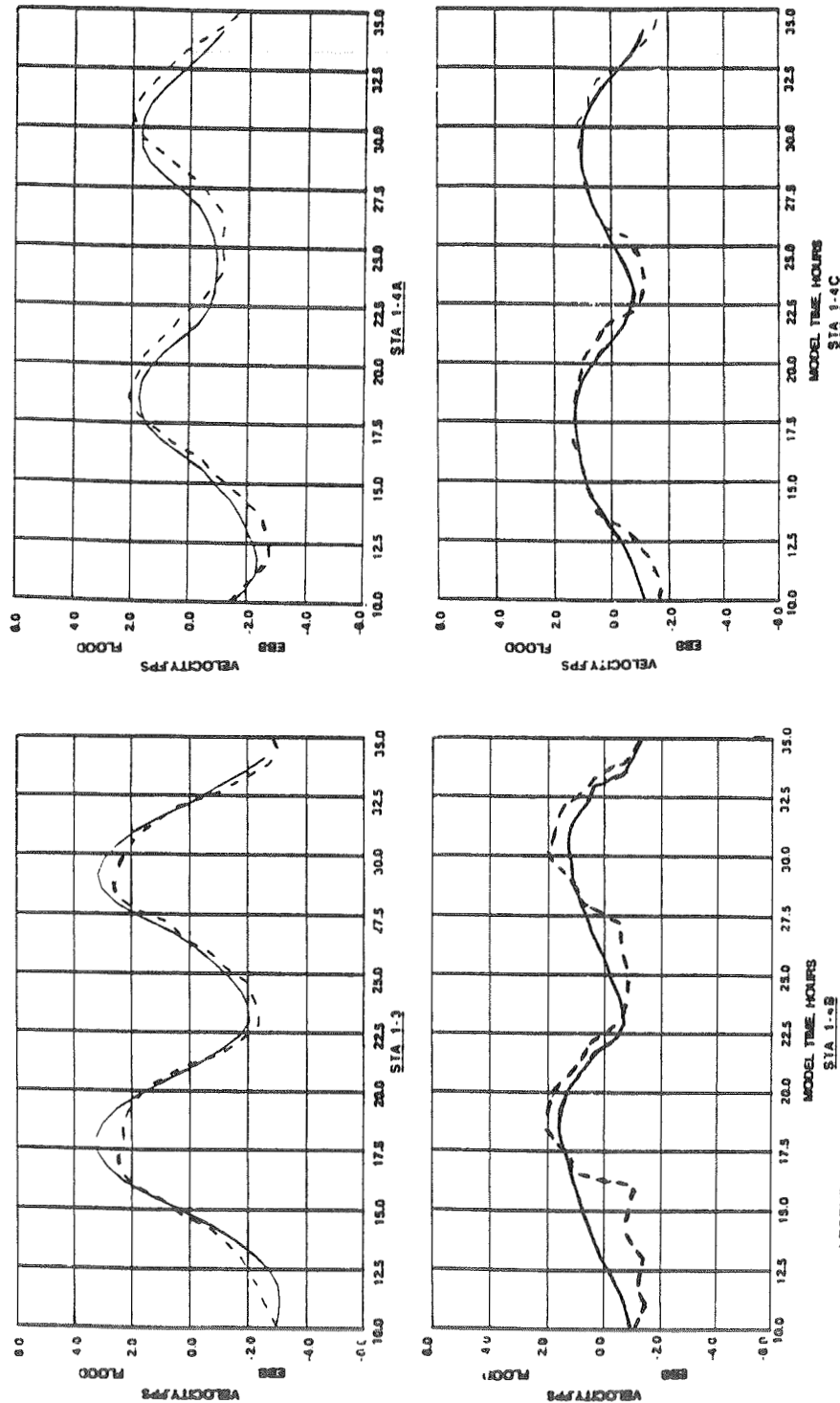
PLATE 3

MESH A
MEAN TIDE VELOCITY DATA
RMA-2V VERSUS PHYSICAL MODEL
STA 1-3, 1-4A, 1-4B, 1-4C
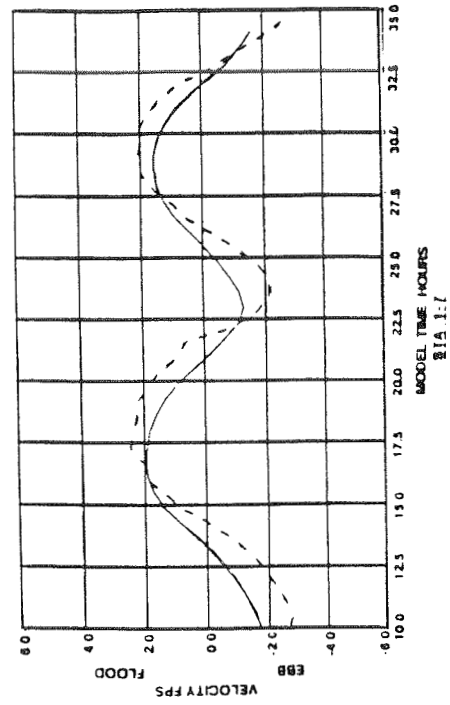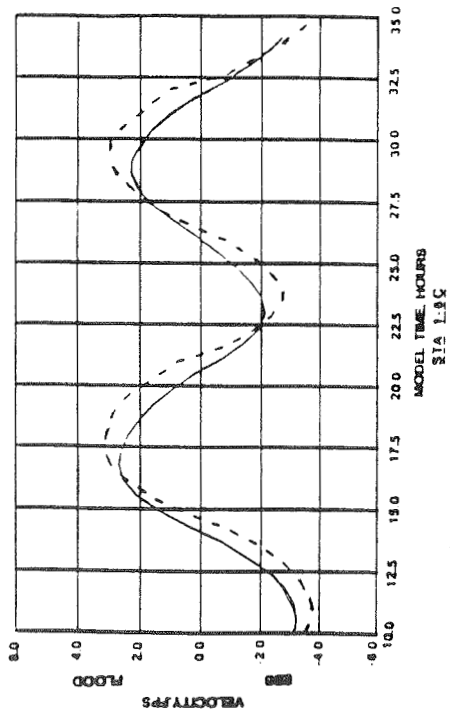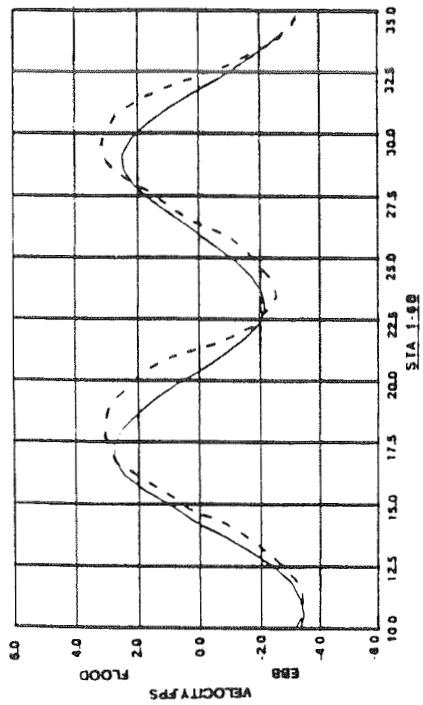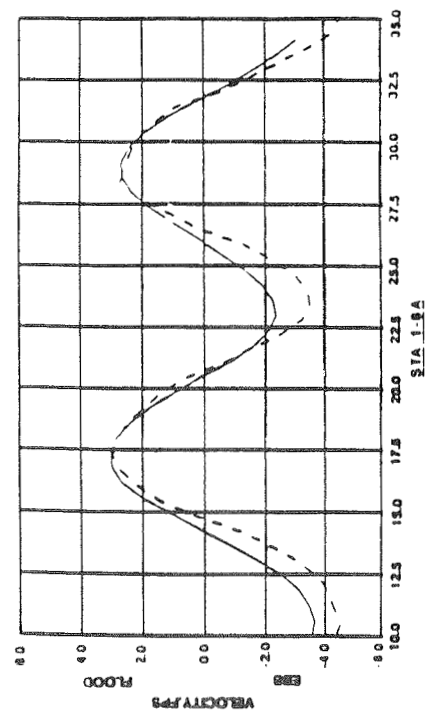
PLATE 4

MESH A

MEAN TIDE VELOCITY DATA

RMA-2V VERSUS PHYSICAL MODEL

STA 1-6A, 1-6B, 1-6C, 1-7
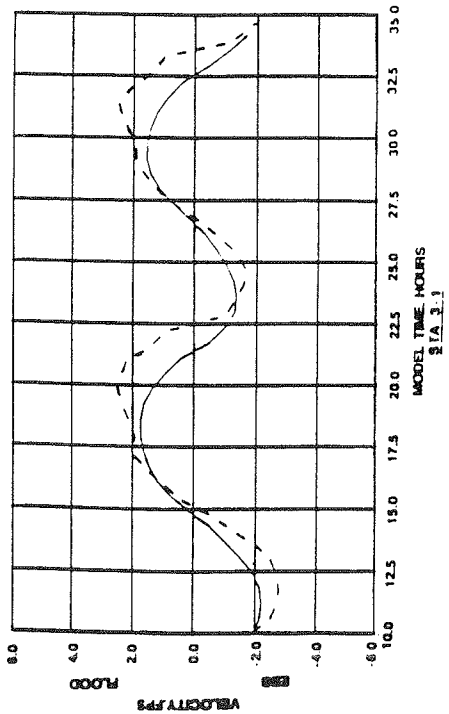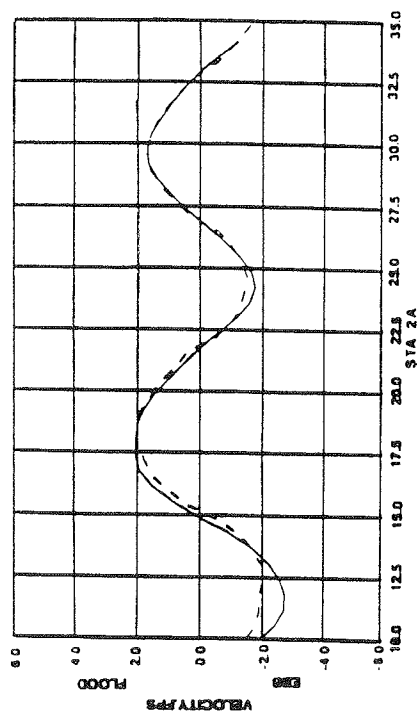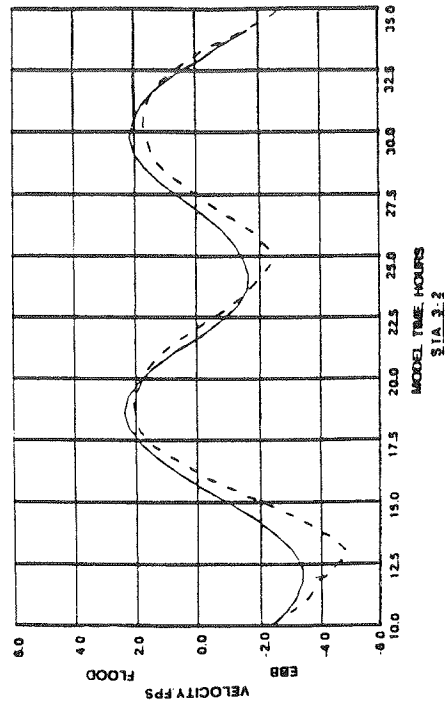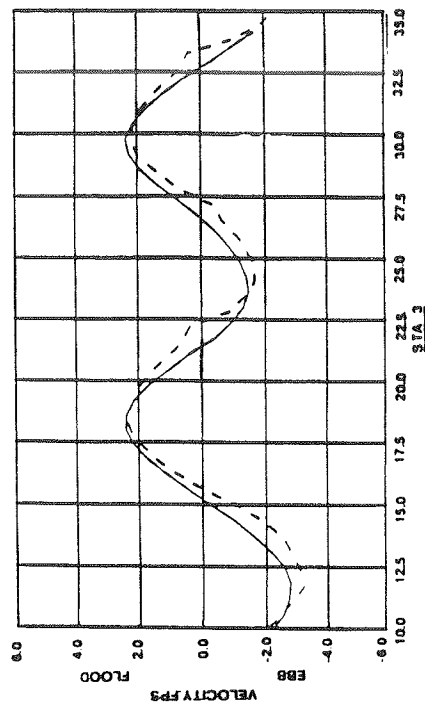
PLATE 5

MESH A
MEAN TIDE VELOCITY DATA
RMA-2V VERSUS PHYSICAL MODEL
STA 2A, 3.3-1, 3.2

LEGEND
— RMA-2V
--- PHYSICAL MODEL

PLATE 6
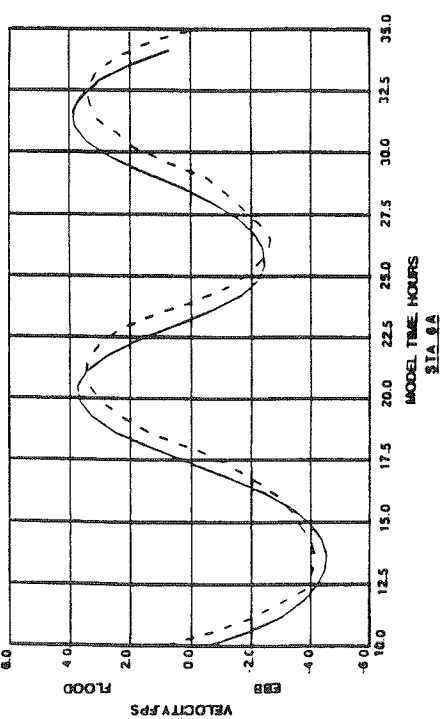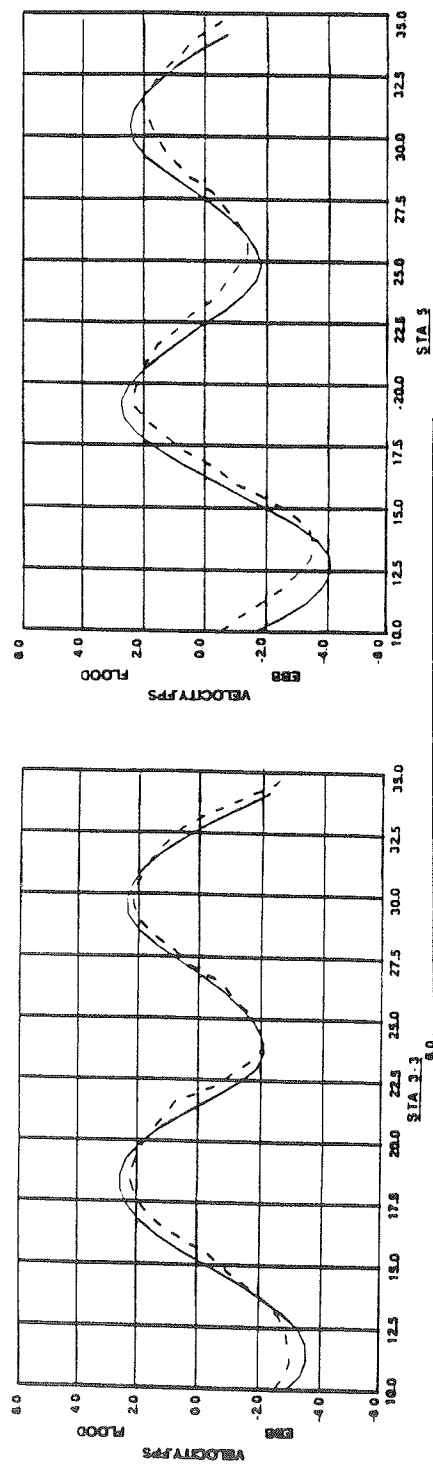
MESH A
MEAN TIDE VELOCITY DATA
RMA-2V VERSUS PHYSICAL MODEL
STA 3-3, 5, 8A

LEGEND
— RMA-2V
--- PHYSICAL MODEL

PLATE 7
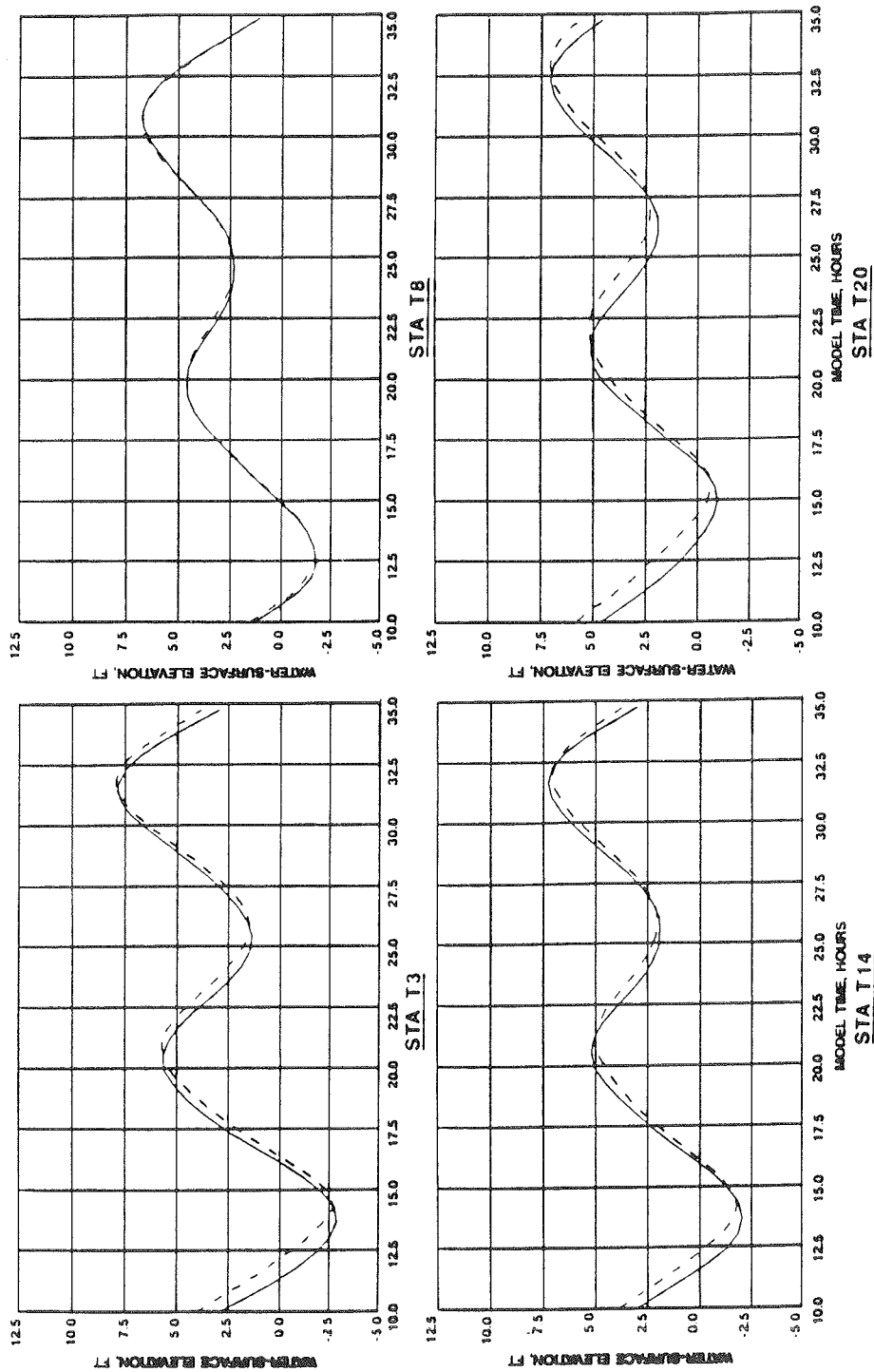
SPRING TIDE WATER-SURFACE DATA

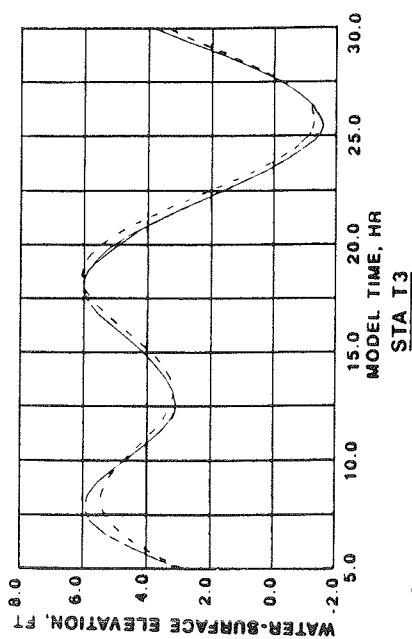RMA-2V VERSUS PHYSICAL MODEL

STA T3, T8, T14, T20

PLATE 8
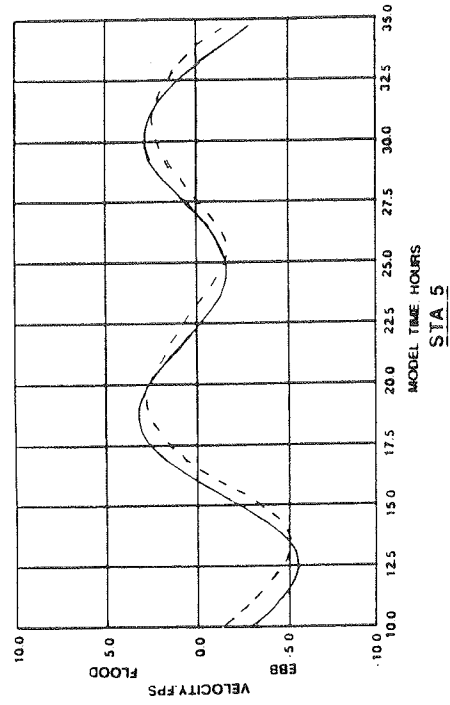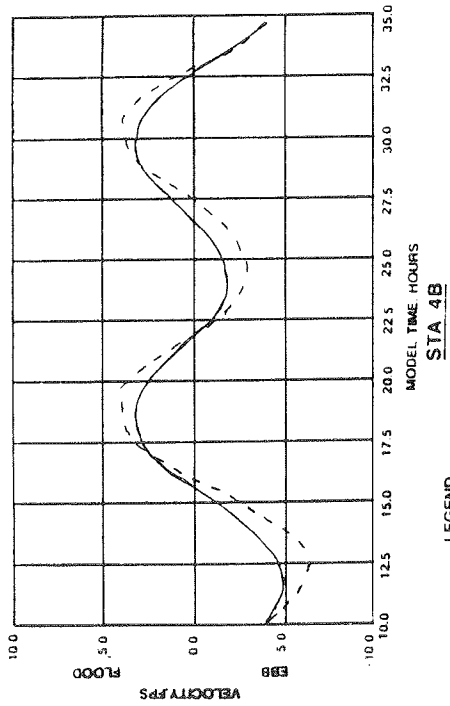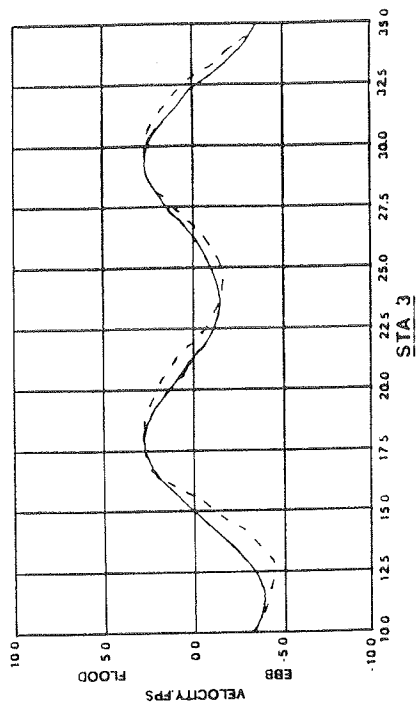
SPRING TIDE VELOCITY DATA
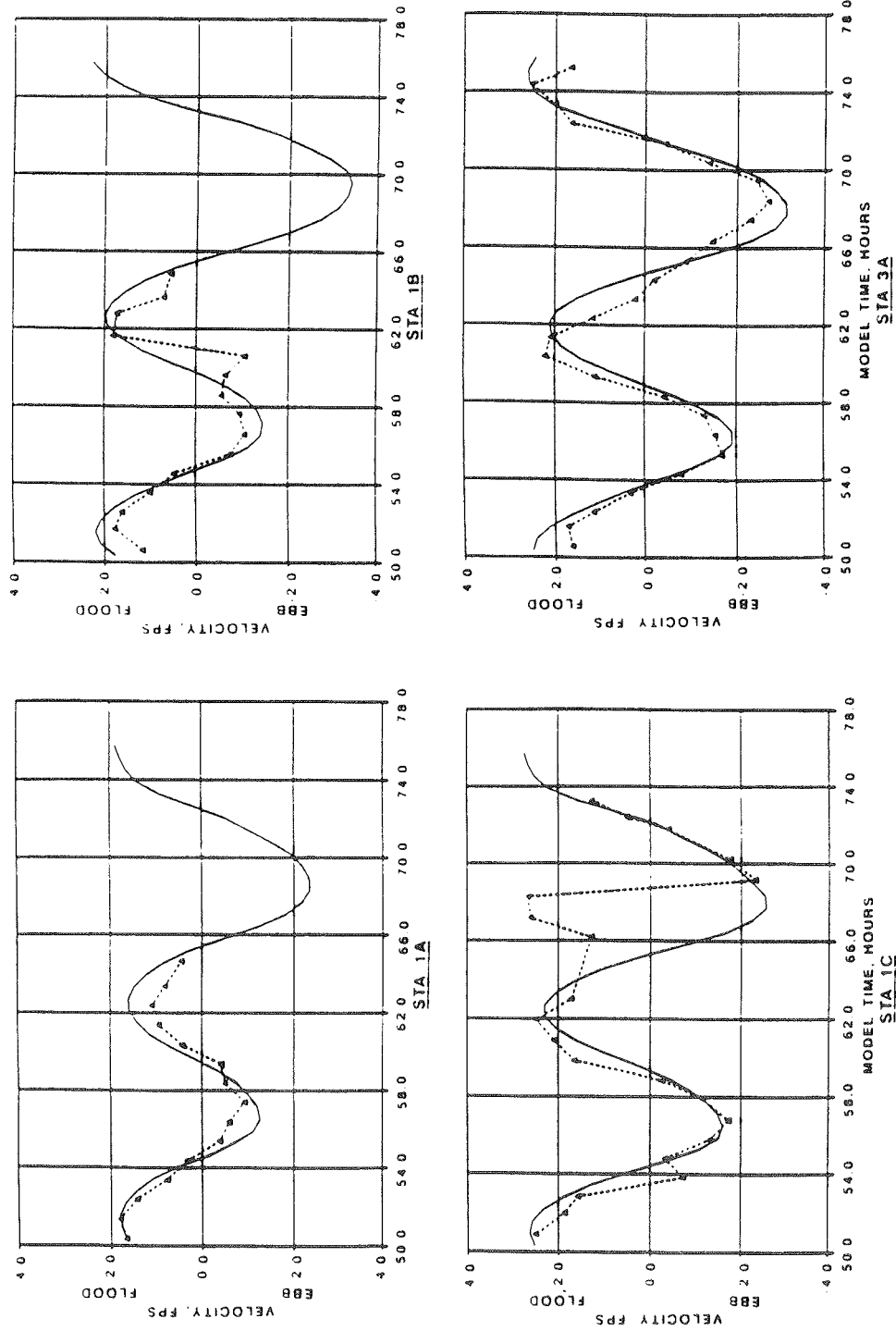RMA-2V VERSUS PHYSICAL MODEL
STA 1, 3, 4B, 5

LEGEND
— RMA-2V
--- PHYSICAL MODEL

PLATE 9
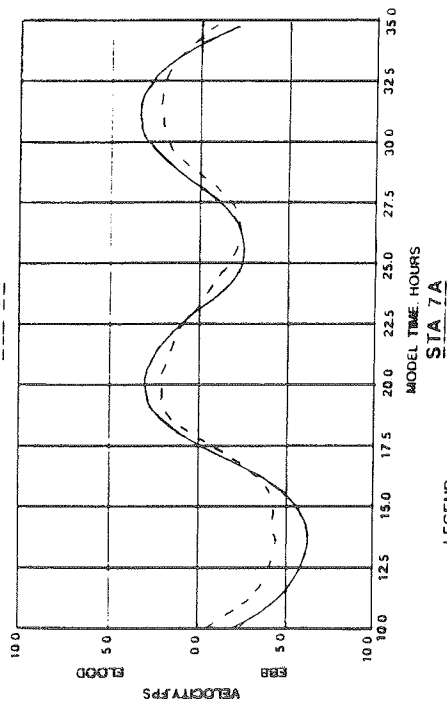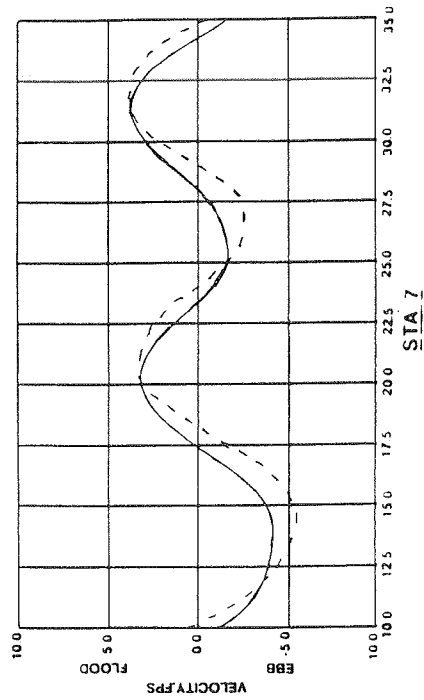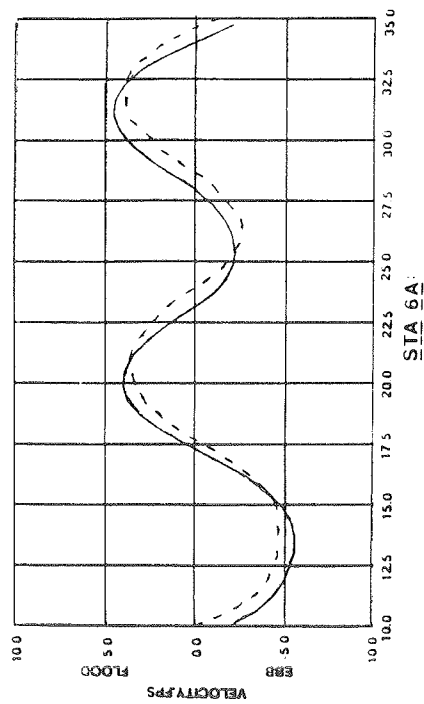
SPRING TIDE VELOCITY DATA
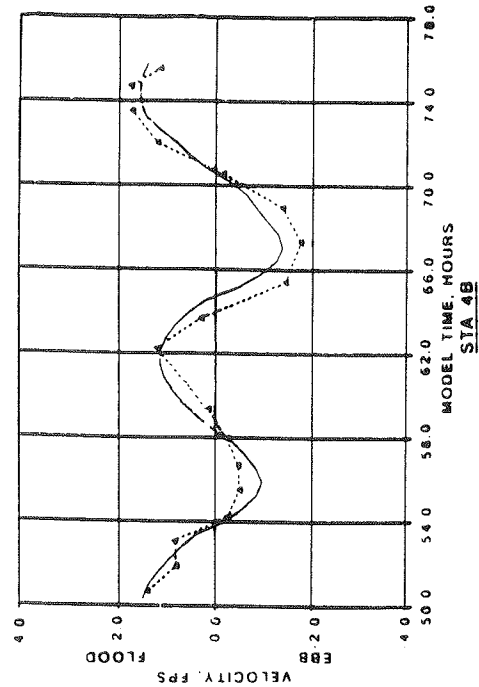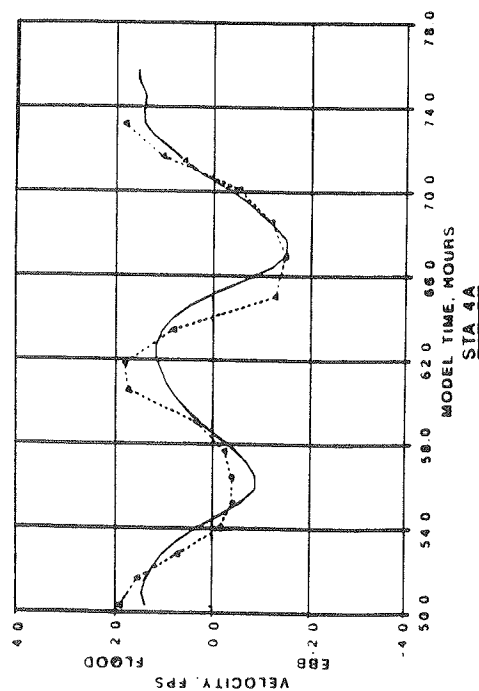RMA-2V VERSUS PHYSICAL MODEL
STA 6A, 7, 7A, 10

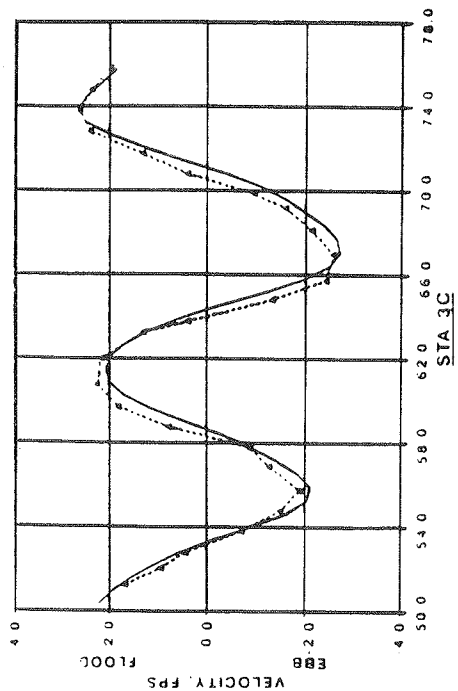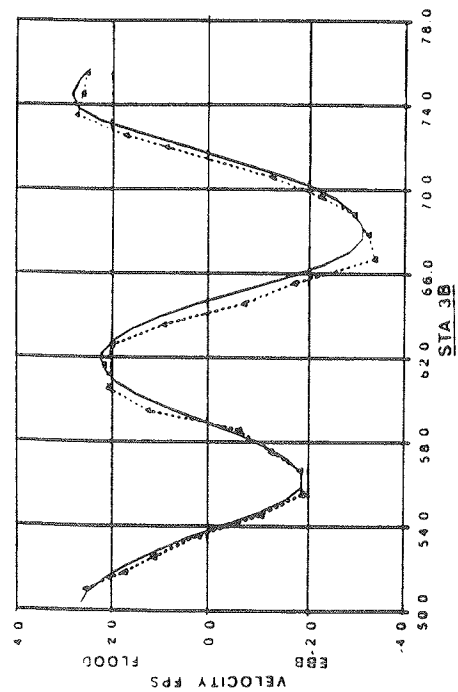PLATE 10
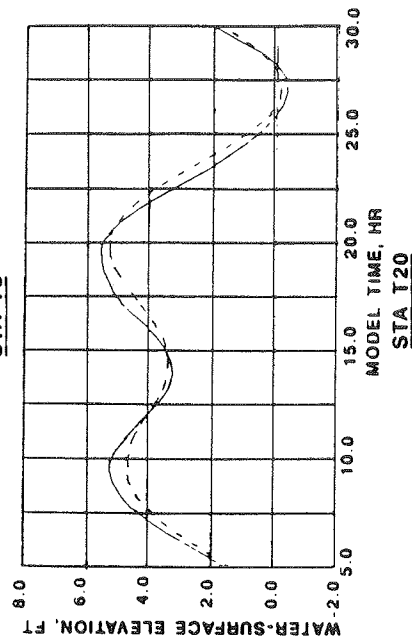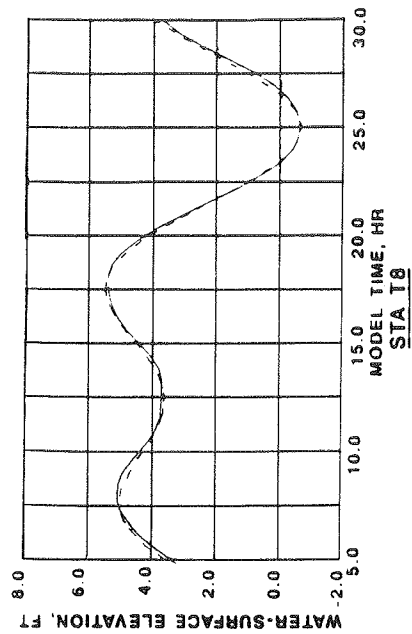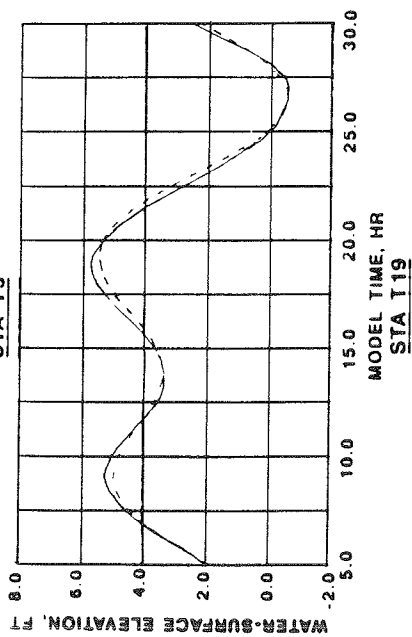
HARMONIC TIDE WATER-SURFACE DATA
RMA-2V VERSUS FIELD DATA
STA T3, T8, T19, T20

PLATE 11

7-8 SEPTEMBER 1988 DATA
RMA-2V VERSUS FIELD MEASUREMENTS
STA 1A, 1B, 1C, 3A

PLATE 12

7-8 SEPTEMBER 1988 DATA
RMA-2V VERSUS FIELD MEASUREMENTS
STA 3B, 3C, 4A, 4B

PLATE 13
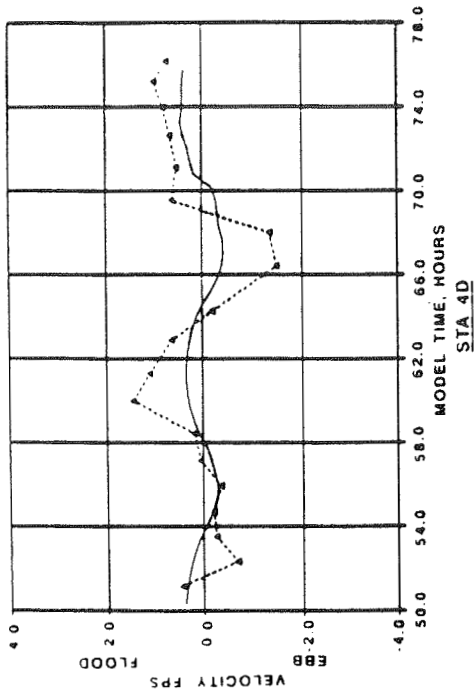
7-8 SEPTEMBER 1988 DATA
RMA-2V VERSUS FIELD MEASUREMENTS
STA 4C, 4D
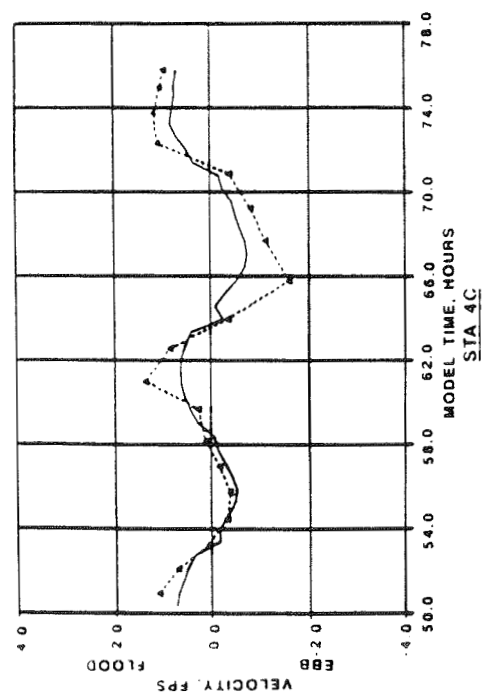
LEGEND
—— RMA-2V
--- FIELD MEASUREMENTS

PLATE 14

NODE 1307 (1A)

NODE 1312 (1B)
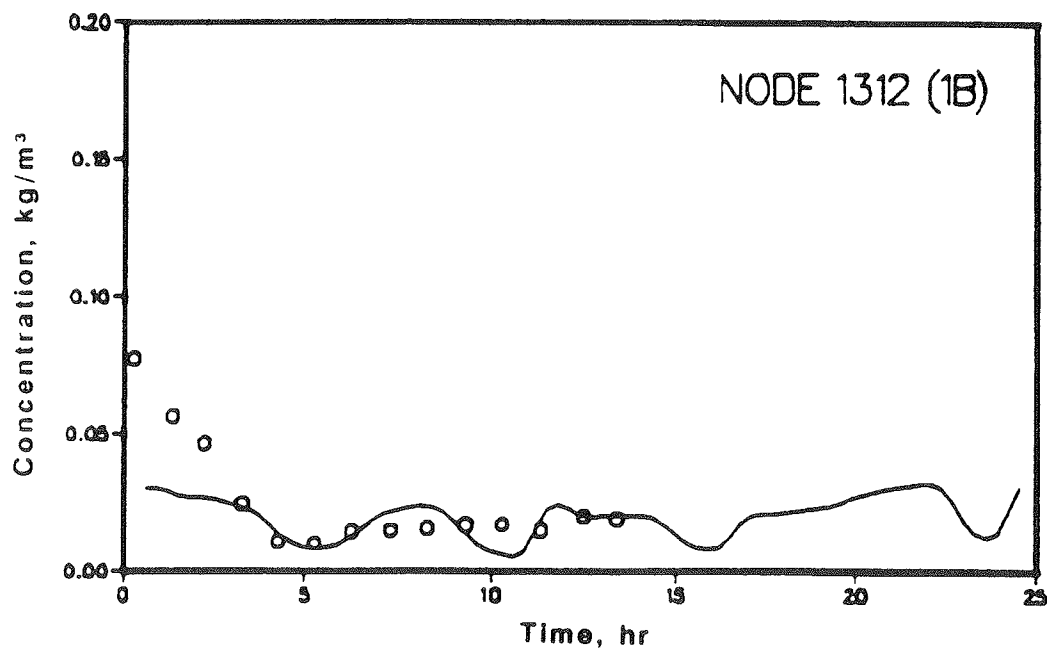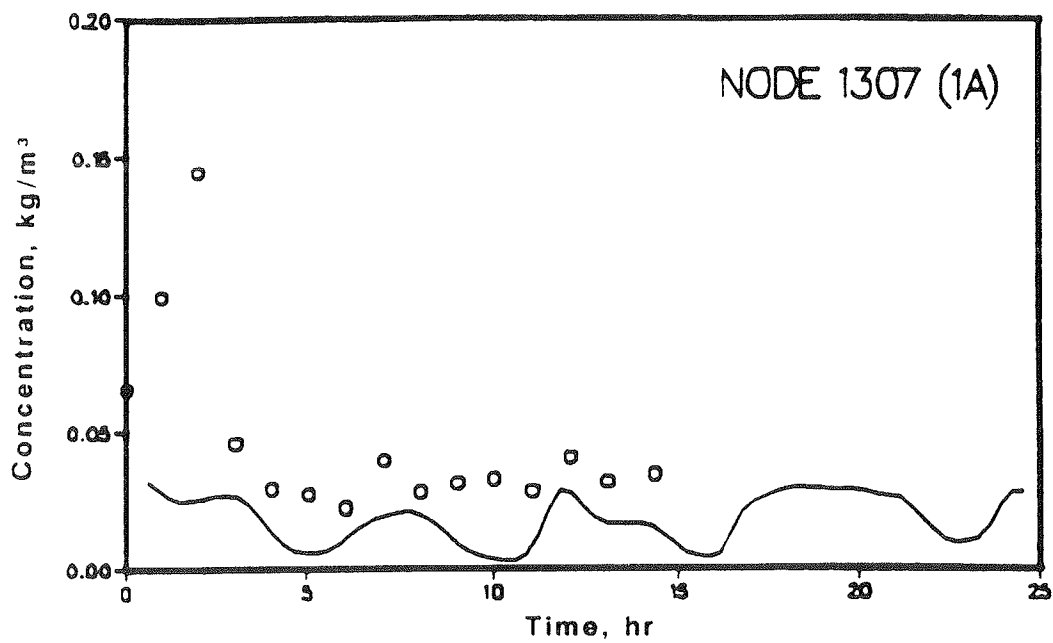
LEGEND
—— STUDH
○ VERTICALLY AVERAGED
FIELD DATA

STUDH Results
Nodes 1307(1A) & 1312(1B)

PLATE 15

NODE 1319 (1C)

NODE 2206 (2A)

LEGEND
—— STUDH
O VERTICALLY AVERAGED
   FIELD DATA

STUDH Results

Nodes 1319 (1C) & 2206 (2A)

PLATE 16

NODE 2250 (2B)

NODE 2300 (2C)
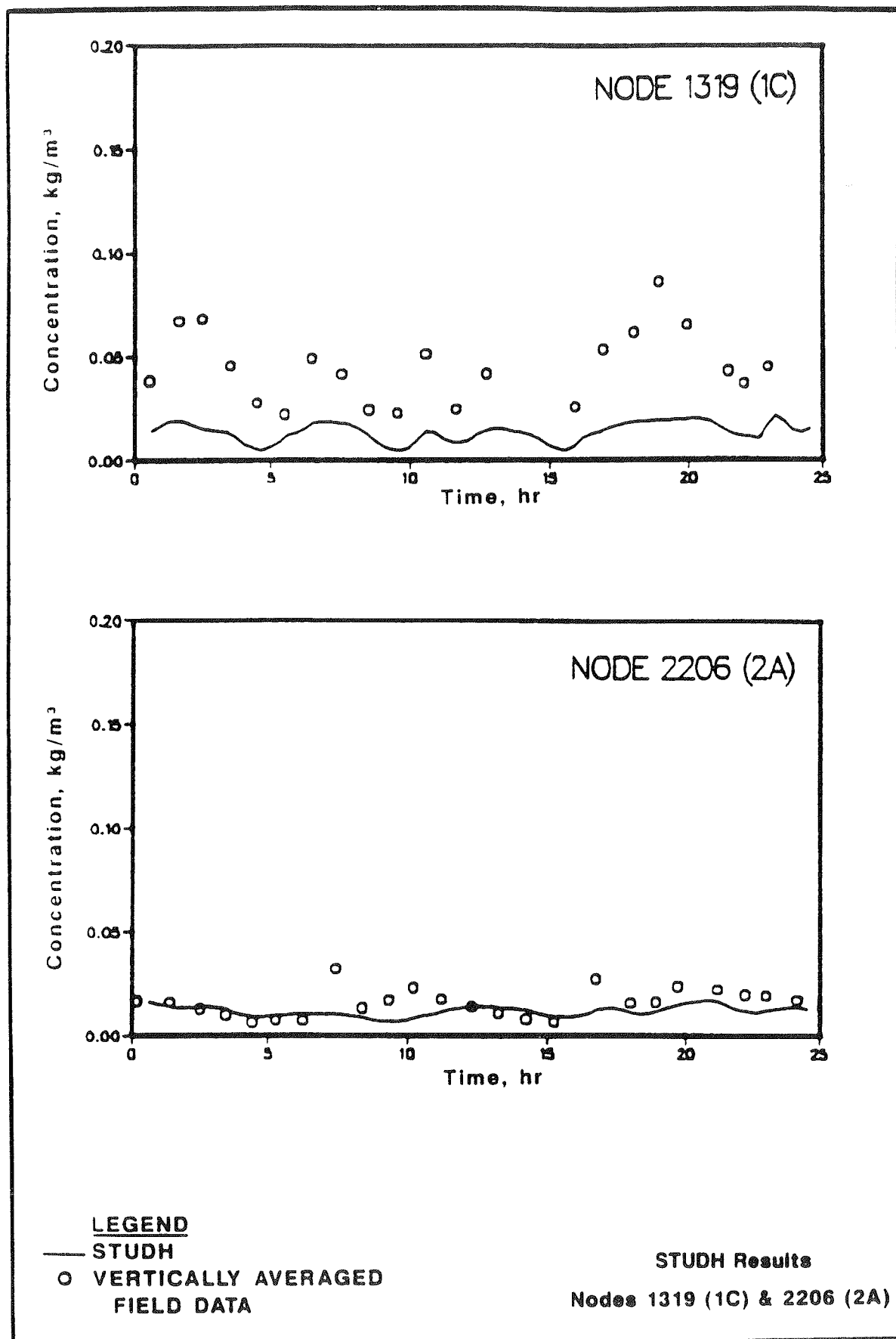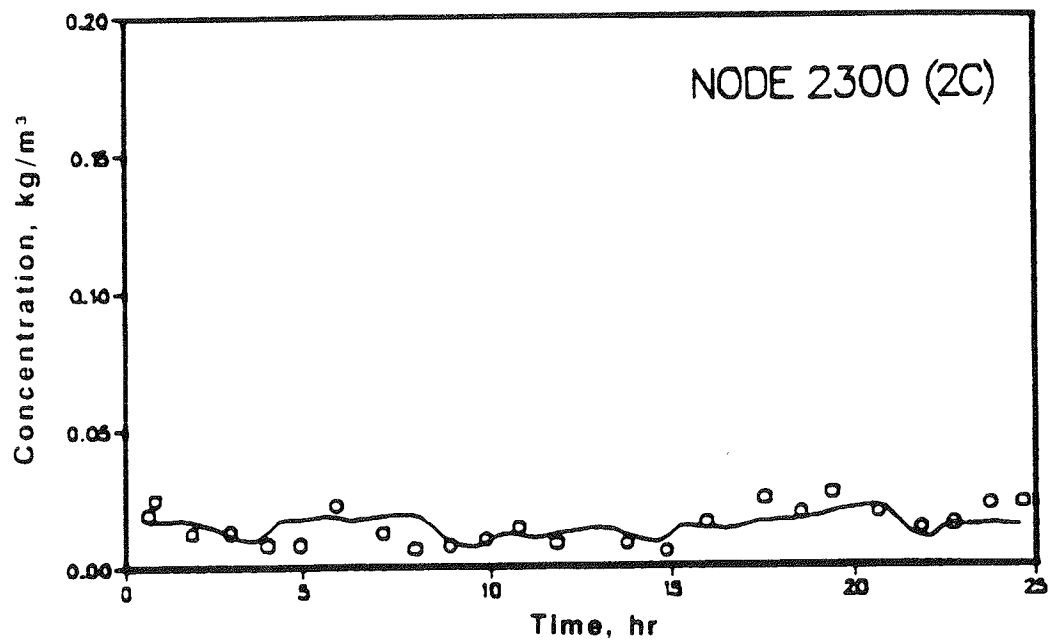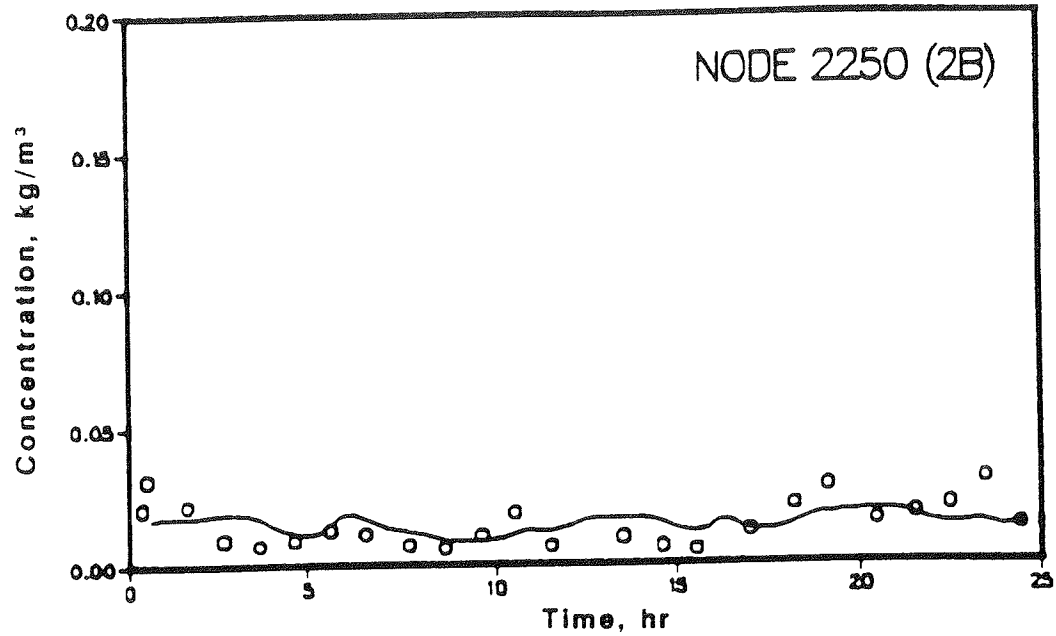
LEGEND

—— STUDH

○ VERTICALLY AVERAGED
   FIELD DATA

STUDH Results

Nodes 2250 (2B) & 2300 (2C)

PLATE 17

NODE 3783 (3A)

NODE 3785 (3B)

LEGEND
—— STUDH
○ VERTICALLY AVERAGED
FIELD DATA

STUDH Results

Nodes 3783 (3A) & 3785 (3B)

PLATE 18
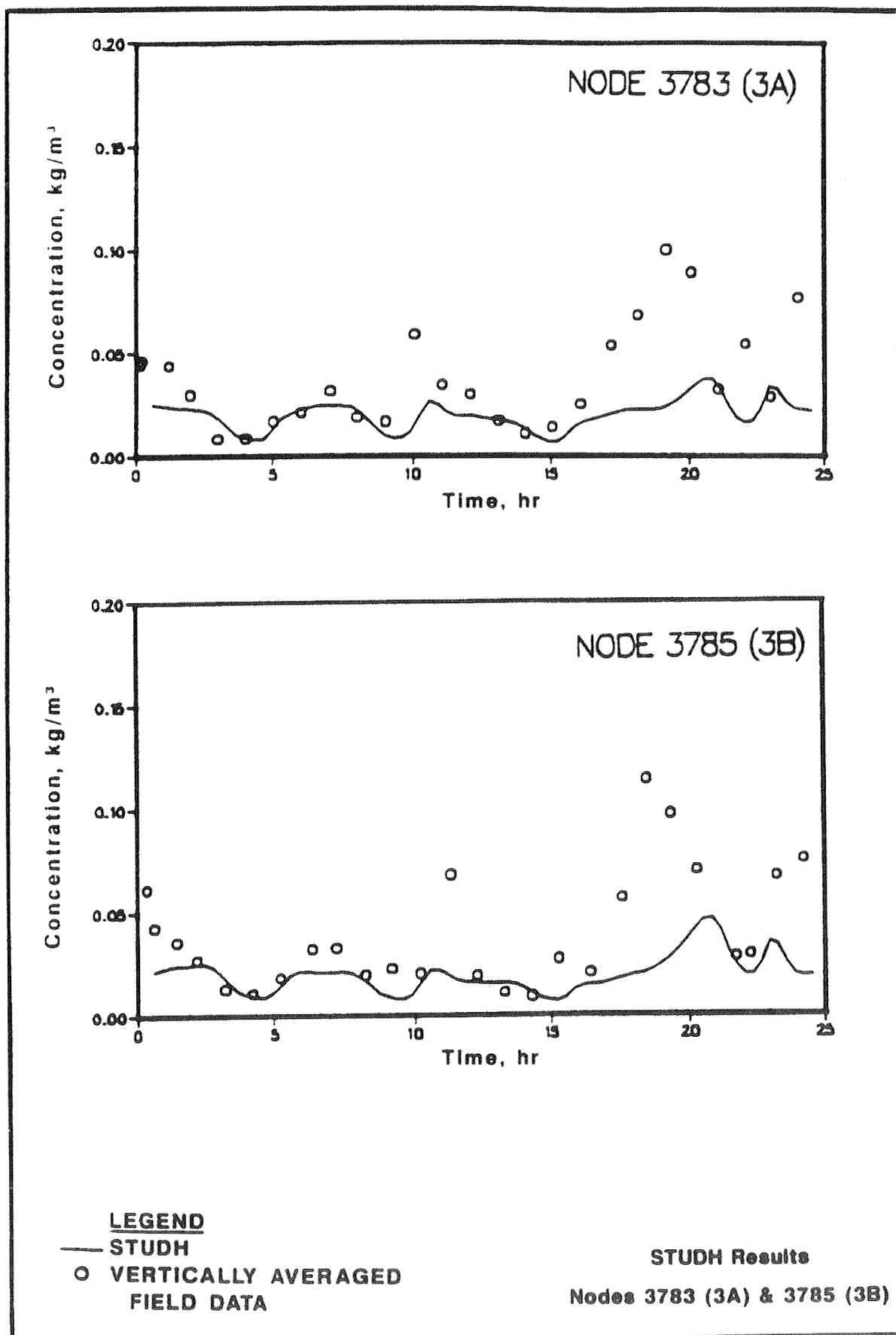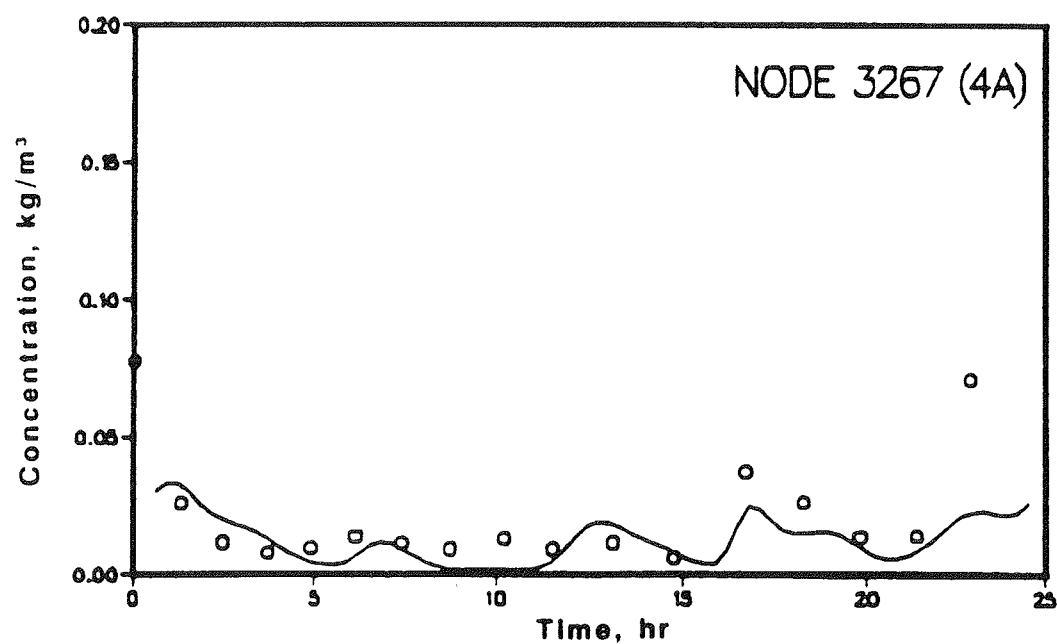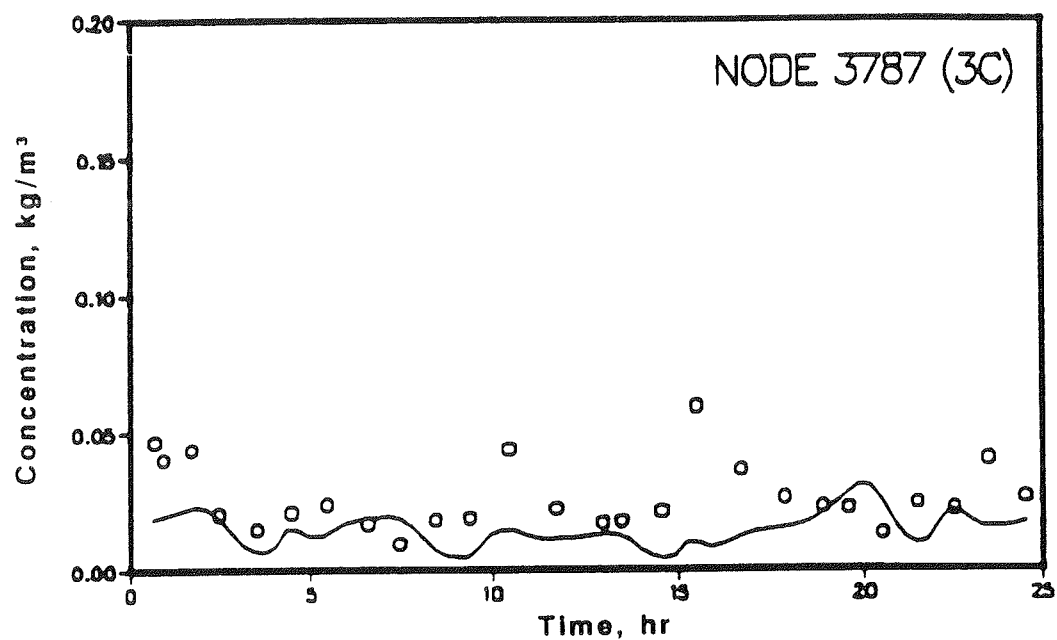
LEGEND
STUDH
○ VERTICALLY AVERAGED
FIELD DATA

STUDH Results
Nodes 3787(3C) & 3267(4A)

PLATE 19

NODE 3275 (4B)
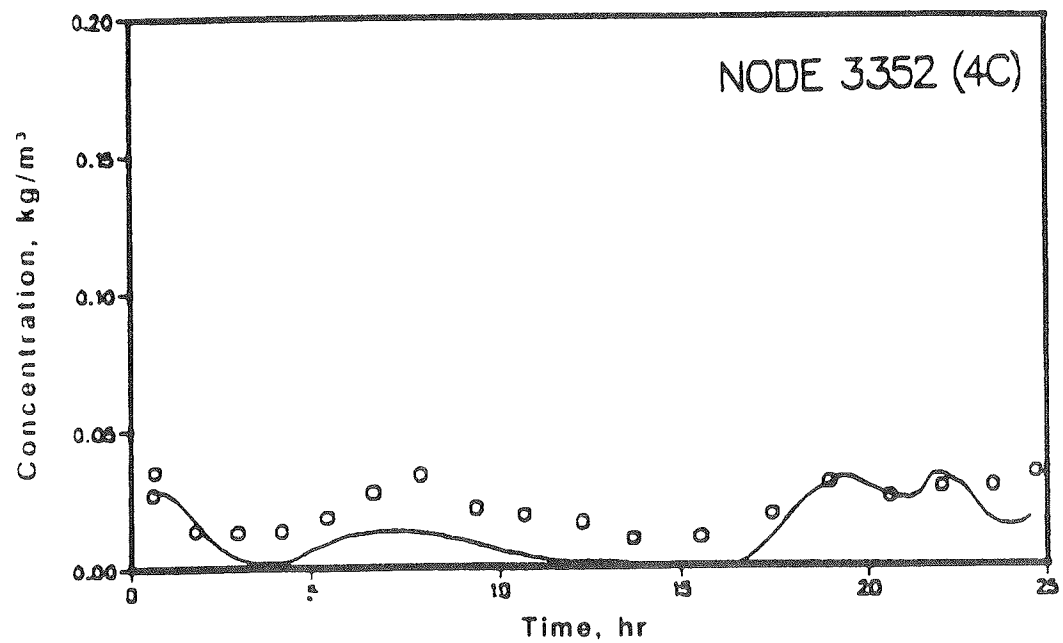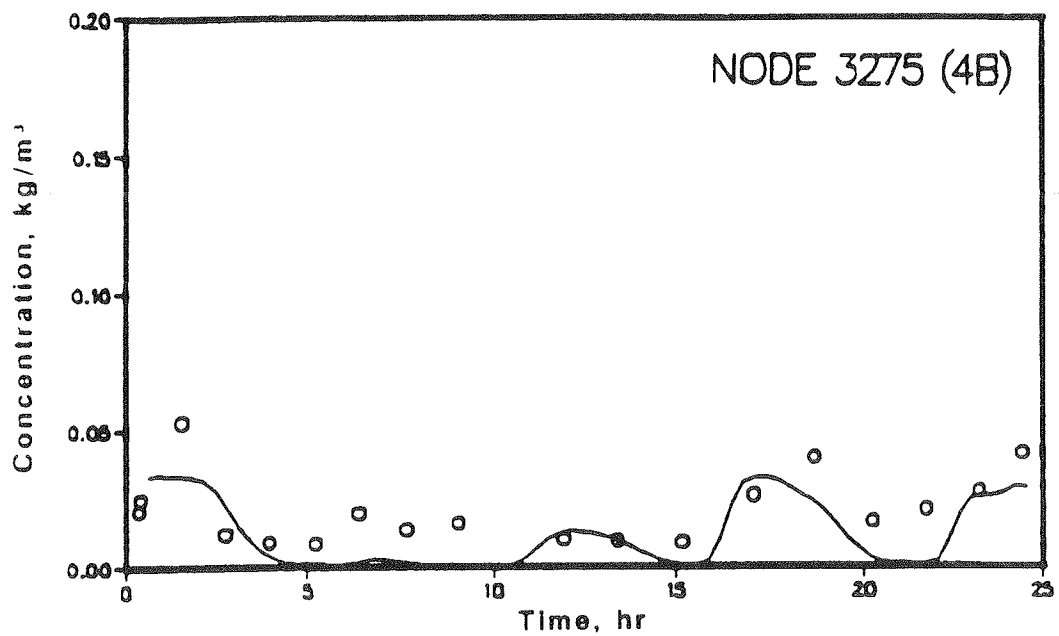
NODE 3352 (4C)

LEGEND
—— STUDH
O VERTICALLY AVERAGED
FIELD DATA

STUDH Results

Nodes 3275(4B) & 3352(4C)

PLATE 20
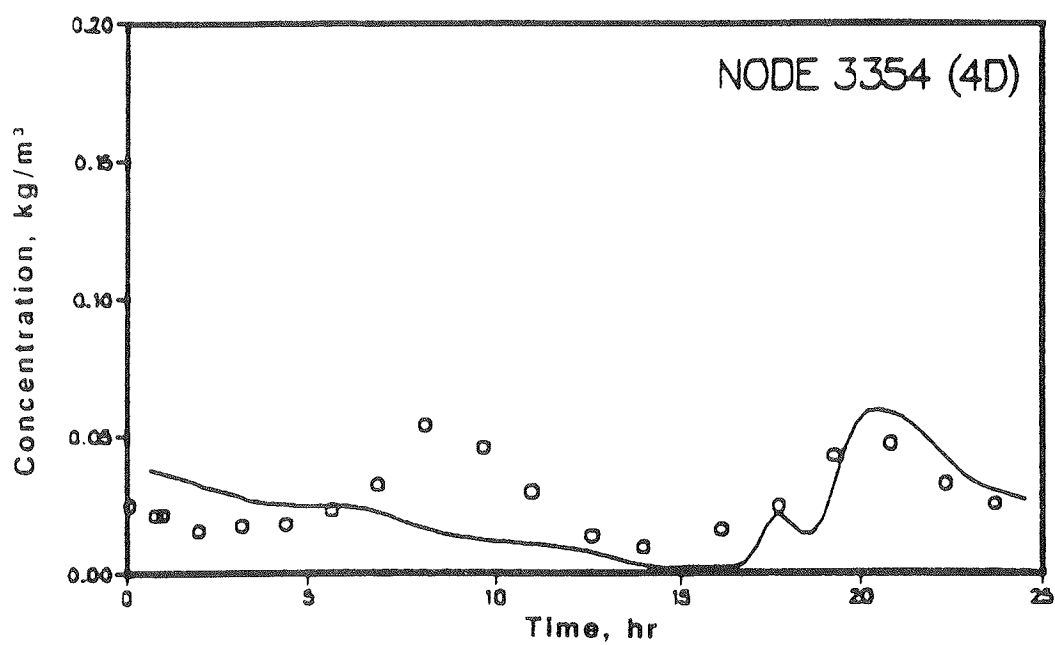
NODE 3354 (4D)

LEGEND
——— STUDH
O VERTICALLY AVERAGED
   FIELD DATA

STUDH Results

Node 3354(4D)

PLATE 21

APPENDIX A: BIBLIOGRAPHY ON SAN FRANCISCO BAY SEDIMENTATION

Arthur, J. F., and Ball, M. D. 1979. "Factors Influencing the Entrapment of Suspended Material in the San Francisco Bay-Delta Estuary," San Francisco Bay: The Urbanized Estuary, American Association for the Advancement of Science, Pacific Division, San Francisco, CA, pp 143-174.

Carlson, P. R., and McCulloch, D. S. 1974 (Oct). "Aerial Observations of Suspended Sediment Plumes in San Francisco Bay and the Adjacent Pacific Ocean," Journal Research of the U.S. Geological Survey, Vol 2, No. 5, pp 519-526.

Cloern, J. E., Powell, T. M., and Huzzey, L. M. 1989. "Spatial and Temporal Variability in South San Francisco Bay (USA); II: Temporal Changes in Salinity, Suspended Sediments, and Phytoplankton Biomass and Productivity Over Tidal Time Scales," Estuarine, Coastal and Shelf Science, Vol 28, pp 599-613.

Committee on Tidal Hydraulics. 1965 (Dec). "San Francisco Bay, California, Disposal of Dredge Spoil," US Army Corps of Engineers, Vicksburg, MS.

Conomos, T. J. 1979. "Properties and Circulation of San Francisco Bay Waters," San Francisco Bay: The Urbanized Estuary, American Association for the Advancement of Science, Pacific Division, San Francisco, CA, pp 47-83.

Conomos, T. J., and Peterson, D. H. 1976. "Suspended-Particle Transport and Circulation in San Francisco Bay: An Overview," Estuarine Processes; Volume II: Circulation, Sediments and Transfer of Material in the Estuary, Academic Press, San Francisco, CA, pp 82-97.

Conomos, T. J., Peterson, D. H., Carlson, P. R., and McCulloch, D. S. 1970. "A Preliminary Study of the Effects of Water Circulation in the San Francisco Bay Estuary - Movement of Seabed Drifters in the San Francisco Bay Estuary and Adjacent Pacific Ocean," Geological Survey Circular 637-A, B, US Department of Interior, Washington, DC.

Conomos, T. J., Smith, R. E., and Gartner, J. W. 1985. "Environmental Setting of San Francisco Bay," Temporal Dynamics of an Estuary: San Francisco Bay, Dr. W. Junk Publishers, Boston, MA, pp 1-12.

Conomos, T. J., Smith, R. E., Peterson, D. H., Hager, S. W., and Schemel, L. E. 1979. "Processes Affecting Seasonal Distributions of Water Properties in the San Francisco Bay Estuarine System," San Francisco Bay: The Urbanized Estuary, American Association for the Advancement of Science, Pacific Division, San Francisco, CA, pp 115-142.

Einstein, H. A., and Krone, R. B. 1961 (Mar). "Estuarial Sediment Transport Patterns," Journal of the Hydraulic Division, American Society of Civil Engineers, Vol 87, No. HY 2, pp 51-59.

Fuller, C. C. 1982 (Dec). "The Use of Pb-210, Th-234 and CS-137 as Tracers of Sedimentary Processes in San Francisco Bay, California," M.S. Thesis, University of Southern California, Los Angeles, CA.

Klingeman, P. C., and Kaufman, W. J. 1965 (Sep). "Transport of Radionuclides with Suspended Sediment in Estuarine Systems," SERL Report No. 65-15, University of California, Berkeley, CA.

Krone, R. B. 1962 (Jun). "Flume Studies of the Transport of Sediment in Estuarial Shoaling Processes," University of California, Berkeley, CA.

Krone, R. B. 1963 (Sep). "A Study of Rheologic Properties of Estuarial Sediments," SERL Report No. 63-8, University of California, Berkeley, CA.

_____. 1976. "Ultimate Fate of Suspended Material in Estuaries," Proceedings of the Specialty Conference on Dredging and its Environmental Effects, American Society of Civil Engineers, Mobile, AL, pp 180-201.

_____. 1979. "Sedimentation in the San Francisco Bay System," San Francisco Bay: The Urbanized Estuary, American Association for the Advancement of Science, Pacific Division, San Francisco, CA, pp 85-96.

Leahy, E. J., Lane, W. B., Tami, T. M., Inman, L. B., McLoud, W. R., and Adams, N. J. 1976 (Jun). "Dredged Sediment Movement Tracing in San Francisco Bay Utilizing Neutron Activation," Technical Report N-76-1, US Army Engineer Waterways Experiment Station, Vicksburg, MS.

McCulloch, D. S., Peterson, D. H., Carlson, P. R., and Conomos, T. J., 1970. "A Preliminary Study of the Effects of Water Circulation in the San Francisco Bay Estuary — Some Effects of Freshwater Inflow on the Flushing of South San Francisco Bay," Geological Survey Circular 637-A, B, US Department of Interior, Washington, DC.

Pankow, V. R. 1988 (Nov). "San Francisco Bay: Modeling System for Dredged Material Disposal and Hydraulic Transport," Technical Report HL-88-27, US Army Engineer Waterways Experiment Station, Vicksburg, MS.

Pestrong, R. (No Date). "Tidal Flat Sedimentation at Cooley Landing, S. W. San Francisco Bay," Department of Geology, San Francisco State College, San Francisco, CA.

Powell, T. M., Cloern, J. E., and Huzzey, L. M. 1989. "Spatial and Temporal Variability in South San Francisco Bay (USA); I: Horizontal Distributions of Salinity, Suspended Sediments, and Phytoplankton Biomass and Productivity," Estuarine, Coastal and Shelf Science, Vol 28, pp 583-597.

Rubin, D. M., and McCulloch, D. S. 1979. "The Movement and Equilibrium of Bedforms in Central San Francisco Bay," San Francisco Bay: The Urbanized Estuary, American Association for the Advancement of Science, Pacific Division, San Francisco, CA, pp 97-113.

Smith, B. J. 1963. "Sedimentation in the San Francisco Bay System," Proceedings of the Federal Inter-Agency Sedimentation Conference, US Department of Agriculture Miscellaneous Publication 970, pp 675-708.

Teeter, A. M. 1987 (May). "Alcatraz Disposal Site Investigation, San Francisco Bay; Alcatraz Disposal Site Erodibility," Report 3, Miscellaneous Paper HL-86-1, US Army Engineer Waterways Experiment Station, Vicksburg, MS.

Trawle, M. J., and Johnson, B. H. 1986a. "Alcatraz Disposal Site Investigation," Miscellaneous Paper HL-86-1, US Army Engineer Waterways Experiment Station, Vicksburg, MS.

_____. 1986b. "Alcatraz Disposal Site Investigation; North Zone of Oakland Outer Harbor and Richmond Inner Harbor Sediments," Report 2, Miscellaneous Paper HL-86-1, US Army Engineer Waterways Experiment Station, Vicksburg, MS.

US Army Engineer District, San Francisco. 1977 (Feb). "Dredge Disposal Study, San Francisco Bay and Estuary," Main Report and Appendices A-M, San Francisco, CA.

APPENDIX B: THE TABS-2 SYSTEM

1.   TABS-2 is a collection of generalized computer programs and utility codes integrated into a numerical modeling system for studying two-dimensional hydrodynamics, sedimentation, and transport problems in rivers, reservoirs, bays, and estuaries. A schematic representation of the system is shown in Figure B1. It can be used either as a stand-alone solution technique or as a step in the hybrid modeling approach. The basic concept is to calculate water-surface elevations, current patterns, sediment erosion, transport and deposition, the resulting bed surface elevations, and the feedback to hydraulics. Existing and proposed geometry can be analyzed to determine the impact on sedimentation of project designs and to determine the impact of project designs on salinity and on the stream system. The system is described in detail by Thomas and McAnally (1985).

2.   The three basic components of the system are as follows:

a.   "A Two-Dimensional Model for Free Surface Flows," RMA-2V.

b.   "Sediment Transport in Unsteady 2-Dimensional Flows, Horizontal Plane," STUDH.

c.   "Two-Dimensional Finite Element Program for Water Quality," RMA-4.

3.   RMA-2V is a finite element solution of the Reynolds form of the Navier-Stokes equations for turbulent flows. Friction is calculated with Manning's equation and eddy viscosity coefficients are used to define the turbulent losses. A velocity form of the basic equation is used with side boundaries treated as either slip or static. The model automatically recognizes dry elements and corrects the mesh accordingly. Boundary conditions may be water-surface elevations, velocities, or discharges and may occur inside the mesh as well as along the edges.
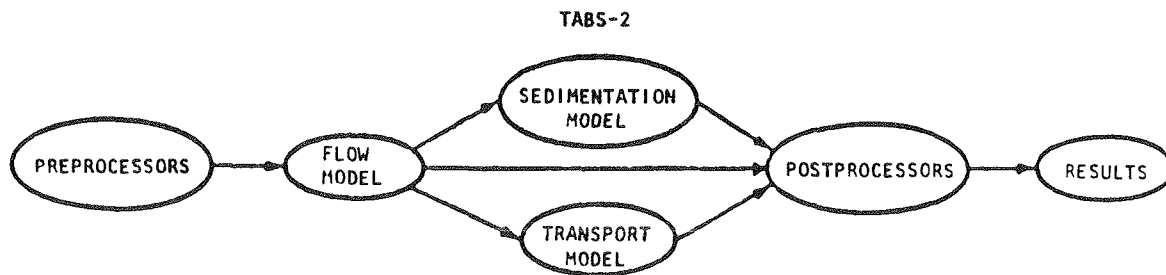

Figure B1.   TABS-2 schematic

4. The sedimentation model, STUDH, solves the convection-diffusion equation with bed source terms. These terms are structured for either sand or cohesive sediments. The Ackers-White (1973) procedure is used to calculate a sediment transport potential for the sands from which the actual transport is calculated based on availability. Clay erosion is based on work by Partheniades (1962) and Ariathurai and the deposition of clay utilizes Krone's equations (Ariathurai, MacArthur, and Krone 1977). Deposited material forms layers, as shown in Figure B2, and bookkeeping allows up to 10 layers at each node for maintaining separate material types, deposit thickness, and age. The code uses the same mesh as RMA-2V.

5. Salinity calculations, RMA-4, are made with a form of the convective-diffusion equation which has general source-sink terms. Up to seven conservative substances or substances requiring a decay term can be routed. The code uses the same mesh as RMA-2V.

6. Each of these generalized computer codes can be used as a stand-alone program, but to facilitate the preparation of input data and to aid in analyzing results, a family of utility programs was developed for the following purposes:

    <u>a</u>. Digitizing

    <u>b</u>. Mesh generation

    <u>c</u>. Spatial data management

    <u>d</u>. Graphical output

    <u>e</u>. Output analysis

    <u>f</u>. File management

    <u>g</u>. Interfaces

    <u>h</u>. Job control language

<u>Finite Element Modeling</u>

7. The TABS-2 numerical models used in this effort employ the finite element method to solve the governing equations. To help those who are unfamiliar with the method to better understand this report, a brief description of the method is given here.

8. The finite element method approximates a solution to equations by dividing the area of interest into smaller subareas, which are called elements. The dependent variables (e.g., water-surface elevations and sediment

B2

concentrations) are approximated over each element by continuous functions
which interpolate in terms of unknown point (node) values of the variables.
An error, defined as the deviation of the approximation solution from the cor-
rect solution, is minimized. Then, when boundary conditions are imposed, a
set of solvable simultaneous equations is created. The solution is continuous
over the area of interest.

9. In one-dimensional problems, elements are line segments. In two-
dimensional problems, the elements are polygons, usually either triangles or
quadrilaterals. Nodes are located on the edges of elements and occasionally
inside the elements. The interpolating functions may be linear or higher
order polynomials. Figure B2 illustrates a quadrilateral element with eight
nodes and a linear solution surface where F is the interpolating function.

10. Most water resource applications of the finite element method use
the Galerkin method of weighted residuals to minimize error. In this method
the residual, the total error between the approximate and correct solutions,
is weighted by a function that is identical with the interpolating function
and then minimized. Minimization results in a set of simultaneous equations
in terms of nodal values of the dependent variable (e.g. water-surface eleva-
tions or sediment concentration). The time portion of time-dependent problems
can be solved by the finite element method, but it is generally more efficient
to express derivatives with respect to time in finite difference form.

The Hydrodynamic Model, RMA-2V

Applications

11. This program is designed for far-field problems in which vertical
accelerations are negligible and the velocity vectors at a node generally
point in the same directions over the entire depth of the water column at any
instant of time. It expects a homogeneous fluid with a free surface. Both
steady and unsteady state problems can be analyzed. A surface wind stress can
be imposed.

12. The program has been applied to calculate flow distribution around
islands; flow at bridges having one or more relief openings, in contracting
and expanding reaches, into and out of off-channel hydropower plants, at river
junctions, and into and out of pumping plant channels; and general flow pat-
terns in rivers, reservoirs, and estuaries.
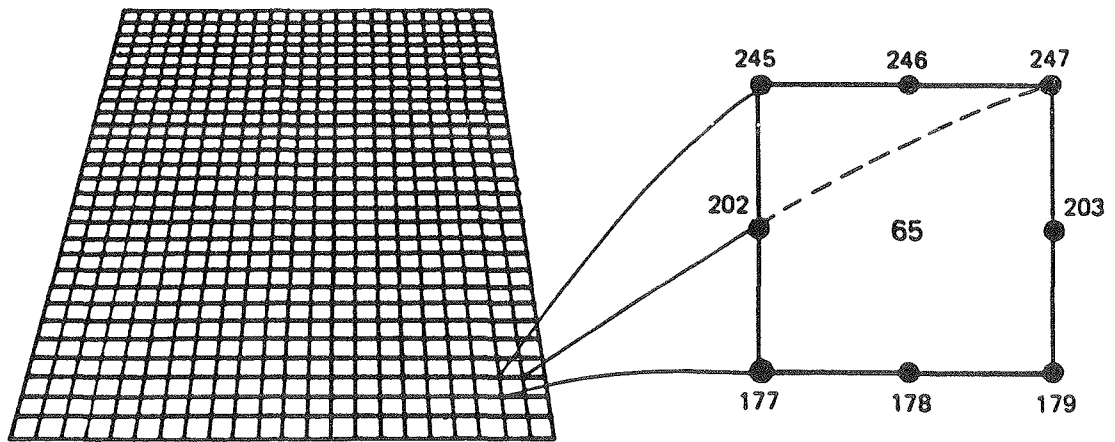
a. Eight nodes define each element
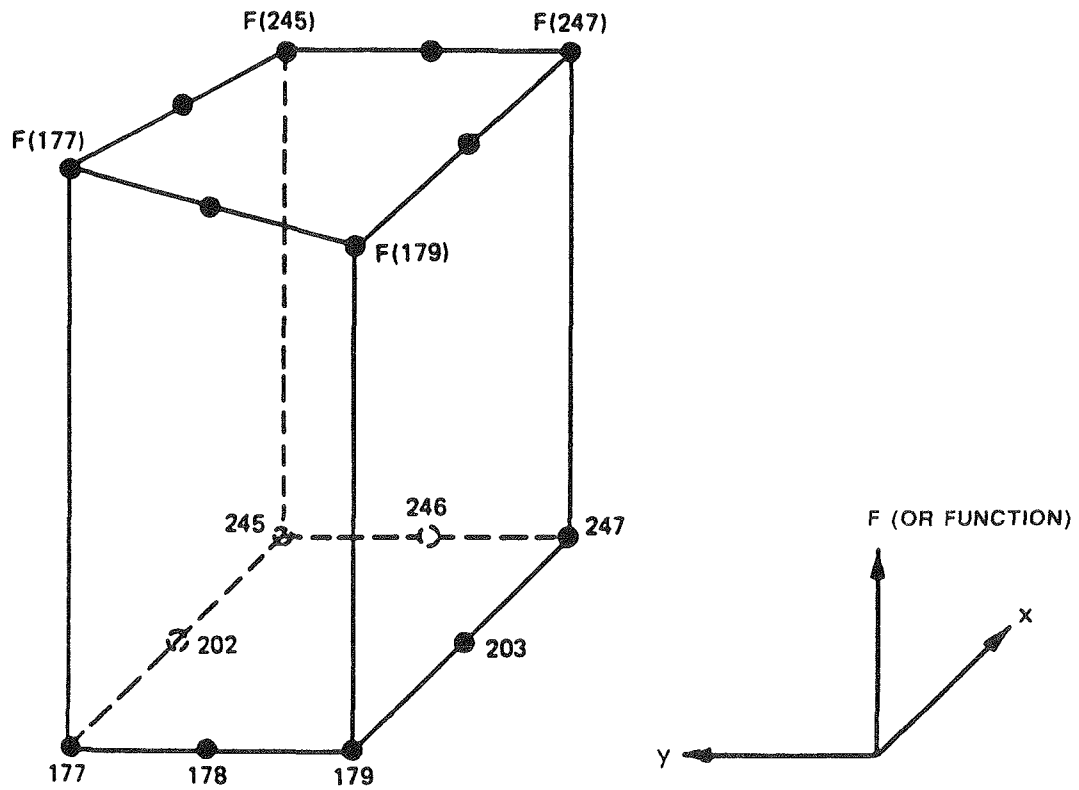
b. Linear interpolation function

Figure B2. Two-dimensional finite element mesh

Limitations

13. This program is not designed for near-field problems where flow-structure interactions (such as vortices, vibrations, or vertical accelerations) are of interest. Areas of vertically stratified flow are beyond this program's capability unless it is used in a hybrid modeling approach. It is two-dimensional in the horizontal plane, and zones where the bottom current is in a different direction from the surface current must be analyzed with considerable subjective judgment regarding long-term energy considerations. It is a free-surface calculation for subcritical flow problems.

Governing equations

14. The generalized computer program RMA-2V solves the depth-integrated equations of fluid mass and momentum conservation in two horizontal directions. The form of the solved equations is

$$h \frac{\partial u}{\partial t} + hu \frac{\partial u}{\partial x} + hv \frac{\partial u}{\partial y} - \frac{h}{\rho} \left[\epsilon_{xx} \frac{\partial^2 u}{\partial x^2} + \epsilon_{xy} \frac{\partial^2 u}{\partial y^2} \right] + gh \left[\frac{\partial a}{\partial x} + \frac{\partial h}{\partial x} \right]$$

$$+ \frac{gun^2}{\left[1.486h^{1/6} \right]^2} \left[u^2 + v^2 \right]^{1/2} - \varsigma V_a^2 \cos \psi - 2h\omega v \sin \phi = 0 \tag{B1}$$

$$h \frac{\partial v}{\partial t} + hv \frac{\partial v}{\partial x} + hv \frac{\partial v}{\partial y} - \frac{h}{\rho} \left[\epsilon_{yx} \frac{\partial^2 v}{\partial x^2} + \epsilon_{yy} \frac{\partial^2 v}{\partial y^2} \right] + gh \left[\frac{\partial a}{\partial y} + \frac{\partial h}{\partial y} \right]$$

$$+ \frac{gvn^2}{\left[1.486h^{1/6} \right]^2} \left[u^2 + v^2 \right]^{1/2} - \varsigma V_a^2 \sin \psi + 2\omega hu \sin \phi = 0 \tag{B2}$$

$$\frac{\partial h}{\partial t} + h \left[\frac{\partial u}{\partial x} + \frac{\partial v}{\partial y} \right] + u \frac{\partial h}{\partial x} + v \frac{\partial h}{\partial y} = 0 \tag{B3}$$

where

$$h = \text{depth}$$

$$u, v = \text{velocities in the Cartesian directions}$$

$$x, y, t = \text{Cartesian coordinates and time}$$

$$\rho = \text{density}$$

ϵ = eddy viscosity coefficient, for xx = normal direction on x-axis surface; yy = normal direction on y-axis surface; xy and yx = shear direction on each surface

g = acceleration due to gravity

a = elevation of bottom

n = Manning's n value

1.486 = conversion from SI (metric) to non-SI units

ζ = empirical wind shear coefficient

V_a = wind speed

ψ = wind direction

ω = rate of earth's angular rotation

ϕ = local latitude

15. Equations B1, B2, and B3 are solved by the finite element method using Galerkin weighted residuals. The elements may be either quadrilaterals or triangles and may have curved (parabolic) sides. The shape functions are quadratic for flow and linear for depth. Integration in space is performed by Gaussian integration. Derivatives in time are replaced by a nonlinear finite difference approximation. Variables are assumed to vary over each time interval in the form

$$f(t) = f(0) + at + bt^c \qquad t_0 \leq t < t \qquad \text{(B4)}$$

which is differentiated with respect to time, and cast in finite difference form. Letters a , b , and c are constants. It has been found by experiment that the best value for c is 1.5 (Norton and King 1977).

16. The solution is fully implicit and the set of simultaneous equations is solved by Newton-Raphson iteration. The computer code executes the solution by means of a front-type solver that assembles a portion of the matrix and solves it before assembling the next portion of the matrix. The front solver's efficiency is largely independent of bandwidth and thus does not require as much care in formation of the computational mesh as do traditional solvers.

17. The code RMA-2V is based on the earlier version RMA-2 (Norton and King 1977) but differs from it in several ways. It is formulated in terms of velocity (v) instead of unit discharge (vh), which improves some aspects of the code's behavior; it permits drying and wetting of areas within the grid;

and it permits specification of turbulent exchange coefficients in directions other than along the x- and z-axes. For a more complete description, see Appendix F of Thomas and McAnally (1985).

The Sediment Transport Model, STUDH

Applications

18. STUDH can be applied to clay and/or sand bed sediments where flow velocities can be considered two-dimensional (i.e., the speed and direction can be satisfactorily represented as a depth-averaged velocity). It is useful for both deposition and erosion studies and, to a limited extent, for stream width studies. The program treats two categories of sediment: noncohesive, which is referred to as sand here, and cohesive, which is referred to as clay.

Limitations

19. Both clay and sand may be analyzed, but the model considers a single, effective grain size for each and treats each separately. Fall velocity must be prescribed along with the water-surface elevations, x-velocity, y-velocity, diffusion coefficients, bed density, critical shear stresses for erosion, erosion rate constants, and critical shear stress for deposition.

20. Many applications cannot use long simulation periods because of their computation cost. Study areas should be made as small as possible to avoid an excessive number of elements when dynamic runs are contemplated yet must be large enough to permit proper posing of boundary conditions. The same computation time interval must be satisfactory for both the transverse and longitudinal flow directions.

21. The program does not compute water-surface elevations or velocities; therefore these data must be provided. For complicated geometries, the numerical model for hydrodynamic computations, RMA-2V, is used.

Governing equations

22. The generalized computer program STUDH solves the depth-integrated convection-dispersion equation in two horizontal dimensions for a single sediment constituent. For a more complete description, see Appendix G of Thomas and McAnally (1985). The form of the solved equation is

$$\frac{\partial C}{\partial t} + u \frac{\partial C}{\partial x} + v \frac{\partial C}{\partial y} = \frac{\partial}{\partial x} \left[D_x \frac{\partial C}{\partial x} \right] + \frac{\partial}{\partial y} \left[D_y \frac{\partial C}{\partial y} \right] + \alpha_1 C + \alpha_2 = 0 \qquad (B5)$$

where

C = concentration of sediment

u = depth-integrated velocity in x-direction

v = depth-integrated velocity in y-direction

D_x = dispersion coefficient in x-direction

D_y = dispersion coefficient in y-direction

α_1 = coefficient of concentration-dependent source/sink term

α_2 = coefficient of source/sink term

23. The source/sink terms in Equation B5 are computed in routines that treat the interaction of the flow and the bed. Separate sections of the code handle computations for clay bed and sand bed problems.

Sand transport

24. The source/sink terms are evaluated by first computing a potential sand transport capacity for the specified flow conditions, comparing that capacity with the amount of sand actually being transported, and then eroding from or depositing to the bed at a rate that would approach the equilibrium value after sufficient elapsed time.

25. The potential sand transport capacity in the model is computed by the method of Ackers and White (1973), which uses a transport power (work rate) approach. It has been shown to provide superior results for transport under steady-flow conditions (White, Milli, and Crabbe 1975) and for combined waves and currents (Swart 1976). Flume tests at the US Army Engineer Waterways Experiment Station have shown that the concept is valid for transport by estuarine currents.

26. The total load transport function of Ackers and White is based upon a dimensionless grain size

$$D_{gr} = D \left[\frac{g(s - 1)}{\nu^2} \right]^{1/3} \tag{B6}$$

where

D = sediment particle diameter

s = specific gravity of the sediment

ν = kinematic viscosity of the fluid

and a sediment mobility parameter

B8

$$F_{gr} = \left[\frac{\tau^{n'} \tau'^{(1-n')}}{\rho g D (s - 1)} \right]^{1/2} \qquad (B7)$$

where

τ = total boundary shear stress

n' = a coefficient expressing the relative importance of bed-load and suspended-load transport, given in Equation A9

τ' = boundary surface shear stress

The surface shear stress is that part of the total shear stress which is due to the rough surface of the bed only, i.e., not including that part due to bed forms and geometry. It therefore corresponds to that shear stress that the flow would exert on a plane bed.

27. The total sediment transport is expressed as an effective concentration

$$G_p = C \left[\frac{F_{gr}}{A} - 1 \right]^m \frac{sD}{h} \left[\frac{\rho}{\tau} U \right]^{n'} \qquad (B8)$$

where U is the average flow speed, and for $1 < D_{gr} \leq 60$

$$n' = 1.00 - 0.56 \log D_{gr} \qquad (B9)$$

$$A = \frac{0.23}{\sqrt{D_{gr}}} + 0.14 \qquad (B10)$$

$$\log C = 2.86 \log D_{gr} - (\log D_{gr})^2 - 3.53 \qquad (B11)$$

$$m = \frac{9.66}{D_{gr}} + 1.34 \qquad (B12)$$

For $D_{gr} < 60$

$$n' = 0.00 \qquad (B13)$$

B9

$$A = 0.17 \qquad\qquad (B14)$$

$$C = 0.025 \qquad\qquad (B15)$$

$$m = 1.5 \qquad\qquad (B16)$$

28. Equations B6-B16 result in a potential sediment concentration G_p. This value is the depth-averaged concentration of sediment that will occur if an equilibrium transport rate is reached with a nonlimited supply of sediment. The rate of sediment deposition (or erosion) is then computed as

$$R = \frac{G_p - C}{t_c} \qquad\qquad (B17)$$

where

$\quad C$ = present sediment concentration

$\quad t_c$ = time constant

For deposition, the time constant is

$$t_c = \text{larger of} \begin{cases} \Delta t \\ \text{or} \\ \dfrac{C_d h}{V_s} \end{cases} \qquad\qquad (B18)$$

and for erosion it is

$$t_c = \text{larger of} \begin{cases} \Delta t \\ \text{or} \\ \dfrac{C_e h}{U} \end{cases} \qquad\qquad (B19)$$

where

$\quad \Delta t$ = computational time-step

$\quad C_d$ = response time coefficient for deposition

$\quad V_s$ = sediment settling velocity

$\quad C_e$ = response time coefficient for erosion

B10

The sand bed has a specified initial thickness which limits the amount of erosion to that thickness.

Cohesive sediments transport

29.   Cohesive sediments (usually clays and some silts) are considered to be depositional if the bed shear stress exerted by the flow is less than a critical value τ_d . When that value occurs, the deposition rate is given by Krone's (1962) equation

$$
S = \begin{cases}
- \dfrac{2V_s}{h} C \left[1 - \dfrac{\tau}{\tau_d}\right] & \text{for } C < C_c & \text{(B20)} \\[4ex]
- \dfrac{2V_s}{hC_c^{4/3}} C^{5/3}\left[1 - \dfrac{\tau}{\tau_d}\right] & \text{for } C > C_c & \text{(B21)}
\end{cases}
$$

where

$\quad$ S = source term

$\quad$ V_s = fall velocity of a sediment particle

$\quad$ h = flow depth

$\quad$ C = sediment concentration in water column

$\quad$ τ = bed shear stress

$\quad$ τ_d = critical shear stress for deposition

$\quad$ C_c = critical concentration = 300 mg/ℓ

30.   If the bed shear stress is greater than the critical value for particle erosion τ_e , material is removed from the bed. The source term is then computed by Ariathurai's (Ariathurai, MacArthur, and Krone 1977) adaptation of Partheniades' (1962) findings:

$$
S = \frac{P}{h}\left[\frac{\tau}{\tau_e} - 1\right] \quad \text{for } \tau > \tau_e \tag{B22}
$$

where P is the erosion rate constant, unless the shear stress is also greater than the critical value for mass erosion. When this value is exceeded, mass failure of a sediment layer occurs and

B11

$$S = \frac{T_L P_L}{h \Delta t} \quad \text{for } \tau > \tau_s \qquad (B23)$$

where

T_L = thickness of the failed layer

P_L = density of the failed layer

Δt = time interval over which failure occurs

τ_s = bulk shear strength of the layer

31.   The cohesive sediment bed consists of 1 to 10 layers, each with a distinct density and erosion resistance.   The layers consolidate with overburden and time.

Bed shear stress

32.   Bed shear stresses are calculated from the flow speed according to one of four optional equations: the smooth-wall log velocity profile or Manning equation for flows alone; and a smooth bed or rippled bed equation for combined currents and wind waves.   Shear stresses are calculated using the shear velocity concept where

$$\tau_b = \rho u_*^2 \qquad (B24)$$

where

τ_b = bed shear stress

u_* = shear velocity

and the shear velocity is calculated by one of four methods:

   a.   Smooth-wall log velocity profiles

$$\frac{\bar{u}}{u_*} = 5.75 \log \left[3.32 \, \frac{u_* h}{\nu} \right] \qquad (B25)$$

which is applicable to the lower 15 percent of the boundary
layer when

$$\frac{u_* h}{\nu} > 30$$

where   u   is the mean flow velocity (resultant of   u   and   v   components)

b. The Manning shear stress equation

$$u_* = \frac{\left(\overline{u}n\right)\sqrt{g}}{CME \ (h)^{1/6}} \qquad \text{(B26)}$$

where   CME   is a coefficient of 1 for SI (metric) units and 1.486 for non-SI units of measurement.

c. A Jonsson-type equation for surface shear stress (plane beds) caused by waves and currents

$$u_* = \sqrt{\frac{1}{2}\left(\frac{f_w u_{om} + f_c \overline{u}}{u_{om} + \overline{u}}\right)\left(\overline{u} + u_{om}\right)^2} \qquad \text{(B27)}$$

where

f_w = shear stress coefficient for waves

u_{om} = maximum orbital velocity of waves

f_c = shear stress coefficient for currents

d. A Bijker-type equation for total shear stress caused by waves and current

$$u_* = \sqrt{\frac{1}{2} f_c \overline{u}^2 + \frac{1}{4} f_w u_{om}^2} \qquad \text{(B28)}$$

Solution method

33. Equation B5 is solved by the finite element method using Galerkin weighted residuals. Like RMA-2V, which uses the same general solution technique, elements are quadrilateral and may have parabolic sides. Shape functions are quadratic. Integration in space is Gaussian. Time-stepping is performed by a Crank-Nicholson approach with a weighting factor (θ) of 0.66.

B13

A front-type solver similar to that in RMA-2V is used to solve the
simultaneous equations.

References

Ackers, P., and White, W. R. 1973. (Nov). "Sediment Transport: New Approach and Analysis," *Journal, Hydraulics Division, American Society of Civil Engineers,* Vol 99, No. HY-11, pp 2041-2060.

Ariathurai, R., MacArthur, R. D., and Krone, R. C. 1977 (Oct). "Mathematical Model of Estuarial Sediment Transport," Technical Report D-77-12, US Army Engineer Waterways Experiment Station, Vicksburg, MS.

Krone, R. B. 1962. "Flume Studies of Transport of Sediment in Estuarial Shoaling Processes," Final Report, Hydraulics Engineering Research Laboratory, University of California, Berkeley, CA.

Norton, W. R., and King, I. P. 1977 (Feb). "Operating Instructions for the Computer Program RMA-2V," Resource Management Associates, Lafayette, CA.

Partheniades, E. 1962. "A Study of Erosion and Deposition of Cohesive Soils in Salt Water," Ph.D. Dissertation, University of California, Berkeley, CA.

Swart, D. H. 1976 (Sep). "Coastal Sediment Transport, Computation of Longshore Transport," R968, Part 1, Delft Hydraulics Laboratory, The Netherlands.

Thomas, W. A., and McAnally, W. H., Jr. 1985 (Aug). "User's Manual for the Generalized Computer Program System; Open-Channel Flow and Sedimentation, TABS-2, Main Text and Appendices A through O," Instruction Report HL-85-1, US Army Engineer Waterways Experiment Station, Vicksburg, MS.

White, W. R., Milli, H., and Crabbe, A. D. 1975. "Sediment Transport Theories: An Appraisal of Available Methods," Report Int 119, Vols 1 and 2, Hydraulics Research Station, Wallingford, England.